SPIE Handbook of Microlithography, Micromachining and Microfabrication

Volume 1: Microlithography

Chapter 2

E Beam Lithography

by

Mark A. McCord, Stanford University
Michael J. Rooks, Cornell University

Table of Contents

2.1 Introduction
- 2.1.1 Definition and historical perspective
- 2.1.2 Applications
- 2.1.3 Alternative techniques

2.2 Elements of electron optics
- 2.2.1 Introduction
- 2.2.2 Electron sources
- 2.2.3 Electron lenses
- 2.2.4 Other electron optical elements
  - 2.2.4.1 Apertures
  - 2.2.4.2 Electron beam deflection
  - 2.2.4.3 Beam blanking
  - 2.2.4.4 Stigmators
- 2.2.5 Other column components
- 2.2.6 Resolution

2.3 Electron-solid interactions
- 2.3.1 Forward scattering
- 2.3.2 Backscattering
- 2.3.3 Secondary electrons
- 2.3.4 Modeling

2.4 Proximity effect
- 2.4.1 Introduction
- 2.4.2 Proximity effect avoidance
- 2.4.3 Proximity effect correction
  - 2.4.3.1 Dose modulation
  - 2.4.3.2 Pattern biasing
  - 2.4.3.3 GHOST
  - 2.4.3.4 Software

2.5 Systems
- 2.5.1 Environment
- 2.5.2 SEM and STEM conversions
- 2.5.3 Commercial SEM conversion systems
  - 2.5.3.1 Nanometer Pattern Generation System (NPGS)
  - 2.5.3.2 Raith pattern generators
  - 2.5.3.3 Leica EBL Nanowriter
- 2.5.4 Gaussian vector scan systems
  - 2.5.4.1 JEOL systems
  - 2.5.4.2 Leica Lithography Systems
  - 2.5.4.3 Leica Lithographie Systeme Jena (Jenoptik) LION
- 2.5.5 Gaussian spot mask writers
  - 2.5.5.1 Etec MEBES systems
  - 2.5.5.2 Lepton EBES4
- 2.5.6 Shaped Spot and Cell Projection Systems
  - 2.5.6.1 IBM EL-4
  - 2.5.6.2 Etec Systems Excaliber and Leica Lithographie Systeme Jena ZBA 31/32
  - 2.5.6.3 JEOL shaped spot systems
  - 2.5.6.4 Cell projection
- 2.5.7 SCALPEL
- 2.5.8 Other e-beam system research
  - 2.5.8.1 STM writing
  - 2.5.8.2 Parallel beam architectures - microcolumns
- 2.5.9 Electron beam fabrication services

2.6 Data preparation
- 2.6.1 Pattern structure
- 2.6.2 Avoiding trouble spots
- 2.6.3 Alignment marks

2.6.4 CAD Programs
2.6.5 Intermediate formats
2.6.5.1 GDSII Stream
2.6.5.2 CIF
2.6.5.3 DXF
2.6.5.4 PG3600
2.6.6 Low-level formats
2.7 Resists
2.7.1 Charge dissipation
2.7.2 Positive resists
2.7.2.1 PMMA
2.7.2.2 EBR-9
2.7.2.3 PBS
2.7.2.4 ZEP
2.7.2.5 Photoresists as e-beam resists
2.7.3 Negative resists
2.7.3.1 COP
2.7.3.2 Shipley SAL
2.7.3.3 Noncommercial negative resists: P(SI-CMS) and EPTR
2.7.4 Multilayer systems
2.7.4.1 Low/high molecular weight PMMA
2.7.4.2 PMMA/copolymer
2.7.4.3 Trilayer systems
2.7.5 Inorganic and contamination resists
2.7.6 Other research: scanning probes and thin imaging layers
2.8 Acknowledgements
2.9 Appendix: GDSII Stream Format
2.10 References

2.1 Introduction

2.1.1 Definition and historical perspective

Electron beam lithography (EBL) is a specialized technique for creating the extremely fine patterns (much smaller than can be seen by the naked eye) required by the modern electronics industry for integrated circuits. Derived from the early scanning electron microscopes, the technique in brief consists of scanning a beam of electrons across a surface covered with a resist film sensitive to those electrons, thus depositing energy in the desired pattern in the resist film. The process of forming the beam of electrons and scanning it across a surface is very similar to what happens inside the everyday television or CRT display, but EBL typically has three orders of magnitude better resolution. The main attributes of the technology are 1) it is capable of very high resolution, almost to the atomic level; 2) it is a flexible technique that can work with a variety of materials and an almost infinite number of patterns; 3) it is slow, being one or more orders of magnitude slower than optical lithography; and 4) it is expensive and complicated - electron beam lithography tools can cost many millions of dollars and require frequent service to stay properly maintained.

The first electron beam lithography machines, based on the scanning electron microscope (SEM), were developed in the late 1960s. Shortly thereafter came the discovery that the common polymer PMMA (polymethyl methacrylate) made an excellent electron beam resist [1]. It is remarkable that even today, despite sweeping technological advances, extensive development of commercial EBL, and a myriad of positive and negative tone resists, much work continues to be done with PMMA resist on converted SEMs. Fig. 2.1 shows a block diagram of a typical electron beam lithography tool. The column is responsible for forming and controlling the electron beam.

Underneath the column is a chamber containing a stage for moving the sample around and facilities for loading and unloading it. Associated with the chamber is a vacuum system needed to maintain an appropriate vacuum level throughout the machine and also during the load and unload cycles. A set of control electronics supplies power and signals to the various parts of the machine. Finally, the system is controlled by a computer, which may be anything from a personal computer to a mainframe. The computer handles such diverse functions as setting up an exposure job, loading and unloading the sample, aligning and focusing the electron beam, and sending pattern data to the pattern generator. The part of the computer and electronics used to handle pattern data is sometimes referred to as the datapath. Fig. 2.2 shows a picture of a typical commercial EBL system including the column, chamber, and control electronics.

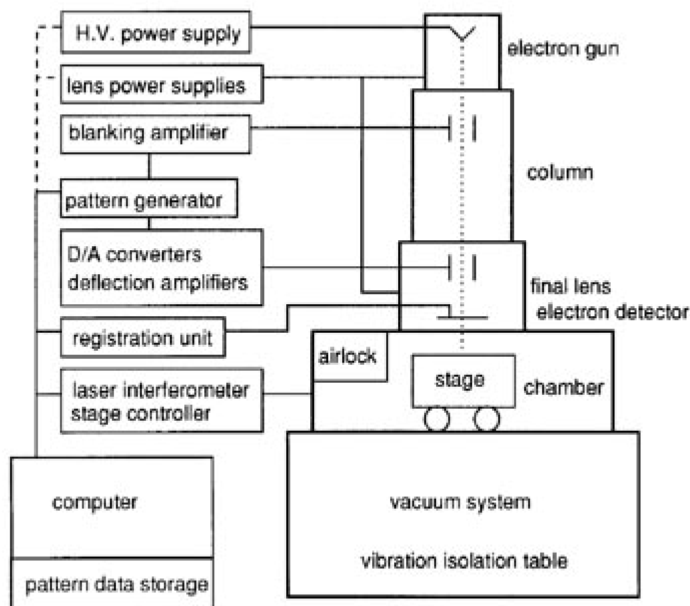

FIGURE 2.1. Block diagram showing the major components of a typical electron beam lithography system.

2.1.2 Applications

Currently, electron beam lithography is used principally in support of the integrated circuit industry, where it has three niche markets. The first is in maskmaking, typically the chrome-on-glass masks used by optical lithography tools. It is the preferred technique for masks because of its flexibility in providing rapid turnaround of a finished part described only by a computer CAD file. The ability to meet stringent linewidth control and pattern placement specifications, on the order of 50 nm each, is a remarkable achievement.

Because optical steppers usually reduce the mask dimensions by 4 or 5, resolution is not critical, with minimum mask dimensions currently in the one to two um range. The masks that are produced are used mainly for the fabrication of integrated circuits, although other applications such as disk drive heads and flat panel displays also make use of such masks.

An emerging market in the mask industry is 1 masks for x-ray lithography. These masks typically have features ranging from 0.25 um to less than 0.1 um and will require placement accuracy and linewidth control of 20 nm or better. Should x-ray technology ever become a mainstream manufacturing technique, it will have an explosive effect on EBL tool development since the combination of resolution, throughput, and accuracy required, while technologically achievable, are far beyond what any single tool today is capable of providing.

The second application is direct write for advanced prototyping of integrated circuits [2] and manufacture of small volume specialty products, such as gallium arsenide integrated circuits and optical waveguides. Here both the flexibility and the resolution of electron beam lithography are used to make devices that are perhaps one or two generations ahead of mainstream optical lithography techniques.

Finally, EBL is used for research into the scaling limits of integrated circuits (Fig. 2.3) [3] and studies of quantum effects and other novel physics phenomena at very small dimensions. Here the resolution of EBL makes it the tool of choice. A typical application is the study of the Aharanov-Bohm effect, [4-6] where electrons traveling along two different paths about a micrometer in length can interfere constructively or destructively, depending on the strength of an applied magnetic field. Other applications include devices to study ballistic electron effects, quantization of electron energy levels in very small structures, [7,8] and single electron

transistors. To see these effects typically requires minimum feature sizes of 100 nm or less as well as operation at cryogenic temperatures.

FIGURE 2.2. A commercial electron beam lithography tool. (courtesy of JEOL Ltd.)

2.1.3 Alternative Techniques

It is prudent to consider possible alternatives before committing to EBL technology. For chrome-on-glass optical mask fabrication, there are optical mask writers available that are based either on optical reduction of rectangular shapes formed by framing blades or by multiple individually controlled round laser beams. Although at present EBL is technologically ahead of optical mask writers, this may not continue in the future. However, EBL will continue to provide a resolution advantage over the optical mask writers which may be important for advanced masks using phase shift or optical proximity correction. For 1 mask fabrication (i.e. x-ray), EBL will continue to be the most attractive option.

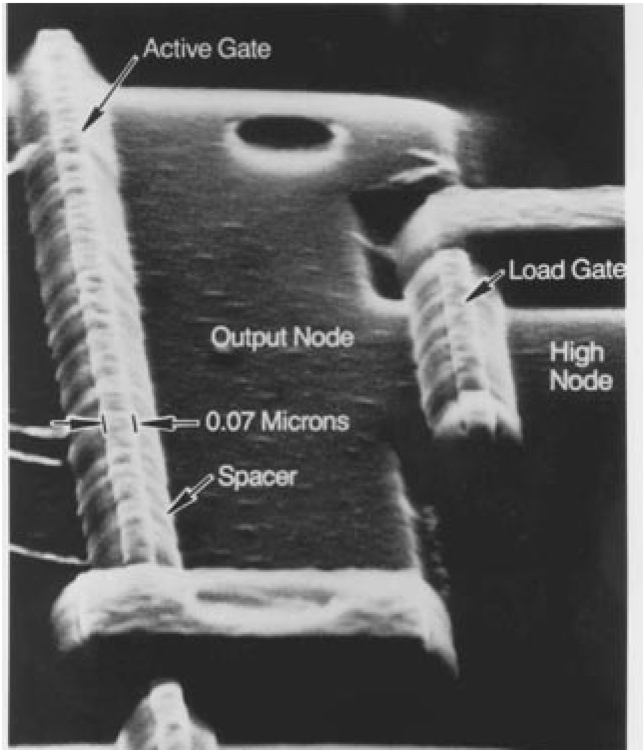

FIGURE 2.3. Micrograph of a portion of an integrated circuit fabricated by electron beam lithography. The minimum dimensions are less than 0.1 um. [Courtesy of S. Rishton and E. Ganin, IBM]

Optical lithography using lenses that reduce a mask image onto a target (much like an enlarger in photography) is the technique used almost exclusively for all semiconductor integrated circuit manufacturing. Currently, the minimum feature sizes that are printed in production are a few tenths of a micrometer. For volume production, optical lithography is much cheaper than EBL, primarily because of the high throughput of the optical tools. However, if just a few samples are being made, the mask cost (a few thousand dollars) becomes excessive, and the use of EBL is justified. Today optical tools can print 0.25 um features in development laboratories, and 0.18 um should be possible within a few years.

By using tricks, optical lithography can be extended to 0.1 um or even smaller. Some possible tricks include overexposing/overdeveloping, phase shift and phase edge masks, and edge shadowing [9]. The problem with these tricks is that they may not be capable of exposing arbitrary patterns, although they may be useful for making isolated transistor gates or other simple sparse patterns. Another specialized optical technique can be used to fabricate gratings with periods as small as 0.2 um by interfering two laser beams at the surface of the sample [10]. Again, the pattern choice is very restricted, although imaginative use of blockout and trim masks may allow for the fabrication of simple devices.

X-ray proximity printing may be a useful lithographic technique for sub-0.25 um features [11]. Again, it requires a mask made by EBL, and since the mask is 1 this can be a formidable challenge. However, if the throughput required exceeds the limited capabilities of EBL, this may be an attractive option. The disadvantage is that x-ray lithography is currently an extremely expensive proposition and the availability of good masks is limited. It also requires either a custom built x-ray source and stepper or access to a synchrotron storage ring to do the exposures. With care, x-ray lithography can also be extended to the sub-0.1 um regime [12].

The final technique to be discussed is ion beam lithography. The resolution, throughput, cost, and complexity of ion beam systems is on par with EBL. There are a couple of disadvantages, namely, limits on the thickness of resist that can be exposed and possible damage to the sample from ion bombardment. One advantage of ion beam lithography is the lack of a proximity effect, which causes problems with linewidth control in EBL. Another advantage is the possibility of in situ doping if the proper ion species are available and in situ material removal by ion beam assisted etching. The main reason that ion beam lithography is not currently widely practiced is simply that the tools have not reached the same advanced stage of development as those of EBL.

Finally, it should also be noted that modern computer simulation tools, together with a detailed understanding of the underlying physics, in many cases allows one to accurately predict exploratory device characteristics without ever having to build actual hardware. This is especially true for silicon transistors.

2.2 Elements of electron optics

2.2.1 Introduction

The part of the EBL system that forms the electron beam is normally referred to as the column. An EBL column (Fig. 2.4) typically consists of an electron source, two or more lenses, a mechanism for deflecting the beam, a blanker for turning the beam on and off, a stigmator for correcting any astigmatism in the beam, apertures for helping to define the beam, alignment systems for centering the beam in the column, and finally, an electron detector for assisting with focusing and locating marks on the sample. The optical axis (Z) is parallel to the electron beam, while X and Y are parallel to the plane of the sample.

Electron optics are a very close analog of light optics, and most of the principles of an electron beam column (except for the rotation of the image) can be understood by thinking of the electrons as rays of light and the electron optical components as simply their optical counterparts. In order to operate an EBL machine, generally it is not necessary to understand the underlying math andphysics, so they will not be discussed here although several excellent texts are available should the reader desire more information. [13,14] In addition, computer programs are available that allow easy and accurate design and simulation of optical components and columns. [15]

2.2.2 Electron Sources

Electrons may be emitted from a conducting material either by heating it to the point where the electrons have sufficient energy to overcome the work function barrier of the conductor (thermionic sources) or by applying an electric field sufficiently strong that they tunnel through the barrier (field emission sources). Three key parameters of the source are the virtual source size, its brightness (expressed in amperes per square centimeter per steradian), and the energy spread of the emitted electrons (measured in electron volts).

The size of the source is important since this determines the amount of demagnification the lenses must provide in order to form a small spot at the target. Brightness can be compared to intensity in light optics, so the brighter the electron source, the higher the current in the electron beam. A beam with a wide energy spread (which is undesirable, as will be shown in the section on lenses) is similar to white light, while a beam with a narrow energy spread would be comparable to monochromatic light. Although the energy spread of the source is important, space charge interactions between electrons further increase the energy spread of the beam as it moves down the column (Boersch effect). [16] An electron source is usually combined with two or more electrodes to control the emission properties, as shown in Fig. 2.5. [17]

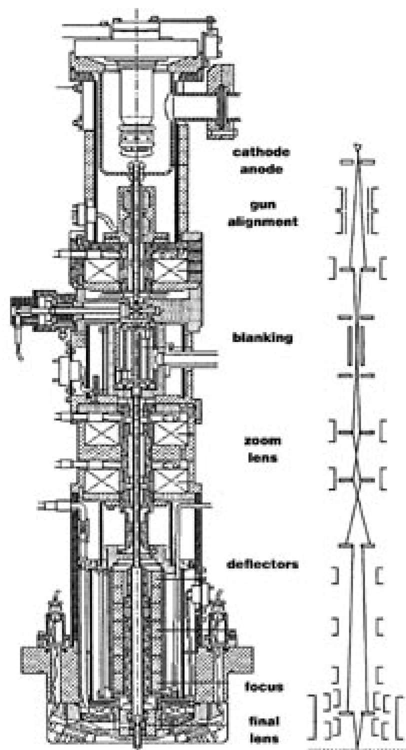

FIGURE 2.4. Cross-section drawing of a typical electron beam column along with a raytrace of the electrons as they pass through the various electron optical components. (Courtesy of Leica Lithography Systems Ltd.)

Table 2.1 summarizes the properties of common sources. For many years the standard thermionic electron source for lithography optics was a loop of tungsten wire heated white hot by passing a current it. Tungsten was chosen for its ability to withstand high temperatures without melting or evaporating. Unfortunately, this source was not very bright and also had a large energy spread caused by the very high operating temperature (2700 K). More recently, lanthanum hexaboride has become the cathode of choice; due to a very low work function, a high brightness is obtained at an operating temperature of around 1800 K. The beam current delivered by thermionic sources depends on the temperature of the cathode. Higher temperatures can deliver greater beam current, but the tradeoff is an exponentially decreasing lifetime due to thermal evaporation of the cathode material.

Field emission sources typically consist of a tungsten needle sharpened to a point, with a radius less than 1 um. The sharp tip helps provide the extremely high electric fields needed to pull electrons out of

the metal. Although cold field emission sources have become common in electron microscopes, they have seen little use in EBL due to their instability with regard to short term noise as well as long term drift, which is a much more serious problem for lithography than microscopy. The noise is caused by atoms that adsorb onto the surface of the tip, affecting its work function and thus causing large changes in the emission current. Heating the tip momentarily (flashing) can clean it, but new atoms and molecules quickly readsorb even in the best of vacuums. In addition, atoms may be ionized by the electron beam and subsequently accelerated back into the tip, causing physical sputtering of the tip itself. To minimize the current fluctuations, the electron source must be operated in an extreme ultra high vacuum environment, 10^{-10} Torr or better.

TABLE 2.1 Properties of the electron sources commonly used in electron beam lithography tools.

source type	brightness ($A/cm^2/sr$)	source size	energy spread (eV)	vacuum requirement (Torr)
tungsten thermionic	~10^5	25 um	2-3	10^{-6}
LaB_6	~10^6	10 um	2-3	10^{-8}
thermal (Schottky) field emitter	~10^8	20 nm	0.9	10^{-9}
cold field emitter	~10^9	5 nm	0.22	10^{-10}

A technology that is now available to EBL (as well as in many electron microscopes) is the thermal field emission source. It combines the sharp tungsten needle of the field emission source and the heating of the thermal source. Because the tip operates at a temperature of about 1800 K, it is less sensitive to gases in the environment and can achieve stable operation for months at a time. Although thermal field emitter is the common name, it is more properly called a Schottky emitter since the electrons escape over the work function barrier by thermal excitation. It features a brightness almost as high as the cold field emission sources, a very small virtual source size, and a moderate energy spread. The tungsten is usually coated with a layer of zirconium oxide to reduce the work function barrier. A heated reservoir of zirconium oxide in the electron gun continuously replenishes material evaporated from the tip. It requires a vacuum in the range of 10^{-9} Torr, which, although much better than required for the thermionic sources, is readily achievable with modern vacuum technology. (A light bakeout might be required to remove water vapor after the system has been vented.) LaB_6 sources are still preferred for shaped beam systems since the total current provided by the thermal field emission source is inadequate for this application.

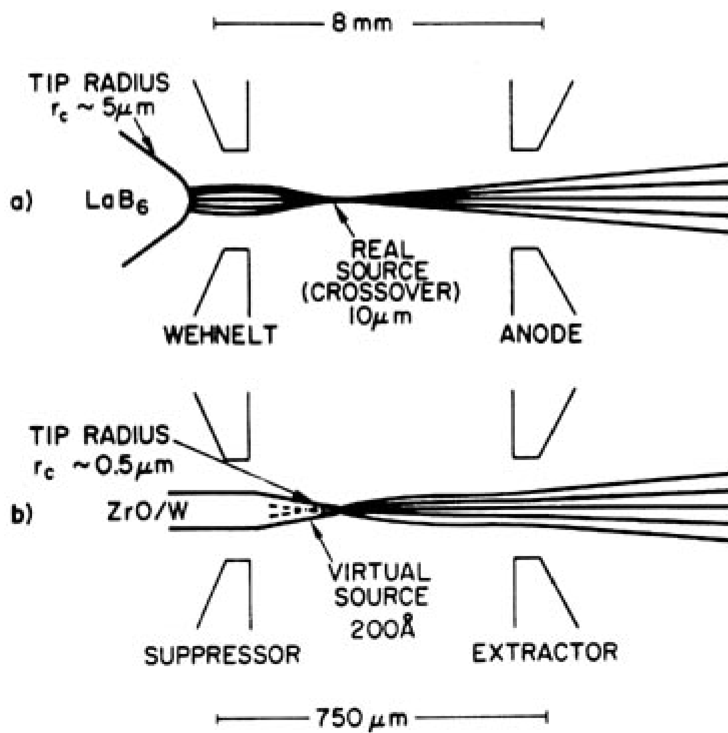

FIGURE 2.5. Electrode structure and relevant dimensions for a) LaB_6 gun and b) thermal field emission gun. The electrodes are circularly symmetric about the optical axis. The Wehnelt and suppressor are biased negative with respect to the cathode, while the anode and extractor are positively biased. [From Gesley, [17] 1989]

2.2.3 Electron Lenses

Electrons can be focused either by electrostatic forces or magnetic forces. Although electron lenses in principle behave the same as optical lenses, there are differences. Except in some special cases, electron lenses can be made only to converge, not diverge. Also, the quality of electron lenses is not nearly as good as optical lenses in terms of aberrations. The relatively poor quality of electron lenses restricts the field size and convergence angle (or numerical aperture) that can be used. The two types of aberrations critical to EBL are spherical aberrations, where the outer zones of the lens focus more strongly than the inner zones, and chromatic aberrations, where electrons of slightly different energies get focused at different image planes. Both types of aberrations can be minimized by reducing the convergence angle of the system so that electrons are confined to the center of the lenses, at the cost of greatly reduced beam current.

A magnetic lens is formed from two circularly symmetric iron (or some other high permeability material) polepieces with a copper winding in-between. Fig. 2.6 shows a cross-section through a typical magnetic lens, along with some magnetic flux lines.

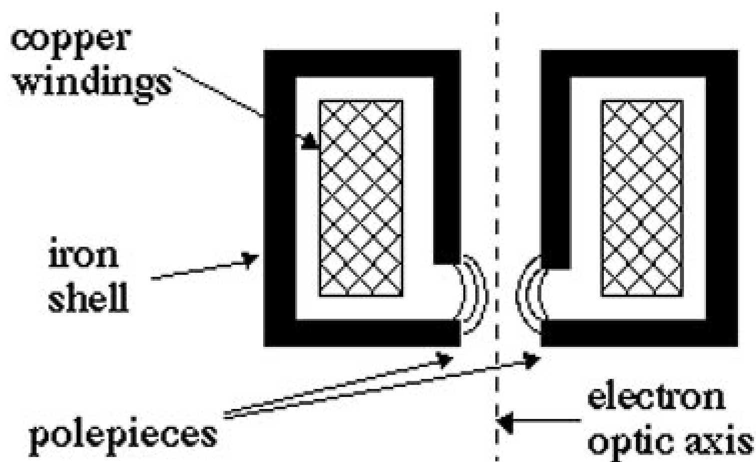

FIGURE 2.6. Cross-section through a magnetic lens with lines showing the magnetic field distribution.

The divergence of the magnetic flux along the optical axis imparts a force on electrons back towards the optical (Z) axis, resulting in focusing action. The magnetic field also causes a rotation of the electrons (and the image) about the Z axis in a corkscrew fashion. Although this does not affect the performance of the lens, it does impact the design, alignment, and operation of the system. For instance, the deflection system must be rotated physically with respect to the stage coordinates. Also, when aligning a column, X and Y displacement in the upper regions of the column will not correspond to the same X and Y displacement at the target. Finally, changes in focus or changes in the height of the sample can cause a slight rotation in the deflection coordinates. This must be properly corrected or stitching and overlay errors will result. Magnetic lenses, particularly the final lens, may be liquid-cooled to maintain a controlled temperature, which is critical for stable operation of a system.

Electrostatic lenses have worse aberrations than magnetic lenses, so they are not as commonly used. They are most often found in the gun region as a condenser lens since they can be combined with the extractor or anode used to pull electrons out of the cathode, and they are easily made for ultrahigh vacuum use and are bakeout compatible. Also, aberrations in the condenser lens tend to be less important; system performance is usually dominated by the aberrations of the final lens. A simple electrostatic lens, as shown in Fig, 2.7, consists of three consecutive elements like apertures, the outer two being at ground potential and the inner at some other (variable) potential that controls the lens strength. The electric potentials set up by such a lens tend to pull an electron that is traveling away from the optical axis back towards the axis, resulting in the focusing action.

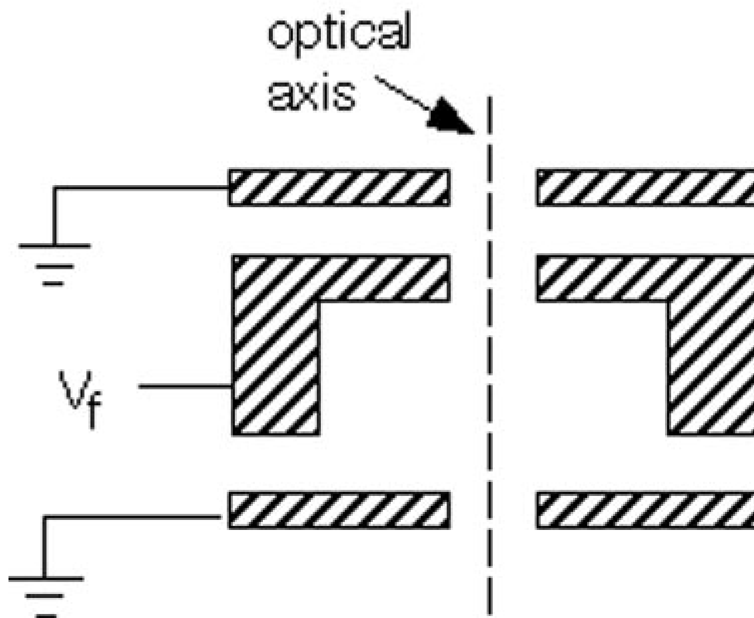

FIGURE 2.7. Cross-section through an electrostatic Einzel lens. The focus of the lens is controlled by the voltage applied to the center electrode.

2.2.4 Other electron optical elements

Other optical elements include apertures, deflection systems, alignment coils, blanking plates, and stigmators.

2.2.4.1 Apertures

Apertures are small holes through which the beam passes on its way down the column. There are several types of apertures. A spray aperture may be used to stop any stray electrons without materially affecting the beam itself. A blanking aperture is used to turn the beam on and off; by deflecting the beam away from the aperture hole, the aperture intercepts the beam when not writing. A beam limiting aperture has two effects: it sets the beam convergence angle [[alpha]] (measured as the half-angle of the beam at the target) through which electrons can pass through the system, controlling the effect of lens aberrations and thus resolution, and also sets the beam current. A beam limiting aperture is normally set in an X-Y stage to allow it to be centered, or aligned, with respect to the optical axis. It is best to have a beam limiting aperture as close to the gun as possible to limit the effects of space charge caused by electron - electron repulsion.

Apertures may be heated to help prevent the formation of contamination deposits, which can degrade the resolution of the system. If not heated, the apertures typically need to be cleaned or replaced every few months. With platinum apertures, cleaning is easily accomplished by heating the aperture orange hot in a clean-burning flame. Shaped beam systems also have one or more shaping apertures, which can be square or have more complicated shapes to allow the formation of a variety of beam shapes, such as triangles, etc.

2.2.4.2 Electron beam deflection

Deflection of the electron beam is used to scan the beam across the surface of the sample. As with lenses, it can be done either magnetically or electrostatically. The coils or plates are arranged so that the fields are perpendicular to the optical axis, as shown in Fig. 2.8(a). Deflecting the beam off axis introduces additional aberrations that cause the beam diameter to deteriorate, and deviations from linearity in X and Y increase as the amount of deflection increases. These effects limit the maximum field or deflection size that can be used. As with lenses, magnetic deflection introduces fewer distortions than electrostatic deflection. Double magnetic deflection using a pair of matched coils is sometimes used to further reduce deflection aberrations. However, electrostatic deflection can achieve

much higher speeds since the inductance of the magnetic deflection coils limits their frequency response, and eddy currents introduced by the magnetic fields may further limit the speed of magnetic deflection. Since deflection systems are frequently placed inside the final lens, care must be taken to prevent the fields from interacting with conducting metal parts. Usually the final lens will be shielded with ferrite to minimize eddy currents. Some tools use multiple deflection systems, where high speed, short range deflection is done electrostatically while long range deflection is magnetic. In either case, the field size of the tool is limited by aberrations of the deflection system; some tools introduce dynamic corrections to the deflection, focus, and stigmators in order to increase the maximum field size, at the cost of additional complexity.

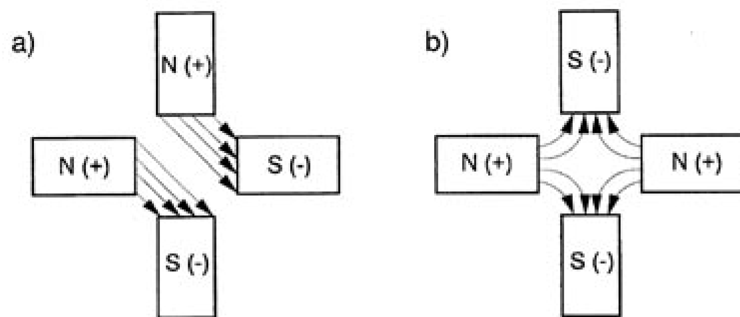

FIGURE 2.8. Schematic showing the magnetic (electrostatic) field distribution for a) a simple beam deflector or alignment device energized for diagonal deflection and b) a stigmator. The optical axis is perpendicular to the plane of the page.

2.2.4.3 Beam blanking

Blanking, or turning the beam on and off, is usually accomplished with a pair of plates set up as a simple electrostatic deflector. One or both of the plates are connected to a blanking amplifier with a fast response time. To turn the beam off, a voltage is applied across the plates which sweeps the beam off axis until it is intercepted by a downstream aperture. If possible, the blanking is arranged to be conjugate so that, to first order, the beam at the target does not move while the blanking plates are activated. Otherwise, the beam would leave streaks in the resist as it was blanked. The simplest way to ensure conjugate blanking is to arrange the column so that the blanking plates are centered at an intermediate focal point, or crossover. In very high speed systems, more elaborate blanking systems involving multiple sets of plates and delay lines may be required to prevent beam motion during the blanking and unblanking processes. [14]

2.2.4.4 Stigmators

A stigmator is a special type of lens used to compensate for imperfections in the construction and alignment of the EBL column. These imperfections can result in astigmatism, where the beam focuses in different directions at different lens settings; the shape of a nominally round beam becomes oblong, with the direction of the principal axis dependent on the focus setting, resulting in smeared images in the resist. The stigmator cancels out the effect of astigmatism, forcing the beam back into its optimum shape. Stigmators may be either electrostatic or magnetic and consist of four or more poles (eight is typical) arranged around the optical axis. They can be made by changing the connections to a deflector, as shown in Fig. 2.8(b). With proper mixing of the electrical signals, a single deflector may sometimes perform multiple functions, including beam deflection, stigmation, alignment, and blanking.

2.2.5 Other column components

A number of other components may be found in the column, which although not important to the electron optics are nonetheless critical to the operation of the system. A Faraday cage located below the final beam limiting aperture is used to measure the beam current in order to ensure the correct dose for resist exposure. It can be either incorporated directly on the stage or a separate movable assembly in the column. The column will also typically have an isolation valve that allows the chamber to be vented for maintenance while the gun is still under vacuum and operational. All parts of an

electron beam column exposed to the beam must be conductive or charging will cause unwanted displacements of the beam. Often a conductive liner tube will be placed in parts of the column to shield the beam from insulating components.

Finally, the system needs a method of detecting the electrons for focusing, deflection calibration, and alignment mark detection. Usually this is a silicon solid state detector similar to a solar cell, mounted on the end of the objective lens just above the sample. Channel plate detectors and scintillators with photomultiplier tubes may also be used. Unlike scanning electron microscopes, which image with low voltage secondary electrons, EBL systems normally detect high energy backscattered electrons since these electrons can more easily penetrate the resist film. The signal from low energy secondary electrons may be obscured by the resist.

2.2.6 Resolution

There are several factors that determine the resolution of an electron beam system. First is the virtual source size d_v divided by the demagnification of the column, M^{-1}, resulting in a beam diameter of $d_g = d_v / M^{-1}$. In systems with a zoom condenser lens arrangement, the demagnification of the source can be varied, but increasing the demagnification also reduces the available beam current.

If the optics of the column were otherwise ideal, this simple geometry would determine the beam diameter. Unfortunately, lenses are far from perfect. Spherical aberrations result from the tendency of the outer zones of the lenses to focus more strongly than the center of the lens. The resultant diameter is $d_s = 1/2 C_s a^3$, where C_s is the spherical aberration coefficient of the final lens and a is the convergence half-angle of the beam at the target. Using an aperture to limit the convergence angle thus reduces this effect, at the expense of reduced beam current. Chromatic aberrations result from lower energy electrons being focused more strongly than higher energy electrons. For a chromatically limited beam, the diameter is $d_c = C_c a \, \mathrm{D}V / V_b$, where C_c is the chromatic aberration coefficient, DV is the energy spread of the electrons, and V_b is the beam voltage.

Finally, quantum mechanics gives the electron a wavelength $L = 1.2/(V_b)^{1/2}$ nm; although much smaller than the wavelength of light (0.008 nm at 25 kV), this wavelength can still limit the beam diameter by classical diffraction effects in very high resolution systems. For a diffraction limited beam, the diameter is given by $d_d = 0.6 \, L / a$. To determine the theoretical beam size of a system, the contributions from various sources can be added in quadrature: $d = (d_g^2 + d_s^2 + d_c^2 + d_d^2)^{1/2}$.

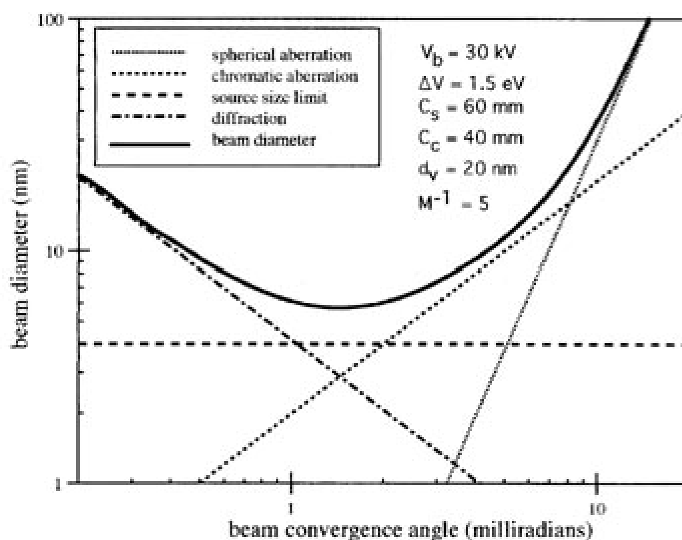

FIGURE 2.9. A plot showing resolution as a function of beam convergence angle for an electron beam column at 30 kV. The plot assumes an energy spread of 1.5 eV, a source diameter of 20 nm, and a fixed demagnification of 5.

The diagram in Fig. 2.9 shows how these sources contribute in a typical column. In systems with thermionic sources, spherical aberrations tend to be the limiting factor for beam diameter, while chromatic aberrations dominate in field emission systems. For a given beam current, there will be an optimum combination of convergence angle and system demagnification. Resolution can generally be improved in most systems by using a smaller beam limiting aperture, at the expense of reduced beam current and throughput. In systems where the demagnification can be varied, increasing the demagnification will also improve resolution, at the expense of reduced beam current.

2.3 Electron-solid interactions

Although electron beam lithography tools are capable of forming extremely fine probes, things become more complex when the electrons hit the workpiece. As the electrons penetrate the resist, they experience many small angle scattering events (forward scattering), which tend to broaden the initial beam diameter. As the electrons penetrate through the resist into the substrate, they occasionally undergo large angle scattering events (backscattering). The backscattered electrons cause the proximity effect, [18] where the dose that a pattern feature receives is affected by electrons scattering from other features nearby. During this process the electrons are continuously slowing down, producing a cascade of low voltage electrons called secondary electrons.

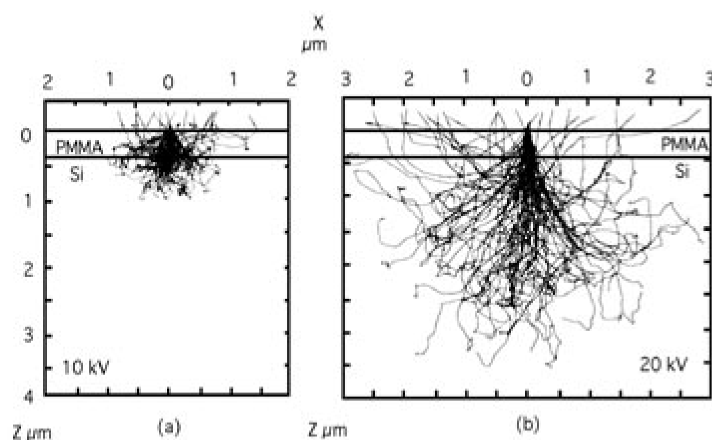

FIGURE 2.10. Monte Carlo simulation of electron scattering in resist on a silicon substrate at a) 10 kV and b) 20 kV. [From Kyser and Viswanathan [19] 1975]

Figure 2.10 shows some computer simulations of electron scattering in typical samples. [19] The combination of forward and backscattered electrons results in an energy deposition profile in the resist that is typically modeled as a sum of two Gaussian distributions, where *a* is the width of the forward scattering distribution, *b* is the width of the backscattering distribution, and e_e is the intensity of the backscattered energy relative to the forward scattered energy. Fig. 2.11 shows an example of a simulated energy profile.

2.3.1 Forward Scattering

As the electrons penetrate the resist, some fraction of them will undergo small angle scattering events, which can result in a significantly broader beam profile at the bottom of the resist than at the fxtop. The increase in effective beam diameter in nanometers due to forward scattering is given empirically by the formula $d_f = 0.9\ (R_t / V_b)^{1.5}$, where R_t is the resist thickness in nanometers and V_b is the beam voltage in kilovolts. Forward scattering is minimized by using the thinnest possible resist and the highest available accelerating voltage.

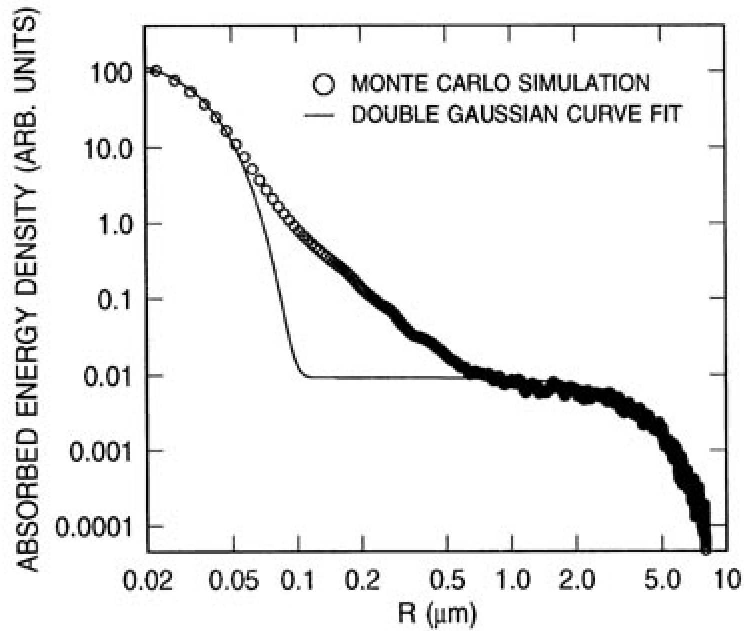

FIGURE 2.11. Simulated profile of the energy absorbed from an electron beam exposure.

Although it is generally best to avoid forward scattering effects when possible, in some instances they may be used to advantage. For example, it may be possible to tailor the resist sidewall angle in thick resist by adjusting the development time. [20] As the time increases, the resist sidewall profile will go from a positive slope, to vertical, and eventually to a negative, or retrograde, profile, which is especially desirable for pattern transfer by liftoff.

2.3.2 Backscattering

As the electrons continue to penetrate through the resist into the substrate, many of them will experience large angle scattering events. These electrons may return back through the resist at a significant distance from the incident beam, causing additional resist exposure. This is called the electron beam proximity effect. The range of the electrons (defined here as the distance a typical electron travels in the bulk material before losing all its energy) depends on both the energy of the primary electrons and the type of substrate. Fig. 2.12 shows a plot of electron range as a function of energy for three common materials. [21]

The fraction of electrons that are backscattered, *e*, is roughly independent of beam energy, although it does depend on the substrate material, with low atomic number materials giving less backscatter. Typical values of *e* range from 0.17 for silicon to 0.50 for tungsten and gold. Experimentally, *e* is only loosely related to e_e, the backscatter energy deposited in the resist as modeled by a double Gaussian. Values for e_e tend to be about twice *e*.

2.3.3 Secondary Electrons

As the primary electrons slow down, much of their energy is dissipated in the form of secondary electrons with energies from 2 to 50 eV. They are responsible for the bulk of the actual resist exposure process. Since their range in resist is only a few nanometers, they contribute little to the proximity effect. Instead, the net result can be considered to be an effective widening of the beam diameter by roughly 10 nm. This largely accounts for the minimum practical resolution of 20 nm observed in the highest resolution electron beam systems and contributes (along with forward scattering) to the bias that is seen in positive resist systems, where the exposed features develop larger than the size they were nominally written.

A small fraction of secondary electrons may have significant energies, on the order of 1 keV. These so-called fast secondaries can contribute to the proximity effect in the range of a few tenths of a

micron. Experimentally and theoretically, the distribution of these electrons can be fit well by a third Gaussian with a range intermediate between the forward scattering distribution and the backscattering distribution.

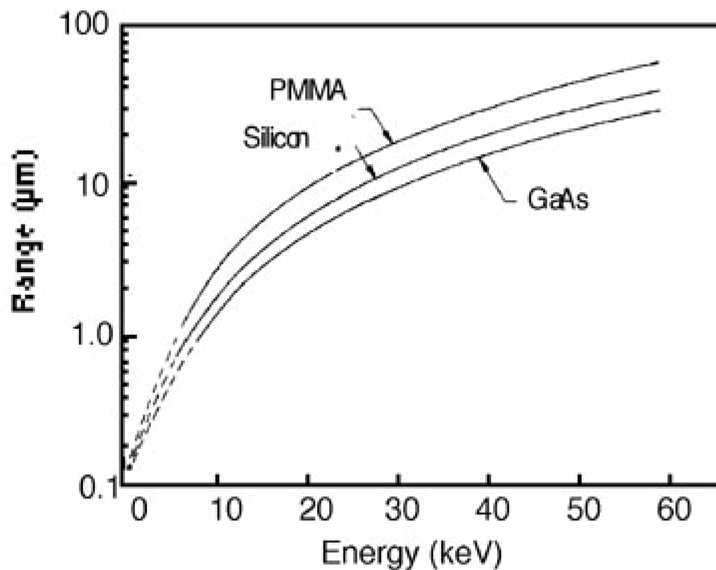

FIGURE 2.12. Electron range as a function of beam energy for PMMA resist, silicon, and gallium arsenide. [From Brewer, 1980]

2.3.4 Modeling

Electron scattering in resists and substrates can be modeled with reasonable accuracy by assuming that the electrons continuously slow, down as described by the Bethe equation, [22] while undergoing elastic scattering, as described by the screened Rutherford formula. [23] Since the different materials and geometries make analytic solutions difficult, Monte Carlo techniques, where a large number of random electrons are simulated, are commonly used. The input to the program contains such parameters as the electron energy, beam diameter, and film thicknesses and densities, while the output is a plot of energy deposited in the resist as a function of the distance from the center of the beam.

Curve fitting with Gaussians and other functions to the simulated energy distribution may also be employed. In order to get good statistics, the energy deposition for a large number (10,000 to 100,000) of electrons must be simulated, which can take a few minutes to an hour or so on a personal computer. Software for Monte Carlo simulation of electron irradiation is available from several sources. [24-27] Such simulations are often used to generate input parameters for proximity effect correction programs (see next section). Alternatively, experimental data can be obtained by measuring the diameter of exposed resist from a point exposure of the beam at various doses [28] or by measuring the linewidths of various types of test patterns such as the "tower" pattern. [29]

2.4 Proximity effect

2.4.1 Introduction

The net result of the electron scattering discussed in the previous section is that the dose delivered by the electron beam tool is not confined to the shapes that the tool writes, resulting in pattern specific linewidth variations known as the proximity effect. For example, a narrow line between two large exposed areas may receive so many scattered electrons that it can actually develop away (in positive resist) while a small isolated feature may lose so much of its dose due to scattering that it develops incompletely. Fig. 2.13 shows an example of what happens to a test pattern when proximity effects are not corrected. [30]

2.4.2 Proximity Effect Avoidance

Many different schemes have been devised to minimize the proximity effect. If a pattern has fairly uniform density and linewidth, all that may be required is to adjust the overall dose until the patterns come out the proper size. This method typically works well for isolated transistor gate structures. Using higher contrast resists can help minimize the linewidth variations. Multilevel resists, in which a thin top layer is sensitive to electrons and the pattern developed in it is transferred by dry etching into a thicker underlying layer, reduce the forward scattering effect, at the cost of an increase in process complexity.

Higher beam voltages, from 50 kV to 100 kV or more, also minimize forward scattering, although in some cases this can increase the backscattering. When writing on very thin membranes such as used for x-ray masks, higher voltages reduce the backscatter contribution as well since the majority of electrons pass completely through the membrane. [31]

Conversely, by going to very low beam energies, where the electron range is smaller than the minimum feature size, the proximity effect can be eliminated. [32] The penalty is that the thickness of a single layer resist must also be less than the minimum feature size so that the electrons can expose the entire film thickness. The electron-optical design is much harder for low voltage systems since the electrons are more difficult to focus into a small spot and are more sensitive to stray electrostatic and magnetic fields. However, this is the current approach in optical maskmaking, where a 10 kV beam is used to expose 0.3 um thick resist with 1 um minimum features on a 5 mask. In more advanced studies, a 1.5 kV beam has been used to expose 70 nm thick resist with 0.15 um minimum features. [33] A technique that can be used in conjunction with this approach in order to increase the usable range of electron energy is to place a layer with a high atomic number, such as tungsten, underneath the resist. This has the effect of further limiting the range of the backscattered electrons.

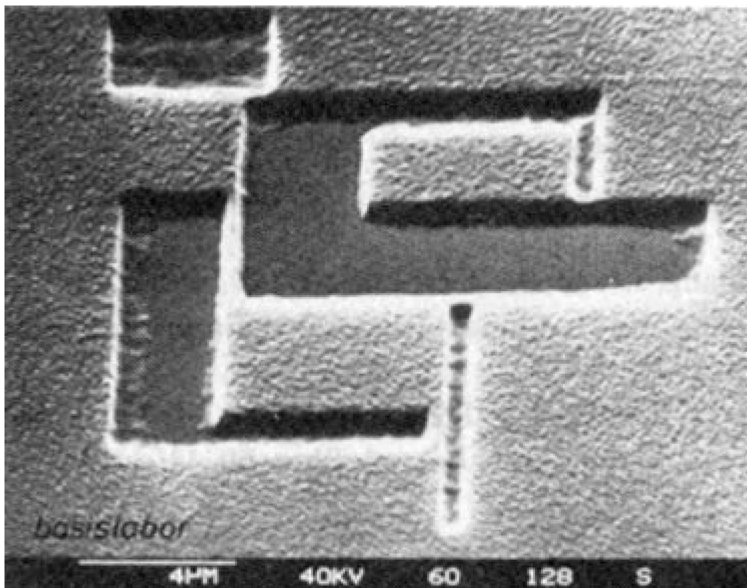

FIGURE 2.13. SEM micrograph of a positive resist pattern on silicon exposed with a 20 kV electron beam demonstrates the proximity effect, where small isolated exposed areas receive less dose relative to larger or more densely exposed areas. [From Kratschmer, [30] 1981]

2.4.3 Proximity Effect Correction

2.4.3.1 Dose modulation

The most common technique of proximity correction is dose modulation, where each individual shape in the pattern is assigned a dose such that (in theory) the shape prints at its correct size. The calculations needed to solve the shape-to-shape interactions are computationally very time consuming. Although the actual effect of electron scattering is to increase the dose received by large areas, for practical reasons proximity correction is normally thought of in terms of the large areas receiving a base dose of unity, with the smaller and/or isolated features receiving a larger dose to compensate.

Several different algorithms have been used. In the self-consistent technique, the effect of each shape on all other shapes within the scattering range of the electrons is calculated. The solution can be found by solving a large number of simultaneous equations; [34] unfortunately, this approach becomes unwieldy as the number of shapes increases and their size decreases. An alternative is to define a grid and compute the interaction of the pattern shapes with the grid and vice versa; [35] however, the accuracy and flexibility of this technique may be limited. An optimal solution may also be arrived at by an iterative approach. [36] Finally, neural network techniques have been applied to the problem of proximity correction; [37] while not an attractive technique when implemented on a digital computer, it might be advantageous if specialized neural network processors become a commercial reality. Many of the algorithms in use assume that the energy distribution has a double Gaussian distribution as discussed in Sec. 2.3.

2.4.3.2 Pattern biasing

A computationally similar approach to dose modulation is pattern biasing. [38-39] In this approach, the extra dose that dense patterns receive is compensated for by slightly reducing their size. This technique has the advantage that it can be implemented on EBL systems that are not capable of dose modulation. However, the technique does not have the dynamic range that dose modulation has; patterns that contain both very isolated features and very dense features will have reduced process latitude compared to when dose modulation is used, since the isolated features will be under-dosed while the dense features will be overdosed. Pattern biasing cannot be applied to features with dimensions close to the scale of the pixel spacing of the e-beam system.

2.4.3.3 GHOST

A third technique for proximity correction, GHOST,[40] has the advantage of not requiring any computation at all. The inverse tone of the pattern is written with a defocused beam designed to mimic the shape of the backscatter distribution (Fig. 2.14). The dose of the GHOST pattern, $e_e / (1 + e_e)$, is also set to match the large area backscatter dose. After the defocussed inverse image is written, the pattern will have a roughly uniform background dose. GHOST is perhaps an underutilized technique; under ideal conditions it can give superb linewidth control. [41] Its disadvantages are the extra data preparation and writing time, a slight to moderate loss of contrast in the resist image, and a slight loss in minimum resolution compared to dose modulation due to the fact that GHOST does not properly correct for forward scattering.

2.4.3.4 Software

A number of companies for some time have had proprietary software for proximity correction. [25] [42-43] Just recently, commercial proximity packages have become available, or are about to become available. [44-45] At present, these are limited in their accuracy, speed, and data volume capability; while excellent for correcting small research patterns, they may have difficulties with complex chips. Finally, several packages have been developed at university and government laboratories, some of which might be available to an adventurous user with excessive amounts of free time. [38] [46]

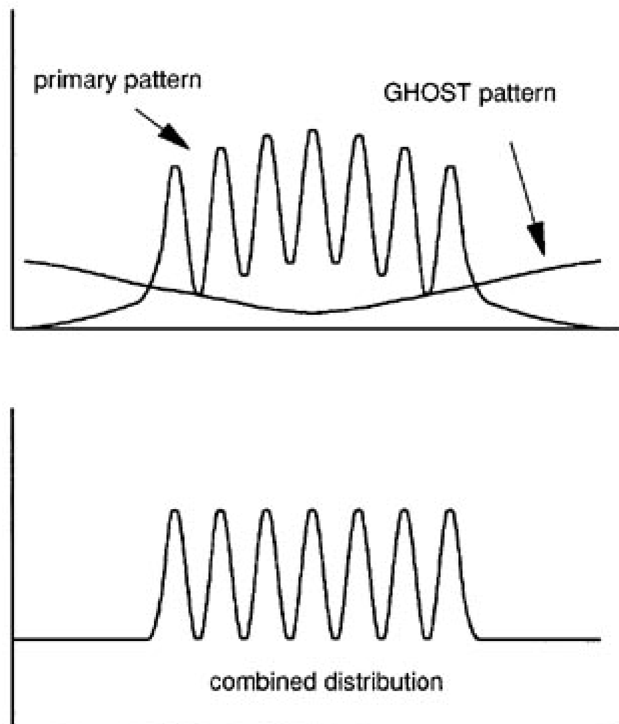

FIGURE 2.14. Schematic showing how the GHOST technique can be used to correct for the proximity effect. The top curves show the energy distribution in the resist for a group of seven lines from the primary exposure and from the GHOST exposure. The bottom curve is the resulting final energy distribution, showing the dose equalization for all the lines.

Section 2.5 Systems

2.5.1 Environment

For best results, systems should be installed in a clean, quiet environment. 60 Hz noise is pervasive in most systems. To minimize this, careful consideration must be paid to the grounding of the system components to prevent ground loops. Also, analog and digital grounds should be kept separate as much as possible to minimize high frequency noise components. One useful method for tracking noise problems is to place the beam on the edge of a mark and monitor the electron detector output with a spectrum analyzer while disconnecting various suspect noise sources.

Acoustical noise can be a significant problem, especially in systems with field-emission electron sources. In such systems the demagnification of the field emission source, and thus the demagnification of vibrations, is much less than that of LaB_6 systems. Stray magnetic fields are also a common problem. Mechanical pumps, transformers, and fluorescent lights should be moved at least 10 ft from the column if possible. The system should be well isolated from mechanical vibrations with a pneumatic table; ideally, it should also be located on the ground floor. Finally, the temperature should be well controlled, ideally to within a tenth of a degree. This is particularly important if good placement accuracy is required.

This section begins with a description of the smallest e-beam systems - namely, SEM conversions - and proceeds to the largest commercial mask production tools. We conclude the section with a listing of e-beam fabrication services.

2.5.2 SEM and STEM Conversions

Any tool for microscopy - optical, electron, or scanning probe - may be adapted to work in reverse; that is, for writing instead of reading. Converted electron microscopes suffer the same limitations as light microscopes used for photolithography, namely, a small field of view and low throughput. Nevertheless, for a subset of research and R&D applications, converted SEMs offer a relatively inexpensive solution.

Of the many custom designed SEM conversions, most use a single set of digital-to-analog converters (DACs), from 12 to 16 bits wide, to drive the scan coils of the microscope. The beam is modulated with an electrostatic or magnetic beam blanker, which is usually located near a crossover of the beam. Alternatively, the beam can be blanked magnetically by biasing the gun alignment coils or not blanked at all. In the later case, the beam must be "dumped" to unused sections of the pattern. Figure 2.15 illustrates the "vector scan" method, in which shapes are filled with a raster pattern and the beam jumps from one shape to the next via a direct vector. By taking over the scan coils and beam blanking, a SEM can be used as a simple but high resolution lithography tool.

SEM conversions have evolved greatly in the past twenty years, primarily due to improvements in small computers and commercially available DAC boards. Early designs used relatively slow computers that sent primitive shapes (rectangles, trapezoids, and lines) to custom hardware. The custom pattern generator filled in the shapes by calculating coordinates inside the shapes and feeding these numbers to the DACs. While this approach is still the best way to avoid data transmission bottlenecks (and is used in commercial systems), inexpensive SEM conversions can now rely on the CPU to generate the shape filling data. A typical configuration uses an Intel CPU based PC, with a DAC card plugged into an ISA bus. In this case, the CPU can generate data much faster than it can be transmitted over an ISA bus.

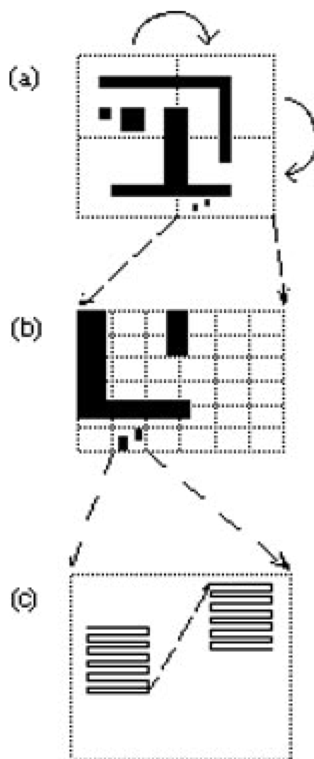

FIGURE 2.15 The vector-scan writing strategy. (a) Patterns are split into "fields". The stage moves from field to field, as shown by the arrows. Full patterns are stitched together from multiple fields. (b) In many vector-scan systems the fields are further tiled into subfields. A major DAC (16 bits) deflects the beam (a small "Gaussian" spot) to a subfield boundary, and a faster DAC (12 bits) deflects the beam within a subfield. SEM conversion kits typically do not include the faster 12-bit DAC. (c) The primitive shape is filled in by rastering the spot. Between shapes the beam is turned off ("blanked") and is deflected in a direct vector to the next shape. An alternative deflection strategy (not shown) is to use the major DAC to deflect the beam to the origin of each primitive shape

The bus limits the deflection speed to around 100 kHz, that is, to a dwell time per point of 10 us.

What dwell time is required? With a 16-bit DAC and a SEM viewing field of 100 um, the size of a pixel (the smallest logically addressable element of an exposure field) is 100 um/2^{16}=1.5 nm, and its area A is the square of this. The charge delivered to this pixel in a time t is It, where I is the beam current. This must equal the dose

times the pixel area. Given a beam current I on the order of 50 pA and a required dose D around 200 uC/cm^2 (typical for PMMA), we have a pixel dwell time

$$t = DA / I = 910^{-8} \text{ s}, (2.1)$$

or a deflection speed of 11 MHz. This being impossible with an ISA bus, we must either space out the exposure points, apply a short strobe to the beam blanker, or use a combination of the two. When the exposure points are spaced every *n* pixels (that is, when the 2^{16} available exposure points are reduced by a factor of *n*) then the "pixel area" and thus the dwell time is increased by a factor of n^2. Note that the *placement* of features can still be specified to a precision of 2^{16} within the writing field, while the shapes are filled in with a more coarse grid.

In the above example, we can set *n* to 11 so that the dwell time is increased to 1.110^{-5} s (91 kHz), increasing the pitch of exposure points to 16.5 nm. This spacing is a good match to the resolution of PMMA, and allows fine lines to be defined without any bumps due to pixelization. However, when we require 100 times the current (5000 pA in this example), the exposure point spacing must be increased by a factor of 10, possibly leading to rough edges. Some pattern generators (see Sect. 2.5.3.1) avoid this problem by allowing different exposure point spacings in the X and Y (or in the r and *theta*) directions, thereby allowing a larger exposure point spacing in the less critical dimension.

To use a SEM *without* a beam blanker, one must consider the large exposure point spacing required for common resists. Lack of a beam blanker leads to the additional problem of artifacts from the settling of scan coils and exposure at beam dump sites. Many SEM manufacturers offer factory-installed beam blankers. Retrofitted blankers are also sold by Raith GmbH. [47]

The scan coils of a SEM are designed for imaging in a raster pattern and so are not commonly optimized for the random placements of a vector scan pattern generator. Settling times are typically around 10 us for a JEOL 840 to as long as 1 ms for the Hitachi S800, where the bandwidth of the scan coils has been purposely limited to reduce noise in the imaging system. Thus, it is important to consider the bandwidth of the deflection system when purchasing a SEM for beamwriting.

The other major limitation of a SEM is its stage. Being designed for flexible imaging applications, SEM stages are not flat, and even when equipped with stepper motor control are no more accurate than ~1 to 5 um. Periodic alignment marks can be used to stitch fields accurately, but this requires extra processing as well as the use of photolithography for printing alignment marks. The mark mask would presumably be fabricated on a commercial system with a laser-controlled stage. Fortunately, alignment with a converted SEM can be quite accurate, especially when using Moiré patterns for manual alignment. Automated alignment in the center of a SEM writing field is at least as good as in large commercial systems. Alignment at the edges of a SEM field will be compromised by distortions, which are typically much larger than in dedicated e-beam systems. Laser-controlled stages can be purchased for SEMs, but these are usually beyond the budgets of small research groups.

Electron beam lithography requires a flat sample close to the objective lens, making secondary electron imaging difficult with an ordinary Everhart-Thornley detector (a scintillator-photomultiplier in the chamber). A few high end SEMs are equipped with a detector above the objective lens or can be equipped with a microchannel plate on the pole-piece. These types of detectors are a great advantage for lithography since they allow the operator to decrease the working distance, and thus the spot size, while keeping the sample flat and in focus.

With patterning speed limited by beam settling and bus speed, it is clear that inexpensive SEM conversions cannot match the high speed writing of dedicated e-beam systems. However, a SEM based lithography system can provide adequate results for a wide variety of applications, at a small fraction of the cost of a dedicated system. The number of applications is limited by stitching, alignment, and automation. Practical applications include small numbers of quantum devices (metal lines, junctions, SQUIDs, split gates), small numbers of transistors, small area gratings, small masks, tests of resists, and direct deposition. The main limitations with SEM lithography are observed with writing over large areas, or when deflection speed and throughput are critical. Specifically, difficulties with stitching and/or distortions due to the electron optics of the microscope can become significant. SEMs are not practical for most mask making, integration of many devices over many fields, large area gratings, multifield optical devices, or any application requiring a large substrate.

2.5.3.1 Nanometer Pattern Generation System (NPGS)

The SEM conversion kit sold by J.C. Nabity Lithography Systems [48] is built around a Windows-based PC-compatible with an ISA bus. A 16 bit multifunction board from Data Translation [49] is used to generate the X and Y beam deflections and to program a second board which provides the signals for blanking control. The beam is deflected from shape to shape in a writing field ("vector scan" mode), with the unique feature that the raster for filling arbitrary polygons can be defined by the user. Arbitrary polygons can be designed with up to 200 vertices and the user can specify the raster to be parallel to any side of the polygon. A unique feature of the NPGS is that the user has control over the exposure spot spacing in X and Y, allowing the critical dimension (e.g. perpendicular to grating lines) to be filled with greater accuracy (see Sect. 2.5.2). Circles and circular arcs are swept using a "polar coordinate" approach, with user control of the exposure spot spacing in *r* and . As with any ISA system, the data throughput is limited to around 100 kHz; and like most pattern generators, exposure points filling the features can be spaced by multiples of the DAC resolution (2^{16}) while still allowing full resolution for feature placement.

To provide for lower doses at reasonable currents, the Nabity system strobes the blanker at each exposure point. [50] For systems without a beam blanker, the Nabity Pattern Generation System (NPGS) can be programmed to "dump" the beam at user-defined locations within the writing field; however, this imposes significant limitations on the exposure spot spacing or on the lowest deliverable dose for a given beam current (refer to discussion above).

Mark alignment on the NPGS is performed by calculating the correlation between the measured mark image and the user-defined mark pattern. Signal processing such as averaging and edge enhancement can be executed before the alignment correlation, allowing the use of low contrast or rough marks. If the user supplies precisely defined marks (usually printed with a mask made on a commercial maskmaking tool) then NPGS can be used to correct for global rotation, scaling, and nonorthogonality. NPGS can control motorized stages, providing fully automated sample movement and pattern alignment. However, SEM stages are typically orders of magnitude slower than those of dedicated e-beam tools, and do not provide feedback to the deflection system (see Sect. 2.5.4).

Angled lines, polygons, and arbitrarily shaped features are all supported, and data can be imported in common e-beam formats: GDSII (Stream), CIF, and a subset of DXF (AutoCAD.)

2.5.3.2 Raith pattern generators

The Proxy-Writer SEM conversion kit is Raith's low end PC-based pattern generator. Like the Nabity system, the Proxy-Writer is a vector-scan system. Unlike the Nabity NPGS, the Proxy-Writer has only manual alignment, and patterns are limited to single writing fields. Corrections for rotation, shift, and orthogonality are applied to single fields (with single patterns); these corrections are not applied globally to correct the workpiece rotation and stage nonorthogonality. The unusual feature of this simple system is its support for exposure simulation and semiautomatic proximity effect correction. Pattern data can be generated with the simple CAD program included or imported from a DXF (AutoCAD) file.

The higher end Raith system, known as Elphy-Plus, supports the full range of e-beam operations, including control of a laser-controlled stage and corrections for workpiece rotation, gain, and orthogonality. The laser stage, also manufactured by Raith, allows field stitching to better than 0.1 m. While the primary control is still a PC-compatible computer, the limitations of the ISA bus are circumvented by using a separate computer and integrated DAC as the pattern generator. In this way, the PC transmits only the coordinates of the corners of a shape, and the patterning hardware generates all of the internal points for exposure. Data throughput is thereby increased to 2.6 MHz (0.4 s/point minimum); however, many SEM deflection systems will be limited to less than 1 MHz due to the inductance of the coils and low pass filters in the imaging system. The Elphy-Plus system supports fully automated mark detection and field stitching. All standard e-beam data formats are supported.

Useful features of the Raith Elphy-Plus system include support of data representation in polar coordinates (greatly reducing the data required to represent circles), bit-mapped pattern exposure, and a "path writing" mode. In the path writing mode, the beam is steered in a circular pattern (defining the width of a line) while the *stage* is moved over the length of the line or curve. This is a relatively slow

way of writing a long line but avoids spatially localized stitching errors. Instead, the placement and drift errors are averaged over the length of the feature. The Raith Elphy-Plus is not only available for SEM conversions but is also used as the pattern generator for Leica's LION-LV1 e-beam system (see below.)

Even the most expensive SEM conversion kit will be limited by the SEM's slow magnetic deflection, large distortion, and small stage. Next, we look at fully integrated commercial systems.

2.5.3.3 Leica EBL Nanowriter

FIGURE 2.16 Leica EBL-100, shown here with a 100 kV LaB6 electron source and a conventional SEM stage. The system is also available with a TFE source and laser-controlled stage. (Courtesy of Leica Lithography Systems Ltd.)

Somewhere between a converted SEM and a full featured e-beam system is the Leica EBL Nanowriter (Fig. 2.16). This system takes its electron gun and upper column from the Leica EBPG e-beam system, its deflection and imaging systems from the Leica 400 SEM series, [51] and adds custom pattern generation hardware. The pattern generator uses 16-bit DACs and has a deflection rate up to 1 MHz for vector scan operation. With an optional laser stage (5.3 nm resolution) this system costs substantially less than large e-beam systems and competes more directly with the high end Raith Elphy-Plus. Without a laser stage, the EBL will suffer from the same limitations as SEM conversions, namely, lack of stage flatness and the need for alignment marks for calibration. The system is available with a LaB_6 or Schottky thermal field emitter (TFE), and acceleration up to 100 kV. The system is unusual in offering such high voltage and a TFE emitter in a low cost system.

2.5.4 Gaussian vector scan systems

Like the converted SEMs, Gaussian vector scan systems use the writing strategy of stopping in each field, deflecting the beam from shape to shape, and filling in the shapes with a raster pattern. Large commercial systems, however, break the deflection into two (or more) sections, usually making use of a 16-bit DAC for "subfield" placement, and a faster 12-bit DAC for deflection inside the subfield (see Fig. 2.15). This is the scheme used in systems from JEOL, and some of the systems from Leica. Leica's EBPG series, and the Vector Scan (VS) tools built by IBM use an alternative technique: the slower DACs are used for placing the origin of each primitive shape and the faster DACs are used for filling in the shape. In addition to deflecting the beam with separate DACs, systems from Hitachi and Leica use these separate DACs to drive physically separate deflectors (magnetic or electrostatic). JEOL systems, in contrast, use a single stage electrostatic deflector. Single stage deflectors have fewer problems with matching deflections of the "fast" and "slow" electronics, but sacrifice some speed.

The largest distinction of these commercial Gaussian spot systems (and in fact all commercial e-beam systems) is the use of high precision laser-controlled stages. Stage controllers from Hewlett-Packard or Zygo use the Zeeman effect to split the line of a He-Ne laser. The split-frequency laser beam is reflected off a mirror attached to the stage, and the beat frequency from the two lines is measured by high speed electronics. When the stage moves, the beat frequency shifts according to the Doppler effect, and the stage position is calculated by integrating the beat counts. While often referred to as "interferometers," these stages actually have more in common with radar speed guns.

Analysis of multiple points on the stage mirror allows the measurement of X, Y, and rotation about Z (yaw). Stage precision is often given in terms of a fraction of the laser's wavelength; a precision of /128 = 5 nm is commonly used in commercial systems, and the best stages now use /1024 = 0.6 nm. Even though the controller reports the stage location to this precision, the accuracy of the stage is limited by unmeasured rotations about the X and Y axes, and by bow in the mirrors. These nonlinearities, called "runout", limit the absolute placement accuracy to the order of 0.1 um over 5 cm of stage travel.

The high precision in reading the stage position means that the stage motors and drive do *not* have to be highly refined. In fact, simple capstan motors and push rods have been used at IBM. [52-53] The stage controller receives a target location from a computer, drives the motors to a point close to this location, then sends an interrupt back to the computer and corrects the field position by applying an electronic shift. This shift is applied continuously, in real time, to compensate also for stage drift and low frequency vibration. In comparison, the laser stage built by Raith for SEM conversions applies corrections to relatively slow piezoelectric translators on the stage itself. By moving and measuring an alignment mark at various locations in the writing field, laser stages are used to calibrate the deflection gain, deflection linearity, and field distortion; that is, the stage is used as an absolute reference, and the deflection amplifiers are calibrated using the stage controller.

Other common features of commercial systems include a flat stage, a fixed working distance (contrasting with a SEM), and automated substrate handling. A flat stage keeps the sample in focus but requires the use of a detector either on or above the objective pole-piece. Most commonly, a microchannel plate or a set of silicon diodes is mounted on the pole-piece.

The market niche for commercial Gaussian spot high resolution e-beam tools has been primarily in research, and to a lesser extent for small-scale production of MMICs, high-speed T-gate transistors, and integrated optics.

Table 2.1. Characteristics of SEM-based lithography systems. In all cases the resolution is high, depending (for Nabity and Raith) on the chosen SEM. All of these systems have relatively small stage motion, ~ 2 in. The Nabity and Raith devices are add-on products, while the Leica Nanowriter is an integrated system.

	JC Nabity Lithography Systems	Raith GmbH	Leica Lithography Systems Ltd.
Model	NPGS	Elphy-Plus	EBL Nanowriter
Alignment	Automated or manual	Automated or manual	Automated
Stitching	Automated, accuracy limited by stage	Automated, 0.1 um accuracy with laser stage	Automated, with laser stage
Energy	0-40 kV for typical SEM, but depends on target instrument	0-40 kVfor typical SEM, but dependson target instrument	10 to 100 kV
DAC speed	Low, > 10 us per exposure point (100 kHz)	Mid-range, >0.4 us per exposure point (2.6 MHz) but may be limited by SEM deflectors	Mid-range, > 1us per exposure point (1 MHz)
Throughput limited by	Settling time of scan coils, transmission rate of ISA bus	Settling time of scan coils	Settling time of scan coils
Stage	Support for any automated stage	optional laser controlled	optional laser controlled
Control computer	PC compatible ISA bus DOS/Windows	PC compatible DOS/Windows	PC compatible
Cost	Low, < \$50k, <\$30k to universities for pattern generator only. SEM purchased separately	Mid-range, > \$100k for pattern generator only. SEM purchased separately	Mid- to high range, >\$1000k for a complete lithography system
Contact	406-587-0848 406-586-9514 jcnabity@aol.com	Germany: 49-0231-97-50000 USA: 516-293-0870, 0187 fax	USA: 708-405-0213 708-405-0147 fax, UK: 44-1223-411-123, -211 fax

2.5.4.1 JEOL systems

JEOL's popular JBX-5DII Gaussian vector scan system uses a LaB_6 emitter running at either 25 or 50 kV. Figure 2.17 shows the 5DII with two condenser lenses and two objective lenses. Only one of the objectives is used at a time; the operator has the choice of using the long working distance lens for a field size of 800 um, or the short working distance lens, for an 80 um field at 50 kV. (The fields are twice as large at 25 kV.) The pattern generator runs at 6 MHz (> 0.167 us per exposure point) and the stage has a precision of /1024 = 0.6nm. As with all commercial systems, alignment, field stitching, and sample handling are fully automated. In fact, one drawback for research purposes is that there is no manual mode of operation. The system is capable of aligning to within 40 nm (2) and writing 30 nm wide features over an entire 5 in. wafer or mask plate. JEOL systems are known for their simple, high quality sample holders. The 5DII is one of the highest resolution (though not one of the fastest) e-beam tools in the LaB_6 class.

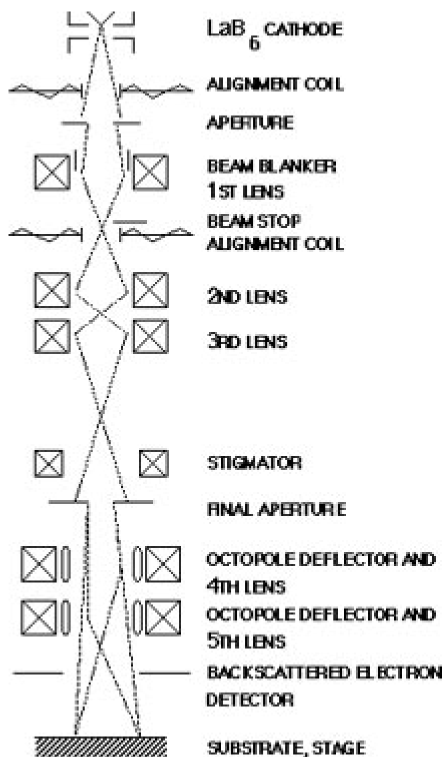

FIGURE 2.17 Schematic of the JEOL JBX-5DII system with LaB_6 emitter. The system features two objective lenses for two different working distances (courtesy of JEOL Ltd.).

JEOL's JBX-6000 implements a number of improvements on the 5DII. The LaB_6 emitter is replaced with a thermal field emitter, eliminating the need for one of the condenser lenses. The pattern generator speed is increased to 12 Mhz, and the PDP-11 controller is replaced with a VAX. The system uses the same set of two objective lenses, and for a given objective lens the magnification is fixed (that is, the DAC's deflection is not scaled with the field size). As can be seen in the graph of figure 2.18, the ultimate spot size is somewhat improved over that of the LaB_6 machine, but more importantly, the current density at smaller spot sizes is greatly improved. The JBX-6000 runs at 25 kV or 50 kV.

With higher current density comes the property that the probe size is sometimes *smaller* than a pixel. For example, consider a pixel grid of spacing 0.0025 um. If the rastering beam skips every *n* grid points, then the pixel area is $(n\ 0.0025\ \text{um})^2$. With a current of 10 nA and a dose of 200 uC/cm^2, we must have $(n\ 0.0025\ \text{um})^2\ 200\ \text{uC/cm}^2$ = 10 nA (exposure time for one pixel), and since the minimum exposure time is 1/(12 MHz) = 0.08 us, the smallest value of *n* is 9. In this case the pixel spacing is 22.5 nm and the spot size, according to Fig. 2.18 is 12 nm. In this example the pixel spacing is *larger* than the spot size, and the exposed features may develop as a lumpy set of connected dots. The problem will be even more pronounced when using high speed resists, large field sizes, and larger currents. One solution would be to implement a faster pattern generator; however, JEOL's approach is to retain the superior noise immunity of the 12 MHz deflector and instead to use less current when necessary, or to increase the spot size by using a larger aperture. Alternatively, one can purposely *defocus* the beam. The NPGS system (see Sect. 2.5.3.1) attacks the problem by allowing different pixel spacings in X and Y (or in r and).

It is interesting to note that future high resolution systems under development at Hitachi [54] are likely to resemble the JEOL Gaussian-spot tools, with field sizes >= 500 um and a single stage electrostatic deflector. Small fields avoid the complexities of dynamic focus and astigmatism corrections, and allow the short working distance needed to reduce the spot size. Single stage deflectors limit the bandwidth (speed) of the system, but improve intrafield stitching between deflections of coarse and fine DACs. The design tradeoff is clearly between high speed and high accuracy.

2.5.4.2 Leica Lithography Systems

Electron beam systems from Leica Lithography Systems Ltd. (LLS) are a combination of products previously manufactured by Cambridge Instruments, the electron beam lithography division of Philips, and most recently products from the former Jenoptik Microlit Division. Leica sells eight different models of Gaussian spot vector scan machines (the EBL Nanowriter has been described above). Systems in the mid-range of resolution include the EBML-300, a LaB_6 tool directly evolved from the Cambridge line, and the EBPG-5, a LaB_6 machine evolved from the Philips line. The EBPG-5 is comparable to the JEOL JBX-5DII in resolution but has accelerating voltage up to 100 kV. The EBMLand EBPG are both known for their versatile control software. On Leica's high end is the VectorBeam, with optics evolved from the Philips EBPG line and control electronics and software evolved from the Cambridge EBML line. The VectorBeam (Fig. 2.19) has a thermal field emission electron source running at 100 kV and a 6 in. stage motion with up to /1024 = 0.6 nm precision. The 25 MHz pattern generator has the useful feature that it is able to hold a small pattern in a buffer, so that repeated patterns do not have to be retransmitted to the pattern generator. This can significantly decrease the transmission overhead time when writing a large array of simple figures.

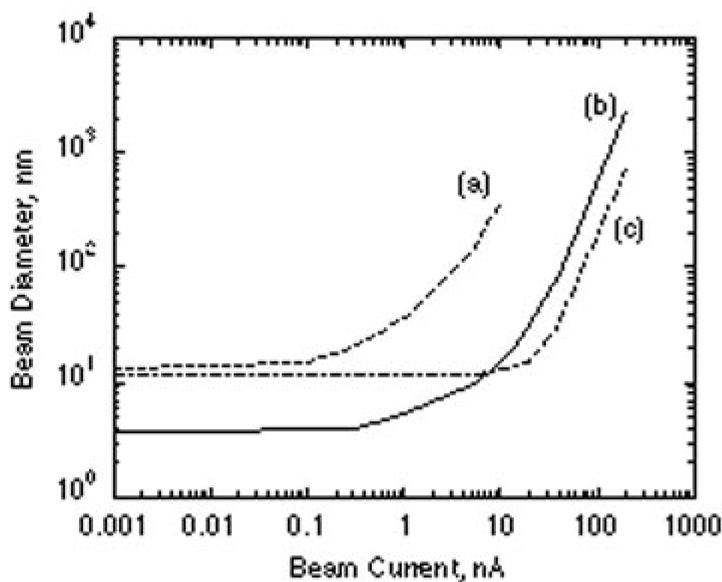

FIGURE 2.18 Probe beam diameter versus current for (a) a LaB_6 cathode with a 120 um objective aperture, (b) a thermal field-emission (TFE) cathode with a 40 um objective aperture, and (c) a thermal field-emission cathode with a 100 um objective aperture. Data is from JEOL Gaussian-spot e-beam systems using 50 kV acceleration and a short working distance objective ("5th lens") (courtesy of JEOL Ltd.).

Leica e-beam tools are also distinguished from those of JEOL by their use of a single objective lens (one working distance), and scaleable writing fields with 2^{15}=32768 or 2^{16} =65536 pixels across the field. In the case of the EBML-300, field sizes up to 3.2 mm may be used, although the benefit of using such a large field is debatable.

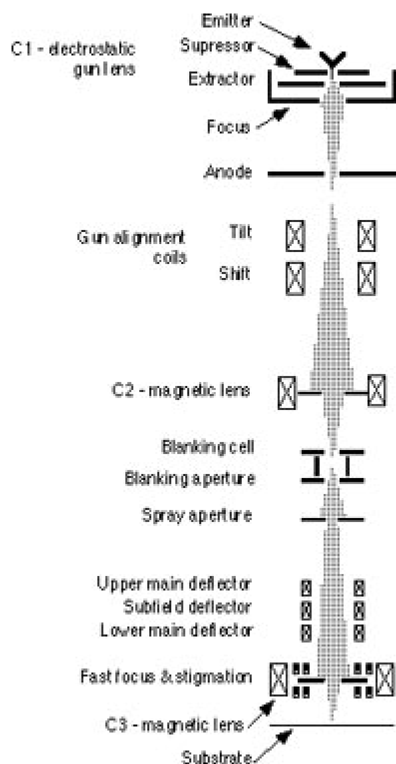

FIGURE 2.19 Schematic of the Leica VectorBeam 100 kV column with a thermally assisted field emission electron source (courtesy of Leica Lithography Systems Ltd.)

The largest systems from Leica are also equipped with 100 kV TFE emitters, and have stages with up to 8 in. travel. Additional features include a glancing-angle laser height sensor for dynamic field size corrections, and dynamic focus/astigmatism corrections -- features more commonly found on high speed maskmaking tools. Systems using large writing fields, with deflection angles exceeding 5 to 10 milliradians, make use of a number of higher order corrections including deflection linearization maps, field rotation maps, dynamic focus and stigmation tables, and even shift corrections for the dynamic focus coil.

2.5.4.3 Leica Lithographie Systeme Jena (Jenoptik) LION

One of the most unique Gaussian vector scan systems is the LION-LV1 from Leica Lithographie Systeme Jena GmbH,[55] a company better known for its large mask making machines (previously sold only in Eastern Bloc countries). The LION-LV1 combines a column designed by ICT GmbH (Heimstetten, Germany) with the pattern generator from Raith GmbH. This pattern generator has the unusual feature that it allows "continuous path control" of curves. In this mode the beam is held close to the center of the field while stage motion defines the shape of a Bezier curve. The ICT column is very similar to that used in the Leo 982 SEM, [51] except for the use of a beam blanker and higher bandwidth deflection coils (see Fig. 2.20). In this system, proximity effects are avoided by using beam energies as low as 1 to 2 keV. Although the voltage may be set as high as 20 kV, the system's selling point is low voltage -- avoiding both damage to the substrate and complications due to the proximity effect.

The column provides a spot size as small as 5 nm at 1 kV, through the use of an unusual compound objective lens. An electrostatic lens produces a diverging field, while the surrounding magnetic lens converges the beam. The complementary lenses reduce chromatic aberration, just as in a compound optical lens. A high resolution automated stage, substrate cassette loader, and substrate height measuring system complete the LION-LV1 as a full-featured system.

Low voltage operation avoids substrate damage and proximity effects, and offers the capability of three dimensional patterning by tailoring the electron penetration depth. However, the disadvantage is in greatly complicated resist processing. If the beam does not penetrate the resist, there will be

significant effects from resist charging, [56] and placement errors due to charging may be dependent on the writing order and on the shape of the pattern itself. Charging may be avoided by using a resist trilayer with a conducting center (e.g., PMMA on Ti on polyimide), or by using a conducting overlayer (see sect. 2.7.1). Increased processing is required also for removing the resist layer over alignment marks. In a production environment this complexity adds significantly to the cost of ownership.

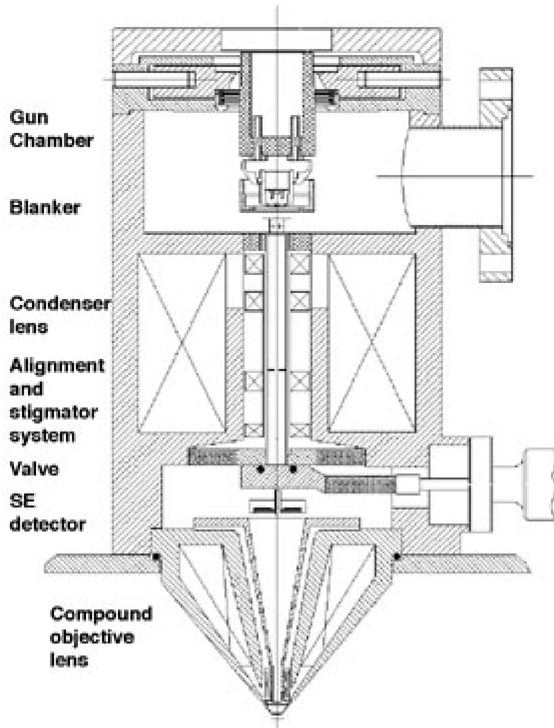

FIGURE 2.20 Low-voltage column developed by ICT GmbH, used in the LION e-beam system from Leica. The beam blanker is directly above the anode. The objective lens combines electrostatic and magnetic elements to reduce the net chromatic aberration. Beam diameter at 1kV is approximately 5nm. (Courtesy of LLS Jena GmbH.)

Table 2.2 Comparison of Gaussian-spot, vector-scan systems. All of these systems are equipped with thermally-assisted (Schottky) field emission electron sources.

	JEOL Inc.	Leica Lithography Systems Ltd.	Leica Lithographie Systeme Jena GmbH
Model	JBX-6000FS	Vectorbeam	LION-LV1
Resolution (minimum spot size)	5 nm	8 nm	5 nm
Alignment	automated	automated	Automated
Stitching	automated	automated	Automated
Field size	maximum 80 or 800 um at 50 kV	scaleable, 16 bits in up to 800 um at 50 kV or 400 um field at 100 kV	scaleable, 16 bits
Energy	25, 50, 100 kV	10 to 100 kV	1 to 20 kV
Speed of pattern generation	high, > 0.08 us per exposure point (12 MHz)	highest of class, >0.04 us per exposure point (25 MHz)	mid-range, > 0.4 us per exposure point (2.6 MHz)
Stage	laser controlled, 0.6 nm, 6 inch travel	laser controlled, 0.6 nm, 6 inch travel	laser controlled, 2.5 nm, 162 mm travel

Control computer	VAX (VMS)	VAX (VMS)	PC compatible
Cost	Expensive, > $3M	Expensive, >$3M	Expensive, >$1M
Contact	USA: 518-535-5900, Japan: 0425-42-2187, 1-2 Musashino 3-chome, Akishima Tokyo 196	USA: 708-405-0213, -0147 fax. UK: 44-1223-411-123, -211 fax	USA: 708-405-0213, -0147 fax. UK: 44-1223-411-123, -211 fax

2.5.5 Gaussian Spot Mask Writers

While both of these systems are promoted for mask making, their basic technologies could be adapted for direct writing on wafers. However, their relatively low throughput compared to photolithography systems has kept them firmly rooted in the maskmaking market.

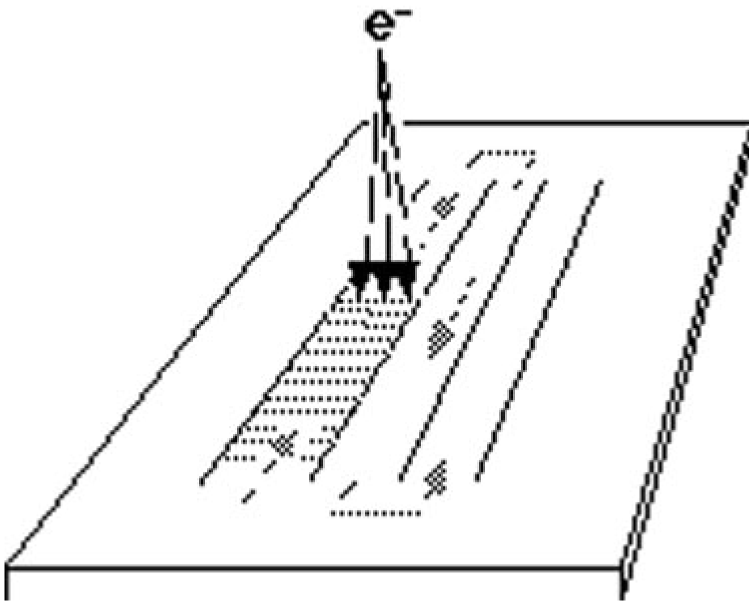

FIGURE 2.21 Gaussian-spot raster-scan writing strategy. The stage is moved continuously while the beam is rastered perpendicular to the stage motion. This technique, used by the Etec MEBES tools, is one of the most common for mask generation.

2.5.5.1 Etec MEBES systems

The most popular and well established mask writing tool is the MEBES from Etec Systems Inc. [57] The MEBES uses a focused ("Gaussian") spot, writing a pattern in stripes while moving the stage continuously. The beam deflection is primarily in one direction, perpendicular to the motion of the stage (Fig. 2.21). Of course, some small deflections are needed in the direction of stage travel, to compensate for stage placement errors. These correction values are provided by the feedback system of the laser-controlled stage. The 10 kV TFE electron gun provides a current density [58] at the mask plate of 400 A/cm^2.

The MEBES is designed for high-throughput mask making, with minimum feature size 0.25m. Figure 2.22 shows the MEBES IV-TFE column design, with three beam crossovers -- compared to one crossover in the Lepton column. A 160 MHz transmission line beam blanker is located at the third crossover. Since Etec Systems has implemented a full range of error compensation techniques, including a glancing-angle height sensor, dynamic focus corrections, periodic drift compensation, and substrate temperature control. Real-time correction of focus, gain, and rotation provide stitching errors (3) of 50nm. [59] The MEBES 4500 can be used as a metrology tool to characterize its own stitching and linearity. However, when errors appear in both the writing and the reading process (as would be

caused by interferometer mirror defects) then a machine cannot measure its own distortions. In this case, two or more MEBES machines can be used to check for consistency.

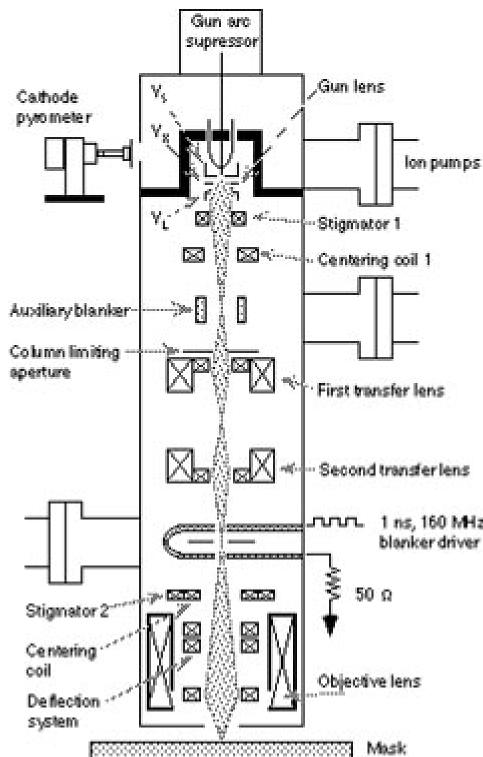

FIGURE 2.22 Schematic of the MEBES IV TFE column (Etec Systems Inc.) The source optics include the extractor (V_x), focus (V_L) and suppressor (V_s). The high-speed beam blanker assembly is a U-shaped transmission line designed to deflect the beam twice with one blanking pulse. [57] (Courtesy of Etec Systems Inc.)

As with any Gaussian beam system, throughput decreases as resolution (density of the pixel writing grid) increases. One way to increase the resolution without sacrificing speed is to implement a "graybeam" strategy, where the pixels on edges of features have dwell times and placements modulated on a per-pixel basis. This allows the bulk of a pattern to be written on a fast, coarse grid while edges are written with a finer resolution. [60]

2.5.5.2 Lepton EBES4

The EBES4 mask writer from Lepton Inc. [61] also uses a Gaussian spot, with a patterning strategy similar to that of the high resolution machines. In this system the coarse/fine DAC beam placement is augmented with an extra (third) deflection stage, and the mask plate is moved continuously, using the laser stage controller to provide continuous correction to the stage position. Unlike the high resolution JEOL machines, each stage of deflection has a separate telecentric deflector (instead of simply a separate set of DACs) for high speed operation. Patterns are separated into stripes (similar to writing fields) 256 m wide (see Fig. 2.23). These stripes are separated into 32 m subfields ("cells") which are further subdivided into 2 um sub-subfields ("microfigures"). A spot of 0.125 m diameter fills in the microfigure with a raster pattern.

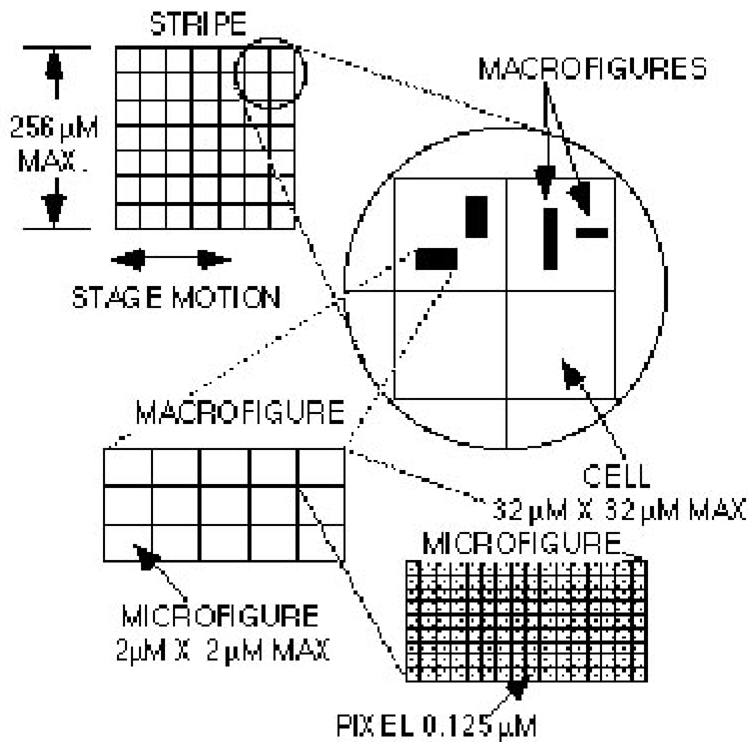

FIGURE 2.23 Writing strategy of the Lepton EBES4 mask writing tool: pattern data is cut into stripes 256 um wide. The stripes are fractured into smaller cells containing macrofigures. The macrofigures are split into even smaller microfigures which are finally written as a set of pixels. [62] (Courtesy of Lepton Inc.)

The entire EBES tool has been designed for high speed, with a current of 250 nA delivered in a 0.125 m spot for a current density at the sample of 1600 A/cm^2. The EBES4 column uses a TFE electron gun operating at 20 kV and a single beam crossover at the center of a high-speed beam blanker. [63] The pattern generator operates at up to 500 MHz, and the high overall throughput allows production of a 16 Mbit DRAM mask in 30 min. [64]

A robot arm is used to load mask plates from a magazine module to the alignment and temperature equilibration chambers, and later to the exposure chamber. The internal mask carrier is made from the glass ceramic Zerodur^{TM}, which minimizes substrate temperature variations during exposure. The EBES4 automatically loads each mask plate into the carrier, establishes electrical contact to the substrate, and verifies the contact resistance.

The EBES4 mask writer has a spot size of 0.12 m, uniformity to 50 nm (3), stitching error of 40 nm, and repeatability (overlay accuracy) of 30 nm over a 6 in. reticle.

Table 2.3 Comparison of Gaussian spot, raster scan mask making systems.

	Lepton Inc.	Etec Systems Inc.
Model	EBES4	MEBES 4500
Resolution	0.125 um spot	0.25 um features
Alignment	automated, optional direct write on wafers	automated, mask writing only
Field	256 um x 32 um stripes, continuous motion	1.1 mm maximum stripe length, continuous motion
Energy	20 kV	10 kV
Current Density	1600 A/cm^2	400 A/cm^2

Speed	500 MHz	160 MHz
Samples	6 inch plates	8 inch plates
Stage	laser controlled, 5 nm resolution controller, 146 mm travel	laser controlled, 6.6 nm resolution controller, 6 inch travel
Contact	USA: 908-771-9490	USA: 510-783-9210 France: 33-42-58-68-94 Japan: 81-425-27-8381

2.5.6 Shaped Spot and Cell Projection Systems

All of the e-beam tools described above focus the beam into a small spot, and shapes are formed by rastering the beam. This spot is the reduced image of the source, often referred to as the "gun crossover," which has a current intensity profile resembling a Gaussian distribution. The time needed to paint a shape can be eliminated by forming the electron beam into primitive shapes (rectangles and triangles) and then exposing large areas with single "shots" of the beam. The optics of these shaped spot systems is shown schematically in Fig. 2.24. The upper aperture typically uses a square to form two sides of a rectangle, and the overlap of the lower aperture defines its length and width. More complex shapes are fractured into rectangles and triangles before exposure.

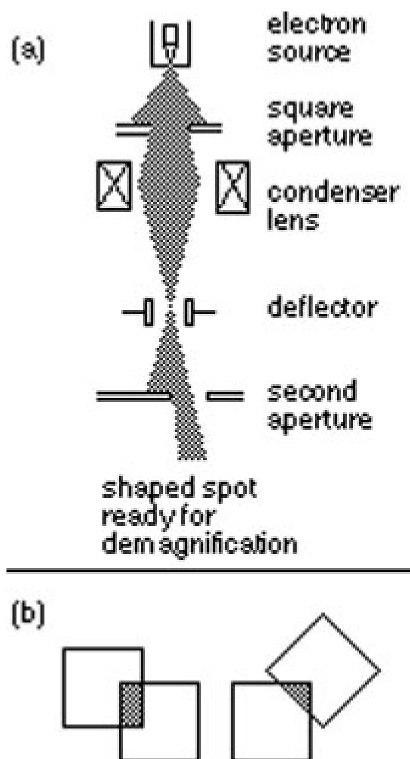

FIGURE 2.24 Shaped spot optics. (a) The first square aperture defines two sides of a rectangle, and the second square aperture defines the other two sides. Deflectors determine the overlap and thus the length and width of the rectangle, as shown in (b). By deflecting over a corner, triangles can be formed. The shaped spot image would be further demagnified by magnetic lenses lower in the column.

Because of their increased parallelism over Gaussian raster-scan tools, shaped spot systems are much faster. However, throughput is still limited by the remaining serialism, by stage movements, and in a few cases by data transfer times. Shaped spot systems can readily be extended to 0.15 m resolution (compared to the 0.25 m resolution of the Gaussian raster beam systems). While there is no well defined standard for the comparison of throughput, we can say that the throughput of shaped spot machines remains under 10 wafers/hour -- making them superior to Gaussian systems but not

competitive with optical steppers which produce, typically, 40 to 80 wafers/hour. The market for high speed shaped spot systems remains in maskmaking, direct-write prototyping, and low volume production of 0.15 m scale features.

2.5.6.1 IBM EL-4

Shaped spot systems have been pioneered, but never sold, by IBM. The latest version, EL-4, combines an extraordinarily large number of lenses [65-67] (Fig. 2.25) with a unique three-stage deflection for optimum speed. The final lens, termed a variable axis immersion lens (VAIL) provides minimized off-axis aberrations (or maximum field coverage) as well as telecentric beam positioning, with the beam landing normal to the substrate, thereby reducing stitching errors due to substrate height variance. The system runs at 75 kV with a LaB_6 emitter, providing up to 50 A/cm^2 at the substrate. Wafers are held on the stage by electrostatic clamping, which is claimed to provide improved flatness, superior thermal stability, and lower contamination than conventional front-surface reference wafer chucks. An advanced feature of the EL-4 is its use of redundant data registers and a cyclic redundancy code for checking the validity of the many gigabytes of data flowing into the system. Another unique feature is the use of a servo guided planar stage which slides on a base plate without guide rails, moved by push rods coupled with friction drives to servo motors outside the vacuum chamber. The stage is positioned entirely through feedback from a multi-axis laser controller. [68-69]

2.5.6.2 Etec Systems Excaliber and Leica Lithographie Systeme Jena ZBA 31/32

The Leica Jena ZBA 31/32 [70] handles plates up to 7 in and wafers up to 8 in. The "31" is a maskmaking tool, and the "32" is a direct-write instrument. Like Etec's AEBLE and Excaliber systems, the ZBA writes while the stage is moving. The ZBA delivers 20 A/cm^2. Its continuous stage motion and cassette-to-cassette wafer loader give it relatively high throughput when using high speed resist.

The latest generation of commercial shaped spot systems will offer resolution to 0.1 m. Under development at Etec is the "Excaliber," with a field emission source, larger stage, and higher resolution than its predecessor, the AEBLE-150. The Excaliber system incorporates a number of features from IBM's EL-4, such as telecentric deflection and the sliding chuck ("wayless") stage with yaw compensation. Unlike EL-4, the Excaliber will keep the field size below 1 mm, thereby decreasing beam settling times while the stage moves continuously.

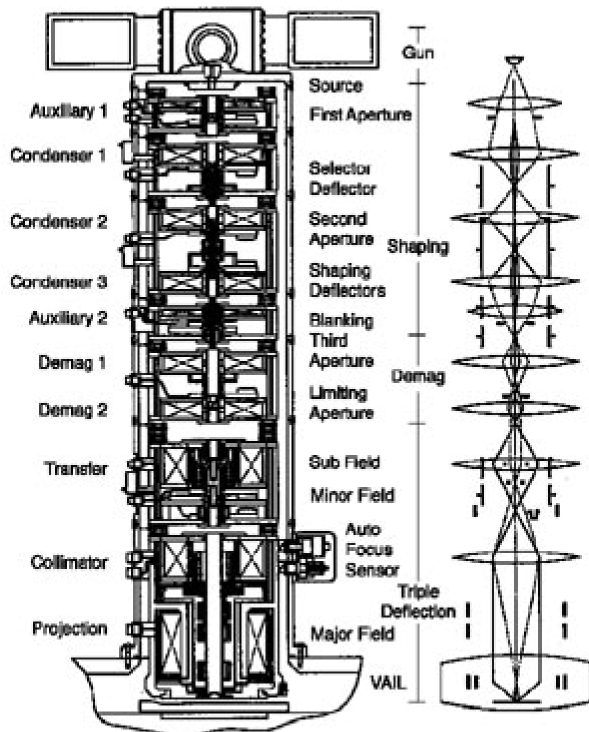

FIGURE 2.25 Schematic of the IBM EL-4 column for shaped-beam lithography. On the right, the dashed ray trace corresponds to the source, and the solid trace to the shaped spot. [66] (Courtesy of IBM Corp.)

2.5.6.3 JEOL shaped spot systems

JEOL's JBX-8600DV [71] provides 0.1 m resolution at 30 A/cm^2 for direct-write applications. The system uses two stage electrostatic deflection, and handles 6 in. wafers. The JBX-7000MVII [72] has been developed as a 4 reticle making system for 256 Mbyte DRAM class devices. As with most shaped spot systems, the JEOL machines can create a map of distortion values for the deflection so that patterns can be mapped more precisely onto optically-generated features. The JBX 7000MVII handles up to 7 in. plates with a laser stage measurement unit of 0.6 nm (/1024). Overlay accuracy is 30 nm (3) and placement accuracy is 40 nm.

The attention to absolute pattern placement accuracy is always much more extensive in dedicated maskmaking tools than in direct-write machines. To control thermal expansion of the plates, temperature monitoring and stabilization is far more elaborate. Like other manufacturers, JEOL creates a map of stage nonlinearity by measuring a set of marks, turning the plate in 90 increments and measuring the set again. The resulting stage distortion map is used to reduce the runout due to imperfections in the stage mirror. In fact, each individual plate holder has its own specific distortion table, which is identified automatically by reading a bar code on the cassette.

2.5.6.4 Cell Projection

The throughput of shaped beam tools is primarily limited by the average beam current in the spot, and by the pattern density. The average beam current for cell projection is modestly larger than for variable shaped beams. Both are limited by Coulomb interaction to a few microamperes. However, by replacing the simple beam shaping aperture with a more complex pattern, a "cell projection" system can greatly increase the pattern density without sacrificing throughput.

In cell projection systems the upper deflector steers the beam into one of a number of hole patterns, or "cells." The shaped beam is deflected back to the center of the column and is demagnified by another lens, forming an image on the substrate. The shaping aperture is made of a silicon membrane, around 20 m thick, patterned with holes and coated with gold or platinum. To maintain small aberrations and

high resolution, the cell is demagnified by a factor of 20 to 100, and the final cell size on the wafer is only 2 to 10 m. The wafer containing these patterns also contains a simple rectangular aperture for general purpose pattern generation in a standard shaped spot mode. While a number of cell patterns may be placed on the beam shaping wafer, it is clear that the cell projection technique is advantageous and economical only for highly repetitive designs with small unit cells, namely, memory chips. Patterns for cell projection will require proximity correction by shape modification [38-39] or through a variation of the GHOST technique [40] (see Sect. 2.4.3).

To achieve throughput comparable to that of optical steppers, cell projection tools must reduce the shot count by a factor of around 100. Current machines have achieved shot reductions on the order of a factor of 10 and have throughputs of less than 10 wafer levels/hour (for a 6 in. wafer populated with 256 Mbyte DRAMs, ~10^9 shots/chip).

IBM, [73] Hitachi, [74-75] Toshiba, [76] Fujitsu, [77-78] and Leica have developed cell projection tools targeted for 256 Mbyte DRAM manufacture. Leica's "WePrint 200" instrument is a modified version of the ZBA-32. Hitachi also offers a cell projection/shaped spot system for sale: the HL-800D. Common features of cell projection systems include continuous stage motion [79] and resolution around 0.2 um. Hitachi's HL-800D reduces the cell reticle by a factor of 25, while Fujitsu uses a factor of 100 and Toshiba uses a factor of 40. The final demagnified cell size is kept below ~10 m to reduce aberrations. [76] Space charge effects also reduce the feature edge sharpness, but these can be compensated by using a current-dependent dynamic refocusing of the image. [75] [80-82] Cell projection has not yet achieved the throughput of optical steppers but as a transitional technology may provide the resolution needed for near-term 256 Mbyte DRAM production.

Table 2.4 Comparison of shaped spot systems.

	IBM Corp.	Etec Systems Inc.	JEOL Inc.	Leica Lithographie Systeme GmbH	Hitachi Inc.
Model	EL-4	Excaliber - *under development*	JBX-7000MVII	ZBA 31/32 WePrint-200	HL-800D *Cell Projection*
Resolution	0.15 um features, 50 nm CD control	0.12 um	0.2 to 0.5 um	0.2, 30 nm CD control	0.25 um, 50 nm CD control
Alignment	automated	automated	automated	automated	automated
Field	10 mm maximum	1 mm	1.5 mm	1.3 mm	
Energy	75 kV	100 kV	20 kV	20 kV	50 kV
Speed	~2-3 wafers/hour	100 kV	20 kV	20 kV	50 kV
Samples	8 inch	8 inch	up to 7 inch plate	8 inch	8 inch
Stage	"wayless" stage: electrostatic clamping, sliding chuck, servo powered, laser control with yaw compensation	"wayless" stage: electrostatic clamping, sliding chuck, servo powered, laser control with yaw compensation	laser controlled conventional stage	laser controlled conventional stage, cassette-to-cassette automated loading	laser controlled conventional stage
Cost	not for sale	*system under development*	high, >$3M	high, >$3M	high, >$3M
Contact	n/a	USA: 510-783-9210 France: 33-42-58-68-94 Japan: 81-425-27-8381	USA: 518-535-5900, Japan: 0425-42-2187	USA: 518-535-5900 Japan: 81-425-43-1111	USA: 415-244-7594, 415-244-7612 fax, or in Japan: 81-3-5294-2061

2.5.7 SCALPEL

Cell projection uses small reticle areas to avoid spherical aberration and to minimize space charge effects. A natural extension of the idea would be to separate a large pattern into many small sections, etch each section into its own area of the aperture wafer, and then select and stitch the patterns together using a set of two deflectors. There are a number of limitations to this extension of cell projection: (1) 20 um of silicon is needed to stop 50 kV electrons, [83] so the pattern must include deep holes. Because the aspect ratio of these holes is limited, lines can be no wider than ~2 um; therefore, the electron optics must demagnify the pattern by a factor of at least 20 to produce linewidths of 0.1 um. This limits the area available for cell patterns. (2) Multiply connected (e.g., doughnut shaped) patterns require complementary stencil masks, so the throughput and available pattern area is further reduced. (3) Residual stress in the stencil mask will distort the mask in a pattern-dependent way, and since stencil masks absorb most of the electron energy, the changing temperature will also cause similar pattern-dependent distortions. [84]

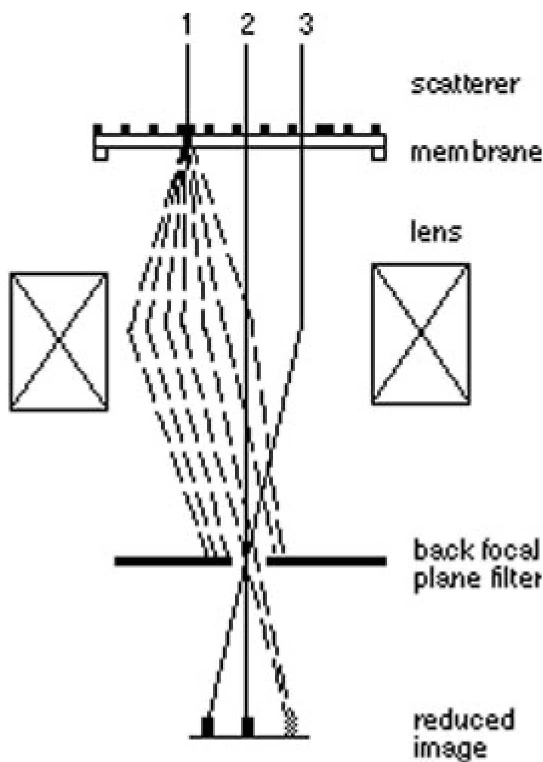

FIGURE 2.26 Schematic of the SCALPEL technique. [87] Electrons (1) that hit the scatterer (the patterns on the mask) are scattered, and most are filtered out by the aperture. Electrons traveling through the membrane (2,3) are demagnified through the aperture and form a high contrast image on the substrate. The mask is a pattern of tungsten supported on a low stress silicon nitride membrane. The membrane is supported on a silicon wafer, with periodic silicon support struts (not shown.) (Courtesy of Lucent Technologies Inc.)

Instead of using an absorbing mask, Koops and Grob [85] proposed and researchers at AT&T Bell Laboratories [86-88] (now known as Lucent Techologies) later implemented the idea of using a *scattering* mask to produce a high contrast image with a technique commonly used in transmission electron microscopy. Figure 2.26 illustrates the technique "scattering with angular limitation in projection electron beam lithography," or SCALPEL. Electrons traveling through a thin (typically 150 nm) silicon nitride membrane are focused by a lens and pass through an aperture (the "back focal plane filter"). Electrons scattered by the adsorber (typically 50 nm of Au or W) are most likely not to pass through the aperture. By choosing an optimal accelerating voltage (95 kV) for the membrane thickness (100 nm of low-stress silicon nitride) and adsorber (50 nm W), the contrast at the substrate can be as high as 95%, with a transmission of 55%. [89]

If the focal plane aperture includes an annular ring, then some of the "dark field" electrons pass through to expose the resist. The unfocused dark field image of the mask can thereby be used to provide a background dose correction to compensate for proximity effect, using a technique similar to GHOST [40] (see Sec. 2.4.3.3). Although this compensation scheme is still in the design stage, it holds the promise of proximity effect correction without any loss of throughput. [90]

As in cell projection, the mask is sequentially scanned and the image shifted and reduced onto the wafer. However, because the scattering features can be much thinner than the holes of cell projection, patterns can be fabricated at smaller dimensions and the demagnification of the mask can be decreased to 5. A much larger chip can then be fabricated, with up to $2 10^{10}$ pixels. [91] Massive support struts between the "cells" are not imaged onto the wafer since the patterns are shifted into place as they are illuminated. While the mask structure is similar to those used for x-ray lithography, the support struts provide greater dimensional stability, [84] and use of reduction optics makes mask fabrication simpler.

The throughput of a fully-developed SCALPEL tools (which to date has only been modeled) is expected to be comparable to that of an optical stepper, while delivering resolution on the scale of 0.1 um. However, several questions remain concerning its practical use: At energies in the 100 kV range resists are proportionally less sensitive, and the energy delivered to the substrate will be larger than in conventional e-beam systems. The effect this may have on transistor thresholds and mobility is still unknown.

2.5.8 Other E-Beam System Research

2.5.8.1 STM writing

The scanning tunneling microscope (STM) has been used to write nanometer-sized patterns in research experiments. It simply consists of a sharp tip used as a field emission cathode that is scanned a few nanometers above the surface of the sample. Resolution is obtained not by lenses but rather by keeping the tip so close to the surface that the electrons do not have a chance to diverge.

However, the technique is severely limited in writing speed and the resist thickness it can expose, and has seen only a few very limited applications. STM lithography is discussed in Sect. 8.8.3, and in the review article by Shedd and Russel. [92]

2.5.8.2 Parallel beam architectures - microcolumns

In addition to the projection systems described above, several other new architectures have been proposed for increasing the parallelism of e-beam lithography. One proposal is to build an integrated matrix of electron sources, producing an array of parallel beams within one column. [93-94] In contrast, researchers at NTT have proposed the use of an array of micromachined beam blankers and objective lenses, illuminated by a single high-current electron gun. [95] Other researchers are developing discrete components for miniaturized single-beam electron sources and columns. [96-98]

In an ongoing effort at IBM, researchers are seeking to shrink the lenses and other optical components to micrometer sizes using micromachining techniques, thereby building a high-performance, low voltage electron beam column. [96] [99-100] Low-voltage has both advantages and disadvantages over high-voltage lithography (see Sect. 2.5.4.3) but is required here simply because of the small size of the components. In this design an entire e-beam column is only several millimeters high, assembled from micromachined silicon membranes supported on anodically bonded silicon and pyrex wafers. This concept is still in the early development stages.

Microcolumn research seeks to provide exposure parallelism by building an array of small columns. If they can be produced cheaply enough, maintenance would be simplified by the use of disposable electron optics. Although the optics may be inexpensive, the control system for a large array of columns may be very expensive. While many technical hurdles have already been overcome, the ultimate success of beam arrays may be decided solely by economics.

2.5.9 Electron Beam Fabrication Services

In addition to commercial mask vendors, many institutions offer services on large, high resolution e-beam tools. Payment for services varies widely, from purely collaborative work to hourly fees or contracts. Public access to many fabrication services is provided in the U.S. by the National Nanofabrication Users Network (NNUN), based primarily at Cornell and Stanford universities. Services provided through this network and the list of other sites changes so often that it is more appropriate to refer the reader to the World Wide Web page, http://www.cnf.cornell.edu/, which provides information about the services of the NNUN and other nonaffiliated U.S. fabrication centers. A list of mask vendors can be found in the *Semiconductor International Buyer's Guide*.

(2005 Note: The National Nanofabrication Users Network is now the **National Nanotechnology Infrastructure Network (NNIN).** More information on this thirteen-member network can be found at www.nnin.org.)

2.6 Data Preparation

2.6.1 Pattern Structure

Preparation of pattern data for electron beam lithography may begin with a high level symbolic or mathematical description of a circuit, with the algorithmic description of a pattern (e.g. a Fresnel lens), or with a simple geometric layout. A computer aided design (CAD) program is usually used to lay out or at least inspect the pattern and to generate output in a standard exchange format. A separate program is then used to convert the intermediate format to machine-specific form. This last step can be quite involved since in most cases all hierarchy must by removed ("flattened"), polygons must be reduced to primitive shapes (e.g., trapezoids or triangles and rectangles), and the pattern must be fractured into fields, subfields, and even sub-subfields.

For shaped beam machines, or if the data is to be proximity corrected, medium and large sized shapes should be "sleeved", so that the edges of shapes are exposed separately from the interiors. For shaped beam machines this allows the edges to be exposed with a small shaped size that has better resolution; for proximity corrected patterns, this allows finer control over the dose delivered to the shapes. Frequently, a bias (also known as sizing) may be applied to the pattern shapes to account for resist characteristics or process steps that affect the final device linewidth.

For Gaussian beam machines, a reasonable pixel size must be selected. A good compromise is usually to use a pixel size of about half the beam diameter. Larger pixel sizes may speed up throughput, while smaller pixel sizes will reduce line edge roughness and improve feature size control. The machine field size is usually a fixed multiple of the pixel size. Field sizes may range from less than 100 um for high resolution, high accuracy work to more than 1 mm for high speed, low resolution lithography.

When designing a device such as a transistor, you would organize the fabrication in a set of steps; e.g., mesa, ohmics, gate, etc. Each step is assigned to a "layer" in the CAD tool, and multiple layers are displayed as overlapping patterns (usually in different colors). Much later on, the layers will be split apart into separate pattern files. Some of these layers may be patterned with photolithography, some with e-beam. For example, you may design the geometry of each layer and place all of this information in the transistor "cell". Now you can put this cell at a number of other locations to create, say, a NAND logic gate. If you have not simply *copied* the transistor but rather have created *instances* of the cell (somewhat like a function called in a program) then any modifications in the transistor cell will be instantiated all over the NAND gate. The NAND gate is now a higher level cell, which can be used as part of, say, a half-adder. The hierarchy of an entire circuit is continued in this way. Of course, when building circuits from a standard technology such as CMOS, all of the basic component cells are usually purchased as part of the CAD program (a library of cells), and may even be placed and connected automatically as part of a symbolic CAD package.

2.6.2 Avoiding Trouble Spots

An e-beam lithographer would be unlikely to use any high level design tools. Rather, the lithographer must deal with data at the lower, geometrical level. If the scale of critical dimensions is far larger than the e-beam tool's placement errors, then the designer is free to place features anywhere. For instance, a set of 5 reticles with 5 um design rules and 0.5 um overlay error budget will demand little (except stability) of a commercial e-beam system. However, when the design requires a direct-write e-beam layer with 0.05 um alignment, the placement of alignment marks becomes critical, and e-beam stitching errors can significantly affect device performance and yield. It is important for the designer to consider the limitations of the e-beam system before laying out any pattern.

Consider the case of a pattern targeted for a high resolution Gaussian beam system, such as the Leica EBPG or the JEOL-JBX series. For high resolution work the writing field may be as small as 80 um. Larger patterns are formed by moving the sample and stitching fields together. Field stitching errors will be around 20 nm, so any fine lines in the pattern (e.g., a narrow gate) should not be placed at a field boundary.

2.6.3 Alignment Marks

Electron-beam lithography may be used to pattern optical masks and their corresponding alignment marks; steppers and contact aligners have specific design requirements for these marks. However, we will discuss here only the marks used for direct-write e-beam layers. There are two phases of alignment: (1) correction for the placement and rotation of the wafer (or piece) and (2) correction for the placement of individual chips on the wafer. The e-beam tool aligns each pattern file (in its final fractured form) to a mark before writing the pattern.

If your alignment tolerance is greater than ~0.5 um, then the individual chip alignment will not be necessary. Global alignment -- that is, correction for the placement and rotation of the workpiece -- can use marks which are separate and larger than those used for chip alignment. Large global alignment marks are useful for the exposure of full wafers since the machine can be programmed to search for the first mark. Typical marks used for global alignment are large crosses of width 2 to 6 um and length ~100 to 200 um, placed at the top, bottom, left, and right sides of the wafer, as illustrated in Fig. 2.27. Alternatively, a few of the marks used for chip alignment could also be used for global alignment; this would allow global alignment on small pieces of a wafer. Alignment to chip marks is especially useful as a diagnostic of the maskmaking tool, allowing the measurement of displacements as a function of chip location.

For large patterns that take a long time to write, it may improve registration and placement accuracy if the machine stops periodically (every 5 to 10 minutes is typical) to reregister to the alignment marks. This corrects for thermal or other drifts that can occur during the writing process. For single level processes or maskmaking, reregistering to a single mark is sufficient to correct for drift.

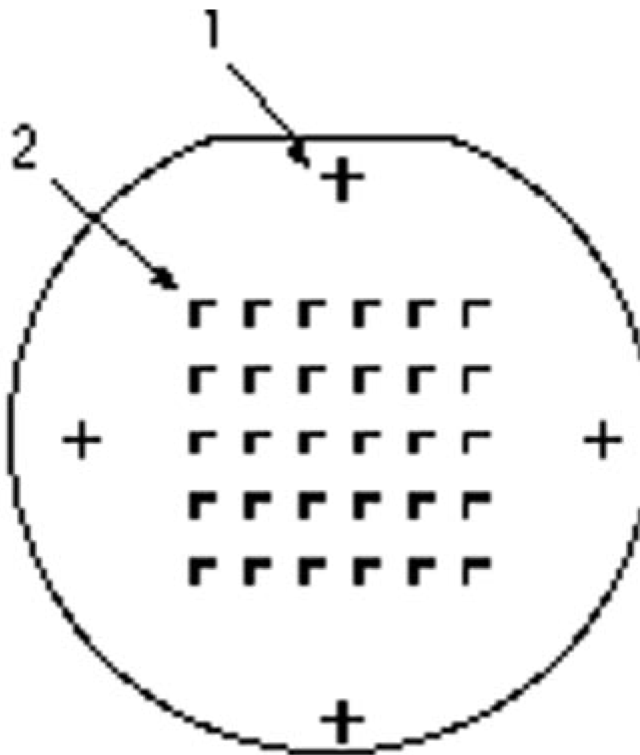

FIGURE 2.27 Alignment marks used for electron-beam lithography. Marks are typically etched pits in the wafer, or high-Z metal such as gold, platinum or tungsten. Global marks (1) are used to correct for the overall shift, rotation, and gain of the wafer, and chip marks (2) are used to correct for the placement of individual patterns. Chip marks can be used to correct for individual chip rotation and gain, to better match a badly adjusted optical stepper. The marks are not shown to scale. Typical wafer marks (1) are 200 um long, and typical chip marks (2) are 10 um long.

The size of a chip may be on the order of centimeters, and in photolithography the chips or entire wafers are aligned at once. While e-beam systems can align to global marks alone, the best tolerance (<0.1 m) will be achieved when the alignment marks are within several hundred micrometers of the critical region. The designer may therefore wish to split the e-beam layer into smaller sections so that critical regions can be aligned individually. If these critical regions (e.g., gates) are arranged in a regular pattern, then arranging the sequence of e-beam writing will be simple. If the critical regions are placed randomly in the chip, the designer will have a time-consuming job of arranging the e-beam sequence and avoiding field boundaries.

Alignment marks must be patterned in previous steps of the device fabrication. A "zero level" is sometimes used for the sole purpose of placing robust alignment marks on the sample before any actual device data are written. Typically the designer includes a photolithography step simply for patterning alignment marks as trenches to be etched into the substrate. The best alignment of layer 2 to layer 1 will be achieved when layer 1 contains the marks used for aligning layer 2 and when the marks are as close as possible to critical areas. If the material of layer 1 is unacceptable for alignment (e.g., a 20 nm thick metal layer) then both layers will have to be aligned to a third reference pattern (the "zero level"). Alignment to a third layer adds a factor of ~1.4 to the overlay error.

Well designed marks are commonly destroyed by processing. For example, ohmic metalizations become very rough when annealed. The rough marks are fine for optical alignment, but the lumps may cause the e-beam alignment hardware to trigger at the wrong locations. A good solution to this problem is to fabricate alignment marks as deep etched trenches (deeper than 1 m). Plasma-etched or wet-etched trenches may be used. Such pits will not change after high temperature processing (unless material is deposited in them), and (unlike Au) are compatible with MOS processing. Other examples of effective alignment marks are W on Ti, Pt on Ti, and Au on Cr. Au is compatible with GaAs processing, but to maintain a smooth film, the alignment marks must be patterned after the annealing steps. In each of these cases the Ti or Cr provides improved adhesion to the substrate. A 200 nm thick layer of Pt or Au provides a good alignment signal, and 10 to 20 nm of Ti or Cr under the high-Z material provides improved substrate adhesion. Metal films can be patterned with very smooth edges by a liftoff process using a bilayer of PMMA and P(MMA/MAA) (see Sect. 2.7.4.2). In all cases, the designer must consider the thickness, roughness, and process compatibility of the material used for e-beam alignment marks, as well as the mark shape required for specific e-beam tools.

2.6.4 CAD Programs

CAD programs range from the very expensive schematic capture tools for VLSI to simple and inexpensive polygon editors. At the high end are widely used circuit capture, simulation, and layout tool sets from Cadence [101] and Mentor Graphics. [102] Other high-end packages are sold by Silvar Lisco, [103] Integrated Silicon Systems, [104] and a number of other vendors. [105] These tools run almost exclusively on UNIX workstations, and generate the standard intermediate format GDSII (also known as "Calma Stream" format) as well as the machine-specific MEBES format. Software tools in these sets include analog and digital simulators, silicon compilers, schematic capture, wire routers, design-rule checkers, and extensive cell libraries for CMOS, BiCMOS, and bipolar technologies.

In the mid-range of expense are the programs from Design Workshop [106] (DW2000) and Tanner Research [107] (L-Edit). Design Workshop implements a fully-functional graphical editor with the unusual feature of providing not only GDSII format, but also output in machine-specific formats for MEBES, JEOL, and Leica systems. DW2000 includes an integrated command language for algorithmic pattern definition. Design Workshop runs under the Macintosh OS, UNIX, and Windows NT. The Tanner Research tools run on PC compatibles, Macintoshes, and several UNIX workstations; output is in CIF or GDSII. Both Design Workshop and Tanner Research have implemented a less extensive set of companion tools (rule checkers, routers, simulators, etc.) and concentrate on the core graphical editors.

Inexpensive graphical editors include AutoCAD and other general-purpose CAD tools for PC compatibles and the Macintosh. AutoCAD and other similar programs generate DXF format, which must be converted to GDSII with a separate program. [108] AutoCAD has the disadvantage that it was not designed for lithography and so can generate patterns (such as 3D structures) that cannot be rendered by e-beam systems. Also, DXF format does not support "datatype" tags, which are used to specify individual dose values for geometrical shapes. Datatype tags are important when compensating (manually or automatically) for the proximity effect (see Sect. 2.4).

At the very low end are the free programs from UC Berkeley: Magic and OCT/VEM, which run on UNIX workstations. Magic is a widely used program geared for MOSIS-compatible CMOS processing. Magic is restricted to rectangles at right angles ("Manhattan geometry") and has no support for polygons. The VEM polygon editor in conjunction with the OCT database manager provides support for polygons. A number of companion simulation and routing tools also work with the OCT database but are distributed "as is," and without support. While these programs are distributed for only a shipping fee, [109] the real cost is the time and expertise required for installation and for working around bugs. Magic and VEM generate patterns in CIF format, which is supported by some mask vendors or may be translated to GDSII.

2.6.5. Intermediate Formats

2.6.5.1 GDSII

GDSII, also known as "Calma Stream", was originally developed by the Calma division of General Electric. Rights to the Calma products have changed hands several times, and are now owned by Cadence Design Systems. GDSII is by far the most stable, comprehensive, and widely used format for lithography. GDSII is a binary format that supports a hierarchical library of structures (called "cells"). Cells may contain a number of objects, including:

- Boundary, which may be used to represent polygons or rectangles,
- Box, which may be used to represent rotated rectangles,
- Path, which may be used to represent wires,
- Text, for annotation either on the CAD screen or the device,
- Sref, to include an instance of one structure (cell) inside another, and
- Aref, similar to Sref but providing an array instance of a cell.

There are 64 available Layers, numbered 0 to 63. Each primitive object (Boundary, etc.) lies on one of these layers. Each layer number typically represents one mask or electron-beam exposure step in a process.

A specification of GDSII format appears in the appendix to this chapter, portions of which are reprinted by permission of Cadence Design Systems.

2.6.5.2 CIF

The Caltech Intermediate Format, or CIF 2.0, is specified officially in *A Guide to LSI Implementation,* Second Edition, by R. W. Hon and C. H. Sequin, [110] and a nearly identical description appears in *Introduction to VLSI Systems*, by C. Mead and L. Conway. [111] This format is far simpler than GDSII and has the advantage that it is readable, using only ASCII characters. While providing nearly all of the functionality of GDSII, there are a few differences:

- Names of cells are not supported. Instead, cells are numbered.
- Datatypes are not supported. These are commonly used to assign different doses within a pattern. Therefore, proximity effect correction requires patterns to be split into multiple layers.
- There is no limit on the number of vertices in a polygon; therefore, CIF interpreters either set arbitrary values or simply run out of memory.
- The array structure (a square array of cells of n m elements) is not supported and so the users of CIF have invented extensions to the format. These extensions have not been added to the CIF standard.

CIF is widely used by universities using the Berkeley CAD tools to design circuits for the MOSIS integrated circuit foundry service. [112] MOSIS requires a number of sensible restrictions on CIF data: [113]

- Polygons (P) must have at least three points; other than this, arbitrary polygons are accepted.
- Wires (W) must have at least one point.
- Round Flashes (R) must have a non-zero diameter.
- The "delete definition" (DD) command is not allowed.
- Symbols (cells) may not be redefined.
- Lines are limited to 509 characters of text.
- The following ASCII characters should not be used as "blanks": square brackets ([]), single quotes ('), and periods (.).
- User extensions are allowed but ignored. Wires are extended beyond the two extreme endpoints by half the wire width.
- The comment layer has a name ending with the letter "X". All geometry on this layer is read by MOSIS but is totally ignored; however, any syntax error in this layer may cause the CIF file to be rejected.
- The bonding pad layer is named "XP" in all technologies.

2.6.5.3 DXF

DXF format is produced by the program AutoCAD as well as by a number of other inexpensive CAD programs for Windows/DOS and the Macintosh. These programs were not designed for lithography and so contain structures (e.g. three-dimensional figures) that have no meaning in this area. Also, the common jargon (e.g., "cell") has been replaced with less familiar terminology (e.g. "block"). Like CIF, this format does not support datatype numbers. DXF is useful only after it has been translated into GDSII by a program such as that sold by Artwork Conversion Software [108] or those of various mask vendors.

In DXF there can be considerable confusion over such issues as whether an enclosed line represents a polygon or an actual line. Translation programs support different subsets of DXF and translate the structures into GDSII using various sets of rules. Users of DXF are advised to submit sample patterns for conversion before investing a lot of time in CAD work, and to bear in mind that the DXF file used for

one vendor may not work at all for a different vendor. Therefore, the cost of data conversion should be considered when choosing an *apparently* inexpensive CAD tool.

2.6.5.4 PG3600

PG3600 and its predecessor PG3000 are used primarily by optical pattern generators built by GCA. These reticle printers use a high brightness lamp and a variable rectangular shutter to print patterns onto mask plates. The rectangle can be rotated to create angled features, and rectangular "flashes" are often overlapped to create curves, circles, and other shapes. Because of its popularity in reticle generation, many e-beam systems support the use of PG3600, even though the format would normally be considered low-level and machine specific. There are a number of disadvantages over GDSII:

- Overlaps must be removed by the conversion software. This can be very time consuming.
- The format is formally a specification for 9-track tape, using the EBCDIC character set. Some conversion programs require the disk format to use EBCDIC, and some allow a mapping into ASCII.
- Polygons in the CAD program are translated into overlapping rotated rectangles. This process is prone to error.
- Like CIF, datatypes are not supported, and so features with different doses must appear in different layers.
- A hierarchy of cells is not supported. The pattern must be "flat" and so may use a great deal of disk space.

2.6.6 Low-Level Formats

Conversion from one of the above formats to a machine-specific format usually involves flattening the hierarchy of cells, fracturing polygons into primitive shapes, and splitting the pattern into fields and subfields. The resulting machine-specific formats (e.g., MEBES, JEOL51, and BPD) usually use far more disk space than the hierarchical forms. These files must be carefully checked for software errors and may require manipulation for sizing, tone-reversal, mirroring, and so on. One way of verifying a conversion is simply to convert the low level format *back* to GDSII so that it can be displayed with the original CAD tool. Unfortunately, the pattern would have lost its cell structure, so the data set may be too large for the graphical editor. A special class of display and manipulation software is required that can handle very large, flat data sets.

The CATS program from Transcription Enterprises [114] and CAPROX from Sigma-C [115] offer not only viewing and manipulation of machine formats, but also will fracture GDSII directly into these formats. These conversion programs support machine formats from Etec Systems (MEBES, AEBLE), Hitachi, JEOL, Leica, GCA, and others. Operations include Boolean functions, tone reversal, rotation, sizing, and overlap removal. Sigma-C also offers a hierarchical proximity effect correction program. CATS can be combined with the proximity effect corrector PROXECCO from AISS GmbH. This software is an important alternative to the converters sold by e-beam manufacturers.

JEBCAD [116] is a less extensive, and less expensive, tool for viewing and manipulating JEOL and Leica formats. JEBCAD will read in GDSII, J01, SPD, and several low-level fractured formats; it will output machine formats for JEOL and Leica systems. Operations in JEBCAD include adding and deleting polygons, moving, copying, and adding arrays of objects.

Design Workshop [117] provides one of the most economical ways of producing machine specific formats for JEOL, Leica, and MEBES tools. DW2000's low-level fracturing modules are quite slow compared to alternative software, but are available at a small fraction of the cost.

2.7 Resists

Electron beam resists are the recording and transfer media for e-beam lithography. This section is not intended as a review of research in resists or as a guide to resist chemistry; for this, the reader is referred to Chap. 4 and to several review papers [118-122]. Instead, we present here a few standard resist systems and some useful recipes for processing and pattern transfer. The commercially available resists described here are summarized in Table 2.5.

The usual resists are polymers dissolved in a liquid solvent. Liquid resist is dropped onto the substrate, which is then spun at 1000 to 6000 rpm to form a coating [123]. Further details on resist application can be found in Chapter 4. After baking out the casting solvent, electron exposure modifies the resist, leaving it either more soluble (positive) or less soluble (negative) in developer. This pattern is transferred to the substrate either through an etching process (plasma or wet chemical) or by "liftoff" of material. In the liftoff process a material is evaporated from a small source onto the substrate and resist, as shown in Fig. 2.28. The resist is washed away in a solvent such as acetone or NMP (photoresist stripper). An undercut resist profile (as shown) aids in the liftoff process by providing a clean separation of the material.

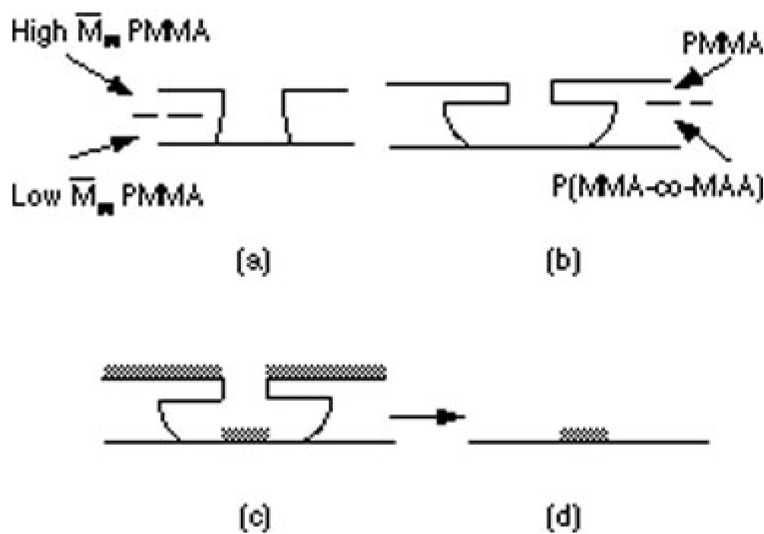

FIGURE 2.28 Two bilayer e-beam resist structures. (a) A high molecular weight PMMA is spun on top of a slightly more sensitive bottom layer of low molecular weight PMMA. The resist is developed in methyl isobutyl ketone:isopropanol (MIBK:IPA), typically 1:3, giving a slight undercut. (b) PMMA is spun on top of the copolymer P(MMA-co-MAA). The structure is typically developed in MIBK:IPA 1:1, giving a large undercut. In this case, MIBK develops PMMA and IPA develops the P(MMA-co-MAA). In the liftoff process metal is evaporated as shown in (c). The resist is then removed in a liquid solvent, leaving the pattern (d). Solvents such as acetone and methylene chloride are used to dissolve the resist.

If we expose a positive resist to a range of doses and then develop the pattern and plot the average film thickness versus dose, we have a graph as shown in Fig. 2.29. The sensitivity of the resist is defined as the point at which all of the film is removed. Ideally, the film thickness would drop abruptly to zero at the critical dose. In practice, the thickness line drops with a finite slope. If D_1 is the largest dose at which no film is lost [actually, the extrapolation of the linear portion of Fig. 2.29(a) to 100%] and if D_2 is the dose at which all of the film is lost [again, actually the extrapolation seen in Fig. 2.29(a)], then we define the contrast of the resist by

$$\log_{10}(D_2/D_1)^{-1} \quad (2.2)$$

The same expression defines the contrast of a negative resist (the film is retained where irradiated), when D_1 and D_2 are the points shown in Fig. 2.29(b).

A higher contrast resist will usually have a wider process latitude as well as more vertical sidewall profiles. In order to help minimize bias and proximity effects, positive resists should usually be exposed and/or developed as lightly as possible while still adequately clearing the resist down to the substrate for all features. In electron beam lithography, especially at beam voltages of 50 kV or more, it is possible to make resist structures with very high aspect ratios. Unfortunately, when the aspect ratio exceeds roughly 5:1, most resists undergo mechanical failure (features will fall over) during development, due primarily to surface tension in the rinse portion of the development sequence. [124] Recently, commercial software for simulating electron-beam exposure of polymer resists has become available. [125]

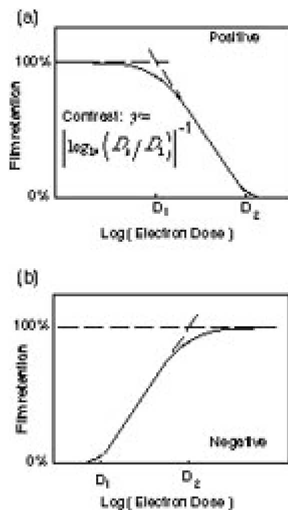

FIGURE 2.29 Film thickness versus exposure dose for (a) positive and (b) negative resist. Contrast is defined as the slope of the linear portion of the falling (or rising) section of the curve.

The primary goals of e-beam lithography are high resolution and high speed (high sensitivity). Unfortunately, the highest resolution resists are usually the least sensitive. We can see a reason for this trend when we consider the limit of resist sensitivity. If a very sensitive resist has a critical dose of 0.1 uC/cm^2, and a pixel is 0.1 um on a side, then only 62 electrons are needed to expose the pixel. [126] At this sensitivity, even small changes in the number of electrons will cause variations in the dose delivered to each pixel. If the sensitivity is increased further, then the number of electrons in each pixel becomes too small to allow an even exposure of the pattern. To look at it another way, if we wish to *decrease* the pixel size, then the resist will have to be made *less* sensitive to avoid statistical variations in the exposure. Although there is room for improving the sensitivity of both high and low resolution resists, the statistics of resist exposure will eventually limit the resist sensitivity and exposure rate.

In the following we describe some common resists, categorized as either positive (removed where exposed), or negative (retained where exposed), single layer or multilayer, and organic or inorganic.

2.7.1 Charge Dissipation

A common problem is the exposure of resist on insulating substrates. Substrate charging causes considerable distortion when patterning insulators and may contribute significantly to overlay errors even on semiconductors. [56] A simple solution for exposure at higher energies (>10 kV) is to evaporate a thin (10nm) layer of gold, gold-palladium alloy, chrome, or aluminum on top of the resist. Electrons travel through the metal with minimal scatter, exposing the resist. The film is removed before developing the resist. When using Au or Au/Pd, the metal film is removed from the top of the resist with an aqueous KI/I solution. [127] A chrome overlayer would be removed with chrome etch. [128] Aluminum can be removed from the resist with an aqueous base photoresist developer. Acid mixtures or photoresist developer for removing aluminum will sometimes react with exposed e-beam resist; therefore, aluminum is not the best choice for charge dissipation. When evaporating any metal, it is

important *not* to use an electron gun evaporator since x-rays and electrons in the evaporator will expose the resist.

Another approach to charge dissipation is the use of a conducting polymer, either as a planarizing layer under the resist or as a coating over the resist. The commercial polymers TQV (Nitto Chemical Industry) and ESPACER100 (Showa Denko) have been used for this purpose. [129-130] Both are coated at a thickness of about 55 nm and have a sheet resistance around 20 M/. TQV uses cyclohexanone as the casting solvent, which swells and dissolves novolac resins (present in most photoresists and SAL), and so a water-soluble PVA (polyvinyl alcohol) layer is needed to separate the resist from the TQV. ESPACER100 has the advantage that it is soluble in water and so can be coated directly onto many resists. TQV is removed with methyl isobutyl ketone/isopropanol (MIBK/IPA), the developer used for PMMA. ESPACER is removed in water. Other water soluble conducting polymers can be prepared from polyaniline doped with onium or triflate salts. [131-132]

2.7.2 Positive Resists

In the simplest positive resists, electron irradiation breaks polymer backbone bonds, leaving fragments of lower molecular weight. A solvent developer selectively washes away the lower molecular weight fragments, thus forming a positive tone pattern in the resist film.

2.7.2.1 PMMA

Polymethyl methacrylate (PMMA) was one of the first materials developed for e-beam lithography. [133-134] It is the standard positive e-beam resist and remains one of the highest resolution resists available. PMMA is usually purchased[135] in two high molecular weight forms (496 K or 950 K) in a casting solvent such as chlorobenzene or anisole. PMMA is spun onto the substrate and baked at 170C to 200C for 1 to 2 hours. Electron beam exposure breaks the polymer into fragments that are dissolved preferentially by a developer such as MIBK. MIBK alone is too strong a developer and removes some of the unexposed resist. Therefore, the developer is usually diluted by mixing in a weaker developer such as IPA. A mixture of 1 part MIBK to 3 parts IPA produces very high contrast [136] but low sensitivity. By making the developer stronger, say, 1:1 MIBK:IPA, the sensitivity is improved significantly with only a small loss of contrast.

The sensitivity of PMMA also scales roughly with electron acceleration voltage, with the critical dose at 50 kV being roughly twice that of exposures at 25 kV. Fortunately, electron guns are proportionally brighter at higher energies, providing twice the current in the same spot size at 50 kV. When using 50 kV electrons and 1:3 MIBK:IPA developer, the critical dose is around 350 uC/cm^2. Most positive resists will show a bias of 20 to 150 nm (i.e. a hole in the resist will be larger than the electron beam size), depending on the resist type, thickness, and contrast and development conditions and beam voltage.

When exposed to more than 10 times the optimal positive dose, PMMA will crosslink, forming a negative resist. It is simple to see this effect after having exposed one spot for an extended time (for instance, when focusing on a mark). The center of the spot will be crosslinked, leaving resist on the substrate, while the surrounding area is exposed positively and is washed away. In its positive mode, PMMA has an intrinsic resolution of less than 10 nm. [137] In negative mode, the resolution is at least 50 nm. By exposing PMMA (or any resist) on a thin membrane, the exposure due to secondary electrons can be greatly reduced and the process latitude thereby increased. PMMA has poor resistance to plasma etching, compared to novolac-based photoresists. Nevertheless, it has been used successfully as a mask for the etching of silicon nitride [138] and silicon dioxide, [139] with 1:1 etch selectivity. PMMA also makes a very effective mask for chemically assisted ion beam etching of GaAs and AlGaAs. [140]

EXAMPLE PROCESS: PMMA POSITIVE EXPOSURE AND LIFTOFF

1. Start with 496K PMMA, 4% solids in chlorobenzene. Pour resist onto a Si wafer and spin at 2500 rpm for 40 to 60 seconds.
2. Bake in an oven or on a hotplate at 180 C for 1 h. Thickness after baking: 300 nm.

3. Expose in e-beam system at 50 kV, with doses between 300 and 500 uC/cm^2. (Other accelerating voltages may be used. The dose scales roughly with the voltage.)
4. Develop for 1 min in 1:3 MIBK:IPA. Rinse in IPA. Blow dry with nitrogen.
5. Optional descum in a barrel etcher: 150W, 0.6 Torr O_2.
6. Mount in evaporator and pump down to 210^{-6} Torr.
7. Evaporate 10 nm Cr, then 100 nm Au.
8. Remove from evaporator, soak sample in methelyne chloride for ~10 min.

Agitate substrate and methylene chloride with an ultrasonic cleaner for ~1 min to complete the liftoff. Rinse in IPA. Blow dry. [141]

2.7.2.2 EBR-9

EBR-9 is an acrylate-based resist, poly(2,2,2-trifluoroethyl--chloroacrylate), [142] sold by Toray Inc. [143] This resist is 10 times faster than PMMA, ~10 C/cm^2 at 20 kV. Its resolution is unfortunately more than 10 times worse than that of PMMA, ~0.2 m. EBR-9 excels for mask writing applications, not because of its speed (PBS is faster) but because of its long shelf life, lack of swelling in developer, and large process latitude.

EXAMPLE PROCESS: EBR-9 POSITIVE MASK PLATE

1. Starting with plate purchased with a coating of EBR-9, skip to step 5. Starting with a mask plate purchased with a coating of photoresist, soak mask plate in acetone > 10 min to remove the photoresist. Rinse in isopropanol, blow dry.
2. Clean the plate with RIE in oxygen. *Do not* use a barrel etcher. RIE conditions: 30 sccm $O_{2,}$ 30 mTorr total pressure, 90 W (0.25 W/cm^2), 2 min
3. Immediately spin EBR-9, 4 krpm, 1 min 400 nm
4. Bake at 170 to 180 C oven for 1 h.
5. Expose with e-beam, 50 kV, 25 C/cm^2 Make sure the plate is well grounded. (Other accelerating voltages may be used. The dose scales roughly with the voltage.)
6. Develop for 4 min in 3:1 MIBK:IPA, rinse in IPA, blow dry in nitrogen
7. Descum -- important. Same as step 2 above, for only 5 s.
8. If this is a Cr plate, etch with Transene Cr etchant, ~1.5 min.
9. If this is a MoSi plate, then RIE etch: 0.05 Torr total pressure, 0.05 W/cm^2, 16 sccm SF_6 4.2 sccm CF_4, 1 min.
10. Plasma clean to remove resist: same as step 2 above, for 3 min.

2.7.2.3 PBS

Poly(butene-1-sulfone) is a common high-speed positive resist used widely for mask plate patterning. For high-volume mask plate production, the sensitivity of 1 to 2 C/cm^2 is a significant advantage over other positive resists. However, the processing of PBS is difficult and the only advantage is the speed of exposure. Plates must be spray developed at a tightly controlled temperature and humidity. [144] Contrast is poor, with ~2. For small to medium scale mask production, the time required for plate processing can make PBS slower than some photoresists. [145] (See Sect. 2.7.2.5.)

EXAMPLE PROCESS: PBS POSITIVE MASK PLATE

1. Start with plates spun with PBS. [146]
2. Expose, 25 kV, 1.0 to 1.6 C/cm^2 (Other accelerating voltages may be used. The dose will be different.)
3. Spray develop, 101 C, humidity 301%, in MIAK (5-methyl-2-hexanone) : 2-*pentanone* 3:1 [147] ~30 s.
4. Rinse in MIAK:2-propanol 3:2, 10 C. Spin dry under nitrogen.
5. Inspect pattern, repeat steps 3 and 4 as necessary.

6. Descum in a barrel etcher, 150 W, 0.6 Torr O_2, 0.5 min.
7. Bake to harden resist, 30 min 120 C. Heat and cool slowly.
8. Etch chrome in wet etch from Transene or Cyantek (acetic acid and ceric ammonium nitrate) ~1 min. Rinse in water. Blow or spin dry.
9. Strip PBS with RIE in O_2 or by soaking in acetone. (rinse in IPA, blow dry).

2.7.2.4 ZEP

A relative newcomer to e-beam lithography is ZEP-520 from Nippon Zeon Co. [148] ZEP consists of a copolymer of -chloromethacrylate and -methylstyrene. Sensitivity at 25 kV is between 15 and 30 C/cm^2, an order of magnitude faster than PMMA and comparable to the speed of EBR-9. Unlike EBR-9, the resolution of ZEP is very high -- close to that of PMMA. ZEP has about the same contrast as PMMA. Lines of width 10 nm with pitch 50 nm have been fabricated with this resist. [149-150] The etch resistance of ZEP in CF_4 RIE is around 2.5 times better than that of PMMA but is still less than that of novolac-based photoresists. ZEP is reported to have a long shelf life. [150] One disadvantage in using this resist is that (like PMMA) its sensitivity to electrons makes it difficult to inspect with a SEM. Resist lines shift and swell under high magnification SEM viewing, so it is necessary to judge the resolution of the resist by inspecting the etched patterns.

EXAMPLE PROCESS: ZEP PATTERNING OF SiO_2 HOLES

1. Prepare oxidized Si wafer. Spin ZEP-520 at 5 krpm for thickness 300 nm.
2. Bake at 170 C, 2 min.
3. Expose at 25 kV, 15 to 30 C/cm^2 (Other accelerating voltages may be used. The dose will be different.)
4. Develop in xylene:p-dioxane (20:1) for 2 min. Blow dry.
5. Descum in barrel etcher, 0.6 Torr of oxygen, 150W, 1 min.
6. Etch oxide in 4 min intervals (to avoid resist flow) 15 mTorr total pressure, 42 sccm CF_4, 5 sccm H_2, 0.03 W/cm^2; oxide etches at ~15 nm/min.
7. Remove residual resist with oxygen RIE: 30 sccm O_2, 30 mTorr total pressure, 0.25 W/cm^2, 5 min.

2.7.2.5 Photoresists as e-beam resists

Most photoresists can be exposed by e-beam, although the chemistry is quite different from that of UV exposure. [151] Because electrons cause both positive exposure and cross-linking at the same time, a photoresist film exposed with electrons must be developed with a strong developer for "positive" behavior, or, the same film can be blanket-exposed with UV light and then developed in a weak developer for "negative" behavior. One of the best photoresists for positive e-beam exposure is AZ5206. [152] [145] This resist has sensitivity around 6 uC/cm^2, contrast =4, and good etch resistance. With resolution around 0.25 um and very simple processing, AZ5206 is one of the best alternatives for high-speed mask production.

EXAMPLE PROCESS: AZ5206 POSITIVE MASK PLATE

1. Soak mask plate in acetone > 10 min to remove the original photoresist. Rinse in isopropanol, blow dry.
2. Clean the plate with RIE in oxygen. *Do not* use a barrel etcher. RIE conditions: 30 sccm O_2, 30 mTorr total pressure, 90 W (0.25 W/cm^2), 5 min.
3. Immediately spin AZ5206, 3 krpm.
4. Bake at 80 C for 30 min.
5. Expose with e-beam, 10 kV, 6 C/cm^2, Make sure the plate is well grounded. (Other accelerating voltages may be used, but the dose will be different.)
6. Develop for 60 s in KLK PPD 401 developer. Rinse in water.
7. Descum - important Same as step 2 above, for only 5 seconds, Or use a barrel etcher, 0.6 Torr oxygen, 150W, 1 min.

8. If this is a Cr plate, etch with Transene Cr etchant, ~1.5 min. If this is a MoSi plate, then RIE etch: 0.05 Torr total pressure, 0.05 W/cm^2, 16 sccm SF_6, 4.2 sccm CF_4,1 min.
9. Plasma clean to remove resist: same as step 2 above, for 3 min.

Other UV sensitive resists used for e-beam include EBR900 [153] from Toray, [143] (8 uC/cm^2 at 20 kV), the chemically amplified resist ARCH [154] from OCG, [155] (8-16 uC/cm^2 at 50 kV), and the deep-UV resists UVIII and UVN from Shipley. [156-157] The latest offerings from Shipley have been optimized for DUV (248 nm) exposure, and have higher resolution than that of AZ5206. The use of DUV resists allows exposure by both photons and electrons in the same film, thereby reducing e-beam exposure time.

2.7.3 Negative Resists

Negative resists work by cross-linking the polymer chains together, rendering them less soluble in the developer. Negative resists tend to have less bias (often zero) than positive resists. However, they tend to have problems with scum (insoluble residue in exposed areas), swelling during development, and bridging between features.

A reasonable starting point for developing a negative resist process is to choose a development time twice as long as the time needed to clear the unexposed resist and an exposure dose just sufficient to ensure acceptable resist thickness loss on all features (e.g., no more than 10%). From there, fine tuning of development time, dose, and postexposure bake conditions may be needed to optimize feature sizes, improve critical dimension control, and minimize resist scum.

2.7.3.1 COP

COP is an epoxy copolymer of glycidyl methacrylate and ethyl acrylate, P(GMA-co-EA), commonly used for negative exposure of mask plates. [147] [122] This is a very high speed resist, 0.3 C/cm^2 at 10 kV, with relatively poor resolution (1 um). [158] COP also has relatively poor plasma etch resistance and requires spray development to avoid swelling. Because cross-linking occurs by cationic initiation and chain reaction, the cross-linking continues after exposure. Therefore, the size of features depends on the time between exposure and development. Unless speed is very critical, COP is probably not a good choice for a negative resist.

EXAMPLE PROCESS: COP NEGATIVE MASK PLATE

1. Soak mask plate in acetone > 10 min to remove photoresist. Rinse in isopropanol, blow dry.
2. Clean the plate with RIE in oxygen. *Do not* use a barrel etcher. RIE conditions: 30 sccm O_2, 30 mTorr total pressure, 90 W (0.25 W/cm^2), 2 min.
3. Immediately spin COP, 3 krpm
4. Expose, 10 kV, 0.3 C/cm^2 (Other accelerating voltages may be used. The dose will be different.)
5. Spray develop, MEK (methyl ethyl ketone) : ethanol 7:3 for ~30 s.
6. Rinse in MIBK (methyl isobutyl ketone) : isopropanol 1:3 for ~30 s (using spray or spinner).
7. Rinse in isopropanol for ~30 s. (spray or spinner). Blow dry with nitrogen.
8. Inspect pattern, repeat steps 5-7 as necessary.
9. Descum in a barrel etcher, 150 W, 0.6 Torr O_2, 0.5 min.
10. Etch chrome in wet etch from Transene or Cyantek (acetic acid and ceric ammonium nitrate) ~1 min. Rinse in water. Blow or spin dry.
11. Strip with RIE in O_2 or by soaking in acetone. (rinse in IPA, blow dry).

2.7.3.2 Shipley SAL

Shipley Inc. [156] produces the popular SAL resist, which comes in a variety of versions and viscocities. SAL has three components: a base polymer, an acid generator, and a crosslinking agent. After exposure, a baking cycle enhances reaction and diffusion of the acid catalyst, leading to resist hardening by cross-linking. Common alkaline photoresist developers will dissolve the unexposed regions. The acid reaction and diffusion processes are important factors in determining the resolution, [159] and a tightly controlled postexposure baking process is required. The postexposure bake is usually on a feedback-controlled hotplate with a suction holder to ensure good thermal contact. The extent of the cross-linking reaction is therefore affected by the thermal conductivity of the sample and by the cooling rate after the bake. Resolution of 30 nm has been demonstrated at very low voltage, [160] and 50 nm wide lines have been fabricated using high voltage. [161] SAL-606 has 0.1 um resolution in 0.4 um thick films, exposed with 40 keV electrons at 8.4 uC/cm^2.

The novolac base polymer has etching properties similar to those of positive photoresists. Unlike photoresist, the shelf life of SAL is on the order of six months at room temperature. Refrigeration extends the shelf life to several years, but care is required to avoid condensation when the resist is dispensed to smaller containers. SAL is a sensitive resist, 7 to 9 uC/cm^2 at either 20 or 40 kV, and so is suitable for mask writing. It is interesting to note that, unlike PMMA, the critical dose of SAL does not scale proportionately with accelerating voltage. Although it is not as sensitive as other negative resists (COP, CMS, or GMC) SAL has far better process latitude and resolution.

EXAMPLE PROCESS: SAL NEGATIVE MASK PLATE

1. Soak mask plate in acetone > 10 min to remove photoresist.
2. Clean the plate with RIE in oxygen. *Do not* use a barrel etcher. RIE conditions: 30 sccm O_2, 30 mTorr total pressure, 90 W (0.25 W/cm^2), 5 min.
3. Immediately spin SAL-601, 4 krpm, 1 min.
4. Bake in 90 C oven for 10 min. This resist is not sensitive to room light.
5. Expose at 50 kV, 11 C/cm^2. Be sure the plate is grounded.
6. Post-bake for 1 min on a large hotplate, 115 C.
7. Cool for > 6 min.
8. Develop for 6 min in Shipley MF312:water (1:1) Be sure to check for underdevelopment.
9. Descum 30 s with oxygen RIE: same as step 2, 10 s.
10. Etch with Transene or Cyantek Cr etchant, ~1.5 min.
11. Plasma clean to remove resist: Same as step 2, 5 min.

2.7.3.3 Noncommercial negative resists: P(SI-CMS) and EPTR

Although not yet commercialized, a very promising negative resist is P(SI-CMS), which combines the high speed of CMS (chloromethylstyrene) with the etch resistance of SI (trimethylsilylmethyl methacrylate). This resist offers at least 10 times the plasma etch resistance of SAL. [162-164] Its silicon component gives excellent resistance to etching in an oxygen plasma by forming a surface layer of silicon oxide. The sensitivity is similar to that of SAL (~10 uC/cm^2 at 40 kV) but the resolution is around 0.2 um. P(SI-CMS) will be a good choice when etch resistance is more important than resolution.

The epoxy type resist [165-167] developed at IBM is a combination of a novolac epoxy resin (*o*-cresol novolac glycidyl ether) and an onium salt (triphenylsulfonium hexafluoroantimonate) photoinitiator. EPTR is a high-speed resist (6 uC/cm^2 at 50 kV) with relatively high contrast (= 6.4) and high resolution (50 nm). While the resolution of EPTR is comparable to that of Shipley SAL, the epoxy formulation allows EPTR to be extended to layer thicknesses exceeding 200 um. [168] The high aspect ratio and thicknesses accessible with EPTR make it uniquely suited for micromechanical applications.

Table 2.5. Comparison of commercially available electron beam resists.

	Tone	Resolution (nm)	Sensitivity at 20 kV (uC/cm^2)	Developer	Contact reference
PMMA	positive	10	100	MIBK:IPA	[135]
EBR-9	positive	200	10	MIBK:IPA	[143]
PBS	positive	250	1	MIAK : 2-Pentanone 3:1	[147]
ZEP	positive	10	30	xylene : p-dioxane	[148]
AZ5206	positive	250	6	KLK PPD 401	[152]
COP	negative	1000	0.3	MEK : ethanol 7:3	[147]
SAL-606	negative	100	8.4	MF312 : water	[156]

2.7.4 Multilayer Systems

2.7.4.1 Low/high molecular weight PMMA

Multilayer resist systems are useful for several purposes: when an enhanced undercut is needed for lifting off metal, when rough surface structure requires planarization, and when a thin imaging (top) layer is needed for high resolution. Figure 2.28 showed the simplest bilayer technique, where a high molecular weight PMMA is spun on top of a low molecular weight PMMA. The low weight PMMA is more sensitive than the top layer, so the resist develops with an enhanced undercut. At high energies (>20 kV), thin PMMA (<0.5 m) will not normally develop an undercut profile; the best resist profile will be perpendicular to the substrate. The moderate undercut from this technique is useful when liftoff is required from densely packed features.

The two-layer PMMA technique was patented in 1976 by Moreau and Ting [169] and was later improved by Mackie and Beaumont [170] by the use of a weak solvent (xylene) for the top layer of PMMA. Use of a weak solvent prevents intermixing of the two layers. A further refinement of the technique [171] substituted MIBK, a solvent of intermediate strength, for the xylene. PMMA of various molecular weights dissolved in MIBK can now be purchased commercially. [172]

EXAMPLE PROCESS: LIFTOFF OF THIN METAL WITH PMMA BILAYER

1. Clean wafer, on the spinner, by spraying with acetone, then isopropanol. Spin dry.
2. Spin 495 K MW PMMA, 2% (in any solvent) 4 krpm for 30 s., for a thickness ~50 nm.
3. Bake at 170-180C for 1 h.
4. Spin 950 K MW PMMA, 2% in MIBK 4krpm for 30 s., for a thickness ~50 nm.
5. Bake at 170-180C for 1 h.
6. Expose at 50 kV, 350 to 450 C/cm^2.
7. Develop in MIBK:IPA, 1:3 for 1 min. Rinse in IPA, blow dry.
8. Optionally, remove surface oxide of GaAs with 10 s dip in NH_4OH : H_2O (1:15). Blow dry.
9. Evaporate 15 nm of Au:Pd (3:2) alloy, 210^{-6} Torr, base pressure, 0.5 nm/s.
10. Lift off by soaking in methylene chloride. Optionally, finish with mild ultrasonic agitation.

2.7.4.2 PMMA/copolymer

A larger undercut resist profile is often needed for lifting off thicker metal layers. One of the first bilayer systems was developed by Hatzakis. [173] In this technique a high sensitivity copolymer of methyl

methacrylate and methacrylic acid [P(MMA-MAA)] [174] is spun on top of PMMA. The exposed copolymer is soluble in polar solvents such as alcohols and ethers but insoluble in nonpolar solvents such as chlorobenzene. A developer such as ethoxyethanol/iso-propanol is used on the top (imaging) layer, stopping at the PMMA. Next, a strong solvent such as chlorobenzene or toluene is used on the bottom layer. This technique has been used to fabricate 1 um memory arrays with thick gate metalizations.

A more common use of P(MMA-MAA) is as the *bottom* layer, with PMMA on top. In this case the higher speed of the copolymer is traded for the higher resolution of PMMA. [175] For simplicity a single developer is used -- the nonpolar solvent working on the PMMA and the polar solvent developing the copolymer. Effective developer combinations include ethylene glycol monoethyl ether : methanol (3:7) and MIBK:IPA (1:1). The undercut of this process is so large that it can be used to form free-standing bridges of PMMA, a technique developed by Dolan [176] and used extensively for the fabrication of very small superconducting tunnel junctions. Other shadowing and "step edge" techniques for fabricating small lines and junctions are covered in the chapter by Howard and Prober. [177] The polymer PMGI (polydimethylglutarimide) is used for the same purpose as P(MAA-MAA). [178-179]

2.7.4.3 Trilayer systems

Bilayer techniques using P(MMA-MAA) or PMGI work well because the polar/nonpolar combination avoids intermixing of the layers. Almost any two polymers can be combined in a multilayer if they are separated by a barrier such as Ti, SiO_2, aluminum, or germanium, [175] [177] forming a so-called trilayer resist. After the top layer is exposed and developed, the pattern is transferred to the interlayer by RIE in CF_4 (or by Cl_2 in the case of aluminum). The interlayer serves as an excellent mask for RIE in oxygen. The straight etch profile available from oxygen RIE allows the fabrication of densely packed, high aspect ratio resist profiles. Such resist profiles can then be used for liftoff or for further etching into the substrate.

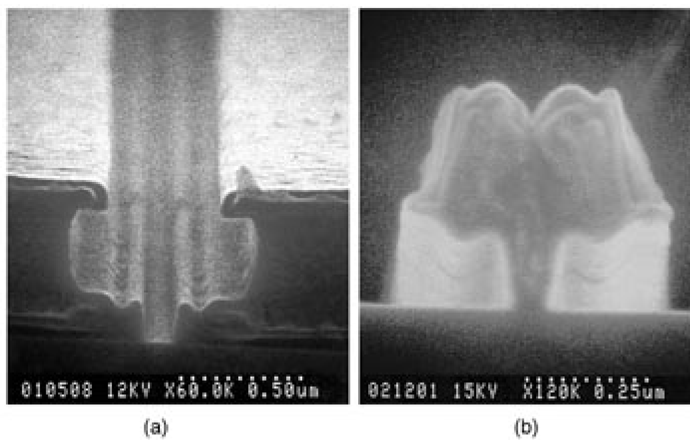

FIGURE 2.30 (a) Resist cross-section (PMMA on P(MMA-MAA) on PMMA) for the lift-off of a "T" shaped gate. (b) Metal gate lifted off on GaAs. (Courtesy of R. C. Tiberio et al. [180])

If we start with Hatzakis's bilayer scheme (PMMA on the bottom and copolymer on the top) and then add another top layer of PMMA, we have a structure that can be developed into a mushroom shape, [180] as shown in Fig. 2.30. In this technique a heavy dose is given to the central line and a lighter dose to the sides. Mutually exclusive developers are used to form the "T-gate" shape, and a thick layer of metal is lifted off. This technique is widely used to form MESFET gates with low capacitance and low leakage (from the small contact area) and low resistance (from the large metal cross-section).

2.7.5 Inorganic and Contamination Resists

Some of the first high-resolution e-beam exposures were made with "contamination lithography" -- by simply using the electron beam to crack contaminants sorbed onto the substrate. These carbonaceous and silicaceous contaminants are produced from oil in the vacuum pumps or from organic residue on the sample surface. By using the contamination as a mask for ion milling, wires as narrow as 50 nm were made in the 1960s. [181] Later, the technique was used for fabricating nanometer-scale superconducting devices [182] and metal lines for the study of electron transport in mesoscopic devices. [183]

The dose required for the deposition of contamination depends on how much oil and other contaminants are in the vacuum system (an untrapped diffusion pump provides an ample supply), but the dose is very high, typically in the range of 0.1 to 1 C/cm^2. The high dose limits its application to very sparse patterns. Cracked hydrocarbons provide poor selectivity for etching or milling, so the choice of metals is also limited (for instance, it is not practical to pattern aluminum this way). The contamination can be easily cleaned by heating the substrate to ~100 C.

Another technique for producing nanometer-scale patterns - again using doses on the order of 1 C/cm^2 -- is the use of metal fluorides. A high current density of electrons causes the dissociation of materials such as AlF_3, MgF_2, NaCl, LiF, KCl, and CaF_2 [184] at doses around 10 to 20 C/cm^2. At lower doses (1 to 3 C/cm^2) AlF_3 acts as a negative resist, developed in water. [185]

One reason for the very high resolution is that these materials are modified by the primary beam of electrons and are insensitive to the much larger spread of secondary electrons. The highest resolution patterns were formed in NaCl crystals, where 50 keV electrons were used to drill holes of ~1.5 nm diameter, [186] but the patterns could not be transferred to any useful material. While negatively exposed AlF_3 makes an excellent etch mask [185] for fluorine-based RIE, the process has not been applied to any useful devices. Recent research in metallic compound resists [187-188] has concentrated on mixing AlF_3 and LiF to reduce the dose needed for dissociation, to provide more uniform films, and to expose these films with the lower current density and lower voltage (20 to 50 kV) available in common e-beam exposure tools. Slots in these films of width 5 nm have been made with 30 keV electrons. [188] At doses similar to those of the metal fluorides, silicon dioxide [189] has also been used for nanometer-scale patterning.

2.7.6 Other Research: Scanning Probes and Thin Imaging Layers

A great deal of research in electron-beam exposure of nanometer-scale patterns is in the field of scanning probe microscopy (SPM), which is covered in Sect. 8.3.3. For an excellent review of SPM lithography, see also the review article by Shedd and Russel. [92]

At low voltage (1 kV) and at higher energies, self-assembled monolayer [190-191] films have demonstrated high resolution but suffer from a very high defect density and difficulty in pattern transfer. Very thin films with lower defect density have been fabricated with Langmuir-Blodgett techniques. [192] Such thin imaging layers are important for low voltage[193] exposures and in-situ processing. However, the imaging layer must be transferred into an intermediate film which is subsequently used as the etch or liftoff mask. This process adds substantially to the cost and complexity of processing. An alternative approach to generating a thin imaging layer on top of a thick resist is the use of surface silylation. In the PRIME silylation process [193-196] electron beam exposure *prevents* the subsequent silylation of (attachment of silicon containing molecules to) the resist surface. The silylated regions act as a mask for oxygen plasma etching of the resist film.

2.8 Acknowledgements

The authors would like to thank the many people who helped in the editing, proofreading, and checking of this chapter; primarily the SPIE reviewer and copy editor, and including also **Sylvia**

Chanak (Cadence), **Dennis Costello** (Cornell), **Mark Gesley** (Etec), **George Lanzarotta** (Raith), **Alex Liddle** (Lucent), **Francois Marquis** (Design Workshop), **Beth Moseley** (Hitachi), **Joseph Nabity** (Nabity Lithography Systems), **Yasutoshi Nakagawa** (JEOL), **Hans Pfeiffer** (IBM), **Rainer Plontke** (Leica Jena), **John Poreda** (Lepton), and **Bernard Wallman** (Leica).

2.9 Appendix: GDSII Stream Format

Portions of the GDSII Stream Format Manual, Documentation No. B97E060, Feb. 1987, reprinted with permission of Cadence Design Systems, Inc., 555 River Oaks Parkway, San Jose, CA 95134. See also the web site http://www.cadence.com.

The following is a description of the GDSII Stream data format (Release 6.0), the most commonly used format for electron beam lithography and photomask production [197]. This appendix omits the description of tape formatting, since disk files and disk file images on tape and other media are now the norm [198].

The pattern data is considered to be contained in a "library" of "cells". Cells may contain geometrical objects such as polygons (boundaries), paths, and other cells. Objects in the cell are assigned to "layers" of the design. Different layers typically represent different processing steps for exposure on separate mask plates. Geometrical objects may also be tagged with "datatypes", which can be used for any purpose, but are most commonly used to group together similarly sized objects for compensation of the proximity effect.

There is no explicitly stated limit to the level of hierarchy (the degree of cell nesting); however, most CAD programs impose a limit of around 32 levels. GDSII interpreters will either impose such a limit explicitly, or will impose an implicit limit by running out of memory during recursive operations.

2.9.1 Order of records:

A GDSII Stream file has a great deal of flexibility, but must contain at least the following:

1. A header record
2. One or more Stream records
3. Library name record
4. End of library token

An example of a common record order (see below for record descriptions) follows:

HEADER	version number
BGNLIB	last modification date
LIBNAME	library name
GENERATIONS	see below
UNITS	data units
BGNSTR	begin structure
STRNAME	structure name
BOUNDARY	begin boundary (polygon)
LAYER	layer number
DATATYPE	a label associated with this item
XY	coordinates
ENDEL	end of element
(etc.)	
ENDSTR	end of structure (cell)
ENDLIB	end of library

2.9.2 Record description

The GDSII Stream file format is composed of variable length records. The minimum record length is four bytes. Records can be infinitely long. The first four bytes of a record are the header. The first two bytes of the header contain a count (in eight-bit bytes) of the total record length. The count tells you where one record ends and another begins. The next record begins immediately after the last byte included in the count. The third byte of the header is the record type (also known as a "token"). The fourth byte of the header describes the type of data contained within the record (see table below). The fifth through last bytes of a record are data.

2.9.3 Data type description

The data type value is found in the fourth byte of the record. Possible types and values are:

Data Type	Value
No data present	0
Bit array	1
Two-byet signed integer	2
Four-byte signed integer	3
Four-byte real (not used)	4
Eight-byte real	5
ASCII string	6

Two- and four-byte signed integers use the usual twos complement format for negative values. The more significant bytes appear first in the file, so that by default no byte swapping is required when reading the integers with a big-endian CPU (e.g., Intel processors). Byte swapping is required when reading or writing integers with a little-endian machine, such as a VAX.

Real numbers are *not* represented in IEEE format. A floating point number is made up of three parts: the sign, the exponent, and the mantissa. The value of the number is defined to be (mantissa) $(16)^{(\text{exponent})}$. If "S" is the sign bit, "E" are exponent bits, and "M" are mantissa bits then an 8-byte real number has the format

SEEEEEEE MMMMMMMM MMMMMMMM MMMMMMMM
MMMMMMMM MMMMMMMM MMMMMMMM MMMMMMMM

The exponent is in "excess 64" notation; that is, the 7-bit field shows a number that is 64 greater than the actual exponent. The mantissa is always a positive fraction greater than or equal to 1/16 and less than 1. For an 8-byte real, the mantissa is in bits 8 to 63. The decimal point of the binary mantissa is just to the left of bit 8. Bit 8 represents the value 1/2, bit 9 represents 1/4, and so on.

In order to keep the mantissa in the range of 1/16 to 1, the results of floating point arithmetic are *normalized.* Normalization is a process whereby the mantissa is shifted left one hex digit at a time until its left *four* bits represent a non-zero quantity. For every hex digit shifted, the exponent is decreased by one. Since the mantssa is shifted four bits at a time, it is possible for the left three bits of a normalized mantissa to be zero. A zero value is represented by a number with all bits zero. The representation of negative numbers is the same as that of positive numbers, except that the highest order bit is 1, not 0.

2.9.4 Record types

Records are always an even number of bytes long. If a character string is an odd number of bytes long it is padded with a null character. The following is a list of record types. The first two numbers in brackets are the record type and the last two numbers in brackets are the data type (see the table

above). *Note that the data type (e.g. "two-byte signed integer") refers to the type of data to follow in the record, not to the number of bytes in the record.* The first two bytes of the record *header* contain a count (in eight-bit bytes) of the total record length. The third byte of the header is the record type (also known as a "token") shown below, and the fourth byte is the data type. All record numbers are shown in hexidecimal. For example, in the HEADER record, "00" is the token, and "02" is the data type.

HEADER [0002]
: Two-byte signed integer: contains data representing the GDSII version number. Values are 0, 3, 4, 5, and 600. With release 6.0 the bersion number changes to three digits.

BGNLIB [0102]
: Two-byte signed integer: contains last modification time of library (two bytes each for the year, month, day, hour, minute, and second) as well as time of last access (same format) and marks beginning of library.

word 1	0x1C (hex) # bytes in record
word 2	0x0102 (the token for bgnlib)
word 3	year of last modification
words 4-8	month, day, hour, minute, second
word 9	year of last access time
words 10-14	month, day, hour, minute, second

LIBNAME [0206]
: ASCII string: contains a string which is the library name. The string must adhere to CDOS file name conventions for length and valid characters, and may contain file extensions such as ".db".

UNITS [0305]
: Eight-byte real: contains 2 8-byte real numbers. The first is the size of a database unit in user units. The second is the size of a database unit in meters. For example, if your library was created with the default units (user unit = 1 m and 1000 database units per user unit), then the first number would be 0.001 and the second number would be 10^{-9}. Typically, the first number is less than 1, since you use more than 1 database unit per user unit. To calculate the size of a user unit in meters, divide the second number by the first.

ENDLIB [0400]
: No data is present. This marks the end of a library.

BGNSTR [0502]
: Two-byte signed integer: contains creation time and last modification time of a structure (in the same format as that of BGNLIB) and marks the beginning of a structure.

STRNAME [0606]
: ASCII string: contains a string which is the structure name. A structure name may be up to 32 characters long. Legal characters are 'A' through 'Z', 'a' through 'z', '0' through '9', underscore, question mark, and the dollar sign, '$'.

ENDSTR [0700]
: No data is present. This marks the end of a structure.

BOUNDARY [0800]
: No data is present. This marks the beginning of a bounary element (polygon).

PATH [0900]
: No data is present. This marks the beginning of a path element.

SREF [0A00]
: No data is present. This marks the beginning of a structure reference element (a reference or "call" to another cell in the library).

AREF [0B00]
: No data is present. This marks the beginning of an array reference element (an array of cells).

TEXT [0C00]
: No data is present. This marks the beginning of a text element.

LAYER [0D02]
: Two-byte signed integer: contains the layer number. The value must be from 0 to 63.

WIDTH [0F03]	Four-byte integer: contains the width of a path or text lines in database units. A negative value for width means that the width is absolute; i.e., I is not affected by the magnification factor of any parent reference. If omitted, zero is assumed.
XY [1003]	Four-byte signed integer: contains an array of XY coordinates in database units. Each X or Y coordinate is four bytes long. Path and boundary elements may have up to 200 pairs of coordinates. A path must have at least 2, and a boundary at least 4 pairs of coordinates. The first and last point of a boundary must coincide. A text or SREF element must have only one pair of coordinates. An AREF has exactly three pairs of coordinates, which specify the orthogonal array lattice. In an AREF the first point locates a position which is displaced from the reference point by the inter-column spacing times the number of columns. The third point locates a position which is displaced from the reference point by the inter-row spacing times the number of rows. A node may have from 1 to 50 pairs of coordinates. A box must have five pairs of coordinates with the first and last points coinciding.
ENDEL [1100]	No data is present. This marks the end of an element.
SNAME [1206]	ASCII string: contains the name of a referenced structure.
COLROW [1302]	Two-byte signed integers: the first 2 bytes contain the number of columns in the array. The third and fourth bytes contain the nunber of rows. Neither the number of columns nor the number of rows may exceed 32,767 (decimal) and both are positive.
NODE [1500]	No data is present. This marks the beginning of a node.
TEXTTYPE [1602]	Two-byte signed integer: contains the text type. The value of the text type must ge in the range of 0 to 63.
PRESENTATION [1701]	Bit array: contains 2 bytes of bit flags for text presentation. Bits 10 and 11, taken together as a binary number, specify the font. Bits 12 and 13 specify the vertical presentaton (00 means top, 01 means middle, and 10 means bottom). Bits 0 through 9 are reserved for future use and must be cleared. If this record is omitted, then top-left justification and font 0 are assumed.
STRING [1906]	ASCII String: contains a character string for text presentation, up to 512 characters long.
STRANS [1A01]	Bit array: contains two bytes of bit flags for SREF, AFREF, and text transformation. Bit 0 (leftmost) specifies reflecton. If it is set, then reflection about the X axis is applied before angular rotation. For AREFs, the entire array lattice is reflected, with the individual array elements riidly attached. Bit 13 flags absolute magnification. Bit 14 flags absolute angle. Bit 15 (rightmost) and all remaining bits are reserved for future use and must be cleared. If this record is omitted, then the element is assumed to have no reflection and its magnification and angle are assumed to be non-absolute.
MAG [1B05]	Eight-byte real: contains a magnification factor. If omitted, a magnification of 1 is assumed.
ANGLE [1C05]	Eight-byte real: contains the angular rotation factor, measured in degrees, counterclockwise. For an AREF, the angle rotates the entire array lattice (with the individual array elements regidly attached) about the array reference point. If this record is omitted, and algle of zero degrees is assumed.
REFLIBS	ASCII string: contains the names of the reference libraries. This record must be

[1F06]	present if there are any reference libraries bound to the current library. The name for the first reference library starts at byte 0 and the name of the second library starts at byte 45 (decimal). The reference library names may include directory specifiers (separated with ":") and an extension (separated with "."). If either library is not named, its place is filled with nulls.
FONTS [2006]	ASCII string: contains names of textfont definition files. This record must be present if any of the 4 fonts have a corresponding textfont definition file. This record must not be present if none of the fonts have a textfont file. The name of font 0 starts the record, followed by the remaining 3 fonts. Each name is 44 bytes long and is null if there is no corresponding textfont definition. Each name is padded with nulls if it is shorter than 44 bytes. The textfont definition file names may include directory specifiers (separated with ":") and an extension (separated with ".").
PATHTYPE [2102]	Two-byte signed integer: contains a value of 0 for square-ended paths that end flush with their endpoints, 1 for round-ended paths, and 2 for square-ended paths that extend a half-width beyond their endpoints. Pathtype 4 signifies a path with variable square-end extensions (see BGNEXTN and ENDEXTN).
GENERATIONS [2202]	Two-byte signed integer: contains a positve count of the number of copies of deleted or backed-up structures to retain. This number must be at least 2 and not more than 99. If the GENERATIONS record is not present, a value of 3 is assumed.
ATTRTABLE [2306]	ASCII string: contains the name of the attribute definition file. This record is present only if there is an attribute definition file bound to the library. The attribute definition file name may include directory specifiers and an extension (see FONTS). Maximum size is 44 bytes.
EFLAGS [2601]	Bit array: contains 2 bytes of bit flags. Bit 15 (rightmost) specifies template data. Bit 14 specifies external data (also referred to as "exterior" data). All other bits are currently unused and must be cleared to 0. If this record is omitted, then all bits are assumed to be 0. Further information about template data can be found in the *GDSII Reference Manual*. Information about external data can be found in the *CustomPlus User's Manual*.
NODETYPE [2A02]	Two-byte signed integer: contains the node type. The value of the node type must be in the range of 0 to 63.
PROPATTR [2B02]	Two-byte signed integer: contains the attribute number. The attribute number is an integer from 1 to 127. Attribute numbers 126 and 127 are reserved for the user integer and user string properties, which existed prior to Release 3.0.
PROPVALUE [2C06]	ASCII string: contains the string value associated with the attribute named in the preceding PROPATTR record. Maximum length is 126 characters. The attribute-value pairs associated with any one element must all have distinct attribute numbers. Also, there is a limit on the total amount of property data that may be associated with any one element: the total length of all the strings, plus twice the number of attribute-value pairs, must not exceed 128 (or 512 of the element is an sref, aref, or node). For example, if a boundary element used a property attribute 2 with property value "metal", and property attribute 10 with property value "property", then the total amount of property data would be 18 bytes. This is 6 bytes for "metal" (odd length strings are padded with a null) plus 8 for "property" plus 2 times the 2 attributes (4) equals 18.

The following records are not supported by Stream Release 3.0:

BOX [2D00]	No data is present. This marks the beginning of a box element.
BOXTYPE [2E02]	Two-byte signed integer: contains the box type. The value of the boxtype must be in the range of 0 to 63.
PLEX [2F03]	Four-byte signed integer: a unique positive number which is common to all elements of the plex to which this element belongs. The head of the plex is flagged by setting the

seventh bit; therefore, plex numbers should be small enough to occupy only the rightmost 24 bits. If this record is omitted, then the element is not a plex member.

Plex numbers are not commonly used.

BGNEXTN [3003]	Four-byte signed integer: applies to pathtype 4. Contains four bytes which specify in database units the extension of a path outline beyond the first point of the path. The value can be negative.
EXDEXTN [3103]	Four-byte signed integer: Applies to pathtype 4. Contains four bytes which specify in database units the extension of a path outline beyond the last point of the path. The value can be negative.
MASK [3706]	ASCII string: Required for Filtered format, and present only in Filtered Stream files. Contains the list of layers and data types included in the data file (usually as specified by the user when generating the Stream file). At least one MASK record must follow the FORMAT record. More than one MASK record may follow the FORMAT record. The last MASK record is followed by the ENDMASKS record. In the MASK list, data types are separated from the layers witha semicolon. Individual layers or data types are separated with a space. a range of layers or data types is specified with a dash. An example MASK list looks like this: 1 5-7 10 ; 0-63
ENDMASKS [3800]	No data is present. This is required for Filtered format, and is present only in a Filtered Stream file. This terminates the MASK records. The ENDMASKS record must follow the last MASK record. ENDMASKS is immediately followed by the UNITS record.
LIBDIRSIZE [3902]	Two-byte signed integer: contains the number of pages in the Library directory. This information is used only when reading the data into a new library. If this record is present, it should occur between the BGNLIB record and the LIBNAME record.
SRFNAME [3A06]	ASCII string: contains the name of the Sticks Rules File, if one is bound to the library. This informationis used only when reading the data into a new library. If this record is present, it should occur between the BGNLIB and LIBNAME records.
LIBSECUR [3B02]	Two-byte signed integer: contains an array of Access Control List (ACL) data. There may be from 1 to 32 ACL entries, each consisting of a group number, a user number, and access rights. This information is used only when reading the data into a new library. If this record is present, it should occur between the BGNLIB and LIBNAME records.

The following record types are either not used, not released, or are related to tape formatting:

TEXTNODE	[1400]
SPACING	[18]
UINTEGER	[1D]
USTRING	[1E]
STYPTABLE	[2406]
STRTYPE	[2502]
ELKEY	[2703]
LINKTYPE	[28]
LINKKEYS	[29]
TAPENUM	[3202]
TAPECODE	[3302]
STRCLASS	[3401]
RESERVED	[3503]

2.9.5 Stream syntax in Bachus Naur representation

An element shown below in CAPITALS is the name of an actual record type. An element shown in lower case means that name can be further broken down in to a set of record types. The following table summarizes the Bachus Naur symbols:

<table>
<tr><th>Symbol</th><th>Meaning</th></tr>
<tr><td>: :</td><td>"Is composed of"</td></tr>
<tr><td>[ ]</td><td>An element which can occur zero or one time.</td></tr>
<tr><td>{ }</td><td>Choose one of the elements within the braces.</td></tr>
<tr><td>{ } *</td><td>The elements within the braces can occur zero or more times.</td></tr>
<tr><td>{ } +</td><td>The elements within braces must occur one or more times.</td></tr>
<tr><td>< ></td><td>These elements are further defined in the Stream syntax list.</td></tr>
<tr><td>|</td><td>"Or"</td></tr>
</table>

<table>
<tr><td><stream format> ::=</td><td>HEADER BGNLIB [LIBDIRSIZE] [SRFNAME] [libsecur] libname [reflibs] [fonts] [attrtable] [generations] [<FormatType>] UNITS {<structure>}* ENDLIB</td></tr>
<tr><td><FormatType> ::=</td><td>FORMAT | FORMAT {MASK}+ ENDMASKS</td></tr>
<tr><td><structure> ::=</td><td>BNGSTR STRNAME [STRCLASS] {<element>}* ENDSTR</td></tr>
<tr><td><element> ::=</td><td>{<boundary> | <path> | <SREF> | <AREF> | <text> | <node> | <box>} {<property>}* ENDEL</td></tr>
<tr><td><boundary> ::=</td><td>BOUNDARY [EFLAGS] [PLEX] LAYER DATATYPE XY</td></tr>
<tr><td><path> ::=</td><td>PATH [EFLAGS] [PLEX] LAYER DATATYPE [PATHTYPE] [WIDTH] [BGNEXTN] [ENDEXTN] XY</td></tr>
<tr><td><SREF> ::=</td><td>SREF [EFLAGS] [PLEX] SNAME [<strans>] XY</td></tr>
<tr><td><AREF> ::=</td><td>AREF [EFLAGS] [PLEX] SNAME [<strans>] COLROW XY</td></tr>
<tr><td><text> ::=</td><td>TEXT [EFLAGS] [PLEX] LAYER <textbody></td></tr>
<tr><td><node> ::=</td><td>NODE [EFLAGS] [PLEX] LAYER NODETYPE XY</td></tr>
<tr><td><box> ::=</td><td>BOX [EFLAGS] [PLEX] LAYER BOXTYPE XY</td></tr>
<tr><td><textbody> ::=</td><td>TEXTTYPE [PRESENTATION] [PATHTYPE] [WIDTH] [<strans>] XY STRING</td></tr>
<tr><td><strans> ::=</td><td>STRANS [MAG] [ANGLE]</td></tr>
<tr><td><property> ::=</td><td>PROPATTR PROPVALUE</td></tr>
</table>

2.9.6 Example GDSII Stream file

The following is a dump of a minimal GDSII Stream file, consisting of just one polygon (boundary). The GDSII file was created with the program DW2000 from Design Workshop. The binary dump was created on a VAX with the VMS command DUMP. The hex numbers are read backwards, from right to left, with each pair of digits representing a byte. Reading the first line below, we see that the file begins with the bytes 00 06 00 02, telling us that the first record contains 6 bytes, that the first record is type 00 (the header), and that record contains data of type 02 (two-byte signed integer). The corresponding ASCII representation on the right is read from left to right.

```
02000200 60000201 1C000300 02000600 ...........'.... 000000
01000E00 02000200 60002500 01000E00 .....%.'........ 000010
42494C45 4C504D41 58450602 12002500 .%....EXAMPLELIB 000020
413E0503 14000300 02220600 59524152 RARY.."......>A 000030
1C00545A 9BA02FB8 4439EFA7 C64B3789 .7K...9D./..ZT.. 000040
60000000 01000E00 02000200 60000205 ...'...........' 000050
58450606 0C001100 01000E00 02000200 ..............EX 000060
0100020D 06000008 04000045 4C504D41 AMPLE........... 000070
0000F0D8 FFFF0310 2C000000 020E0600 .......,........ 000080
FFFF204E 00001027 0000204E 00001027 '...N ..'...N .. 000090
0000F0D8 FFFFF0D8 FFFFF0D8 FFFFF0D8 ................ 0000A0
00000004 04000007 04000011 04001027 '............... 0000B0
00000000 00000000 00000000 00000000 ................ 0000C0
```

The following is an ASCII representation of this file created by the program SDUMP, [198] which translates the token numbers into the names listed in the previous section.

```
HEADER
3
BGNLIB
96
2
2
14
1
37
96
2
2
14
1
37
LIBNAME EXAMPLELIBRARY
GENERATIONS
3
UNITS
1.0000000000000E-03
1.0000000000000E-09
BGNSTR
96
2
2
14
1
0
96
2
2
14
1
17
STRNAME EXAMPLE
BOUNDARY
LAYER
1
DATATYPE
0
XY
-10000
10000
20000
10000
20000
```

```
-10000
-10000
-10000
-10000
10000
ENDEL
ENDSTR
ENDLIB
```

2.10 References

1. M. Hatzakis, "Electron resists for microcircuit and mask production," *J. Electrochem. Soc.* **116**, 1033-1037 (1969).

2. M. G. Rosenfield, M. G. R. Thomson, P. J. Coane, K. T. Kwietniak, J. Keller, D. P. Klaus, R. P. Volant, C. R. Blair, K. S. Tremaine, T. H. Newman, and F. J. Hohn, "Electron-beam lithography for advanced device prototyping: Process tool metrology," *J. Vac. Sci. Technol.* **B11** (6), 2615-2620 (1993).

3. S. A. Rishton, H. Schmid, D. P. Kern, H. E. Luhn, T. H. P. Chang, G. A. Sai-Halasz, M. R. Wordeman, E. Ganin, and M. Polcari, "Lithography for ultrashort channel silicon field effect transistor circuits," *J. Vac. Sci. Technol.* **B6** (1), 140-145 (1988).

4. C. P. Umbach, C. Van Haesendonck, R. B. Laibowitz, S. Washburn, R. A. Webb, "Direct observation of ensemble averaging of the Aharonov-Bohm effect in normal metal loops," Phys. Rev. Lett. **56** 386 (1986).

5. V. Chandrasekhar, M. J. Rooks, S. Wind, and D. E. Prober, "Observation of Aharonov-Bohm Electron Interference Effects with Periods h/e and h/2e in Individual Micron-Size, Normal-Metal Rings," *Phys. Rev. Lett.* **55**, 1610-1613 (1985).

6. S. Washburn, R. A. Webb, "Aharonov-Bohm effect in normal metal quantum coherence and transport," Advances in Physics **35,** 375 (1986).

7. B. J. van Wees, H. van Houten, C. W. J. Beenakker, J. G. Williamson, L. P. Kouwenhoven, D. van der Marel, C. T. Foxon, "Quantized conductance of point contacts in a two-dimensional electron gas," Phys. Rev. Lett. **60**, 848 (1988).

8. M. J. Rooks, C. C. Eugster, J. A. del Alamo, G. Snider, E. Hu, "Split-gate electron waveguide fabrication using multilayer PMMA," J. Vac. Sci. Technol. B 9, 2856 (1991).

9. P. H. Woerlee, G. A. M. Hurkx, W. J. M. J. Josquin, and J. F. C. M. Verhoeven, "Novel method of producing ultrasmall platinum silicide gate electrodes," *Appl. Phys. Lett.* **47** (7), 700-702 (1985).

10. E. Anderson, V. Boegli, M. Schattenburg, D. Kern, and H. Smith, "Metrology of electron-beam lithography systems using holographically produced reference samples," *J. Vac. Sci. Technol.* **B9** (6), 3606-3611 (1991).

11. R. Viswanathan, D. Seeger, A. Bright, T. Bucelot, A. Pomerene, K. Petrillo, P. Blauner, P. Agnello, J. Warlaumont, J. Conway, and D. Patel, "Fabrication of high performance 512K static-random access memories in 0.25 um complementary metal-oxide semiconductor technology using x-ray lithography," *J. Vac. Sci. Technol.* **B11** (6), 2910-2919 (1993).

12. S. Y. Chou, H. I. Smith, and D. A. Antoniadis, "Sub-100-nm channel-length transistors fabricated using x-ray lithography," *J. Vac. Sci. Technol.* **B4** (1), 253-255 (1986).

13. P. W. Hawkes and E. Kasper, *Principles of Electron Optics,* Academic Press, London (1989).

14. P. Grivet, *Electron Optics*, Elsevier, Oxford, Pergamon imprint (1965).

15. E. Munro, "Numerical modelling of electron and ion optics on personal computers," *J. Vac. Sci. Technol.* **B8** (6), 1657-1665 (1990).

16. H. Boersch, "Experimentelle Bestimmung der Energieverteilung in Thermisch Ausgelosten Elektronenstrahlen," *Z. Phys.* **139**, 115-146 (1954).

17. M. Gesley, "Thermal field emission optics for nanolithography," *J. Appl. Phys.* **65** (3), 914-926 (1989).

18. T. H. P. Chang, "Proximity effect in electron beam lithography," *J. Vac. Sci. Technol.* **12**, 1271-1275 (1975).

19. D. F. Kyser and N. S. Viswanathan, "Monte Carlo simulation of spatially distributed beams in electron-beam lithography," *J. Vac. Sci. Technol.* **12**(6), 1305-1308 (1975).

20. M. Hatzakis, "Recent developments in electron-resist evaluation techniques," *J. Vac. Sci. Technol.* **12** (6), 1276-1279 (1975).

21. G. Brewer, ed., *Electron-Beam Technology in Microelectronic Fabrication,* Academic Press (1980).

22. R. Birkhoff, in *Handbuck der Physik,* E. Fluegge, ed., Springer, Berlin and New York, 53 (1958).

23. K. Murata, D. Kyser, and C. Ting, "Monte Carlo simulations of fast secondary electron production in electron beam resists," *J. Appl. Phys.* **52**, 4396-4405 (1981).

24. University of Califronia, Berkeley, Department of Electrical Engineering, Berkeley, CA USA.

25. Leica Ltd., Cambridge, UK; USA: 708-405-0213, -0147 fax. UK: 44-223-411-411, -211-310 fax.

26. Sigma-C GmbH, Rosenheimer Landstr. 74 D-85521 Ottobrunn Germany, 49 89 609 60 51.

27. AISS GmbH, represented byTranscription Enterprises Limited, 101 Albright Way, Los Gatos, CA 95030. 408-866-1851, fax: 408-866-4839.

28. S. A. Rishton and D. P. Kern, "Point exposure distribution measurements for proximity correction in electron beam lithography on a sub-100 nm scale," *J. Vac. Sci. Technol.* **B5** (1), 135-141 (1987).

29. M. Rosenfield, S. Rishton, D. Kern, and D. Seeger, "A study of proximity effects at high electron-beam voltages for x-ray mask fabrication. 1. Additive mask processes," *J. Vac. Sci. Technol.* **B8** (6), 1763-1770 (1990).

30. E. Kratschmer, "Verification of a proximity effect correction program in electron beam lithography," *J. Vac. Sci. Technol.* **19** (4), 1264-1268 (1981).

31. K. K. Christenson, R. G. Viswanathan, and F. J. Hohn, "X-ray mask fogging by electrons backscattered beneath the membrane," *J. Vac. Sci. Technol.* **B8**(6), 1618-1623 (1990).

32. Y. Yau, R. F. W. Pease, A. Iranmanesh, and K. Polasko, "Generation and applications of finely focused beams of low-energy electrons," *J. Vac. Sci. Technol.* **19**(4), 1048 (1981).

33. M. A. McCord and T. H. Newman, "Low voltage, high resolution studies of electron beam resist exposure and proximity effect," *J. Vac. Sci. Technol.* **B10**(6), 3083-3087 (1992).

34. M. Parikh, "Self-consistent proximity effect correction technique for resist exposure (SPECTRE)," *J. Vac. Sci. Technol.* **15**(3), 931-933 (1978).

35. H. Eisenmann, T. Waas, and H. Hartmann, "PROXECCO - Proximity effect correction by convolution," *J. Vac. Sci. Technol.* **B11** (6), 2741-2745 (1993).

36. K. Harafuji, A. Misaka, K. Kawakita, N. Nomura, H. Hamaguchi, and M. Kawamoto, "Proximity effect correction data processing system for electron beam lithography," *J. Vac. Sci. Technol.* **B10** (1), 133-142 (1992).

37. K. Cummings, R. Frye, E. Rietman, "Using a neural network to proximity correct patterns written with a Cambridge electron beam microfabricator 10.5 lithography system," *Appl. Phys. Lett.* **57**, 1431-1433 (1990).

38. J. Jacob, S. Lee, J. McMillan, and N. MacDonald, "Fast proximity effect correction: An extension of PYRAMID for circuit patterns of arbitrary size," *J. Vac. Sci. Technol.* **B10** (6), 3077-3082 (1992).

39. B. D. Cook, S.-Y. Lee, "Fast proximity effect correction: An extension of PYRAMID for thicker resists", J. Vac. Sci. Technol. **B11**, 2762 (1993).

40. G. Owen and P. Rissman, "Proximity effect correction for electron beam lithography by equalization of background dose," *J. Appl. Phys.* **54** (6), 3573-3581 (1983).

41. M. Gesley and M. A. McCord, "100 kV GHOST electron beam proximity correction on tungsten x-ray masks," *J. Vac. Sci. Technol.* **B12** (6), 3478-3482 (1994).

42. Y. Kuriyama, S. Moriya, S. Uchiyama, and N. Shimazu, "Proximity effect correction for x-ray mask fabrication," *Jpn. J. Appl. Phys.* **33**, 6983-6988 (1994).

43. T. Abe, S. Yamasaki, T. Yamaguchi, R. Yoshikawa, and T. Takigawa, "Representative Figure Method for Proximity Effect Correction [II]," *Jpn. J. Appl. Phys.* **30** (11), 2965-2969 (1991).

44. CAPROX, trademark of Sigma-C GmbH, Rosenheimer Landstr. 74 D-85521 Ottobrunn Germany, 49 89 609 60 51. Distributed by Raith GmbH, Hauert 18, D-44227 Dortmund, Germany (0231-97-50-000) or Raith USA, 6 Beech Rd, Islip, NY 11751, 516-224-1764, 516-224-2620 fax, 73164.1330@compuserve.com.

45. PROXECCO, distributed byTranscription Enterprises Limited, 101 Albright Way, Los Gatos, CA 95030. 408-866-1851, fax: 408-866-4839.

46. Y. Pati, A. Teolis, D. Park, R. Bass, K. Rhee, B. Bradie, and M. Peckerar, "An error measure for dose correction in e-beam nanolithography," *J. Vac. Sci. Technol.* **B8** (6), 1882-1888 (1990).

47. Raith GmbH, Hauert 18, D-44227 Dortmund, Germany (0231-97-50-000) or Raith USA, 6 Beech Rd, Islip, NY 11751, 516-224-1764, 516-224-2620 fax, 73164.1330@compuserve.com.

48. J.C. Nabity Lithography Systems, PO Box 5354, Bozeman, MT 59717 USA, (406-587-0848), jcnabity@aol.com.

49. Data Translation Inc., 800-525-8528.

50. J. C. Nabity, M. N. Wybourne, "A versatile pattern generator for high-resolution electron-beam lithography," Rev. Sci. Instrum. **60** (1) (1989).

51. The Leica SEM division and the Zeiss SEM/TEM division have merged to form a new, separate comany, Leo Electron Optics. US Address: One Zeiss Drive, Thornwood, NY 10594, 800-356-1090.

52. R. Kendall, S. Doran, E. Weissmann, "A servo guided X-Y-theta stage for electron-beam lithography," J. Vac. Sci. Technol. **B9**, 3019 (1991).

53. R. Innes, "Yaw compensation for an electron-beam lithography system", J. Vac. Sci. Technol. **B12**, 3580 (1994).

54. H. Ohta, T. Matsuzaka, N. Saitou, "New electron optical column with large field for nanometer e-beam lithography system", Proc. SPIE **2437** 185 (1995).

55. Jenoptik Technologie GmbH, Microfabrication Division, D-07739 Jena, Germany, 49-3641-653181 (voice) 49-3641-653654 (fax). The electron beam lithography division of Jenoptik has recently been acquired by Leica Ltd. , Cambridge, UK, to form Leica Lithographie Systeme Jena GmbH; USA: 708-405-0213, -0147 fax. UK: 44-223-411-411, -211-310 fax.

56. J. Ingino, G. Owen, C. N. Berglund, R. Browning, R. F. W. Pease, "Workpiece charging in electron beam lithography," J. Vac. Sci. Technol. **B12** (3) 1367 (1994).

57. M. Gesley, F. Abboud, D. Colby, F. Raymond, S. Watson, "Electron beam column developments for submicron- and nanolithography," Jpn. J. Appl. Phys. **32** 5993 (1993).

58. M. Gesley, "MEBES IV thermal-field emission tandem optics for electron-beam lithography," J. Vac. Sci. Technol. **B9** (6) 2949 (1991).

59. H. Pearce-Percy, R. Prior, F. Abboud, A. Benveniste, L. Gasiorek, M. Lubin, F. Raymond, "Dynamic corrections in MEBES 4500," J. Vac. Sci. Technol. **B12** (6) 3393 (1994).

60. A. Murray, F. Abboud, F. Raymond, C. N. Berglund, "Feasibility study of new graybeam writing strategies for raster scan mask generation," J. Vac. Sci. Technol. **B11** (6) 2390 (1993).

61. Lepton Inc., Murray Hill NJ 07974, 908-771-9490.

62. D. M. Walker, D. C. Fowlis, S. M. Kugelmass, K. A. Murray, C. M. Rose, "Advanced mask and reticle generation using EBES4," Proc. SPIE **2322**, 56 (1994).

63. M. G. R. Thomson, R. Liu, R. J. Collier, H. T. Carroll, E. T. Doherty, R. G. Murray, "The EBES4 electron-beam column," J. Vac. Sci. Technol. **B5** (1) 53 (1987).

64. D. W. Peters, D. C. Fowlis, A. von Neida, C. M. Rose, H. A. Waggener, W. P. Wilson, "EBES4: Performance of a new e-beam reticle generator," SPIE vol. 1924, 193 (1993).

65. H. C. Pfeiffer, D. E. Davis, W. A. Enichen, M. S. Gordon, T. R. Groves, J. G. Hartley, R. J. Quickle, J. D. Rockrohr, W. Stickel, E. V. Weber, "EL-4, a new generation electron-beam lithography system," J. Vac. Sci. Technol. **B11** (6) 2332 (1993).

66. P. F. Petric, M. S. Gordon, J. Senesi, D. F. Haire, "EL-4 column and control," J. Vac. Sci. Technol. **B11** (6) 2309 (1993).

67. J. D. Rockrohr, R. Butsch, W. Enichen, M. S. Gordon, T. R. Groves, J. G. Hartley, H. C. Pfeiffer, "Performance of IBM's EL-4 e-beam lithography system", Proc. SPIE **2437** 160 (1995).

68. R. Kendall, S. Doran, E. Weissmann, "A servo guided X-Y-theta stage for electron-beam lithography," J. Vac. Sci. Technol. **B9**, 3019 (1991).

69. R. Innes, "Yaw compensation for an electron-beam lithography system", J. Vac. Sci. Technol. **B12** 3580 (1994).

70. H. Elsner, P. Hahmann, G. Dahm, H. W. P. Koops, "Multiple beam-shaping diaphragm for efficient exposure of gratings," J. Vac. Sci. Technol. **B11**(6) 2373 (1993).

71. K. Nakamura, T. Okino, S. Nakanoda, I. Kawamura, N. Goto, Y. Nakagawa, W. Thompson, M. Hassel Shearer, "An advanced electron beam lithography system for sub-half-micron ultra-large-scale production: the distortion corrector technology," J. Vac. Sci. Technol. **B8**(6) 1903 (1990).

72. T. Komagata, H. Takemura, N. Gotoh, K. Tanaka, "Development of EB lithography system for next generation photomasks," Proc. SPIE **2512**, 190 (1995).

73. H. C. Pfeiffer, "Projection exposure with variable axis immersion lenses:a high-throughput electron beam approach to "suboptical" lithography," Jpn. J. Appl. Phys. **34** 6658 (1995).

74. Y. Someda, H. Satoh, Y. Sohda, Y. Nakayama, N. Saitou, H. Itoh, M. Sasaki, "Electron-beam cell projection lithography: Its accuracy and its throughput," J. Vac. Sci. Technol. B12(6) 3399 (1994).

75. G. H. Jansen, "Coulomb interactions in particle beams", J. Vac. Sci. Technol. **B6** 1977 (1988).

76. K. Hattori, R. Yoshikawa, H. Wada, H. Kusakabe, T. Yamaguchi, S. Magoshi, A. Miyagaki, S. Yamasaki, T. Takigawa, M. Kanoh, S. Nishimura, H. Housai, S. Hashimoto, "Electron-beam direct writing system EX-8D employing character projection exposure method," J. Vac. Sci. Technol. **B11**(6) 2346 (1993).

77. K. Sakamoto, S. Fueki, S. Yamazaki, T. Abe, K. Kobayashi, H. Nishino, T. Satoh, A. Takemoto, A. Ookura, M. Oono, S. Sago, Y. Oae, A. Yamada, H. Yasuda, "Electron-beam block exposure system for a 256 M dynamic random access memory," J. Vac. Sci. Technol. **B11**(6) 2357 (1993).

78. A. Yamada, K. Sakamoto, S. Yamazaki, K. Kobayashi, S. Sago, M. Oono, H. Watanabe, H. Yasuda, "Deflector and correction coil calibrations inan electron beam block exposure system," J. Vac. Sci. Technol. **B12**(6) 3404 (1994).

79. M. Kawano, K. Mizuno, H. Yoda, Y. Sakitani, K. Andou, N. Saitou, "Continuous writing method for high speed electron-beam direct writing system HL-800D," J. Vac. Sci. Technol. **B11**(6) 2323 (1993).

80. G. H. Jansen, *Coulomb Interactions in Particle Beams* (Academic, Boston, 1990).

81. S. Berger, D. J. Eaglesham, R. C. Farrow, R. R. Freeman, J. S. Kraus, J. A. Liddle, "Particle-particle interaction effects in image projection lithography systems," J. Vac. Sci. Technol. **B11**(6) 2294 (1993).

82. Y. Someda, H. Satoh, Y. Sohda, Y. Nakayama, N. Saitou, H. Itoh, M. Sasaki, "Electron-beam cell projection lithography: Its accuracy and its throughput," J. Vac. Sci. Technol. **B12**(6) 3399 (1994).

83. Y. Nakayama, S. Okazaki, N. Saitou, H. Wakabayashi, "Eelctron-beam cell projection lithography: A new high-throughput electron-beam direct-writing technology using a specially tailored Si aperture," J. Vac. Sci. Technol. **B8** 1836 (1990).

84. J. A. Liddle, C. A. Volkert, "Stress-induced pattern-placement errors in thin membrane masks," J. Vac. Sci. Technol. **B12**(6) 3528 (1994).

85. H. P. W. Koops, J. Grob, *Springer Series in Optical Sciences: X-ray Microscopy* (Springer, Berlin, 1984) vol. 43.

86. S. D. Berger, J. M. Gibson, "New approach to projection-electron lithography with demonstrated 0.1um linewidth," Appl. Phys. Lett. **57** (2) 153 (1990).

87. S. D. Berger, J. M. Gibson, R. M. Camarda, R. C. Farrow, H. A. Huggins, J. S. Kraus, "Projection electron-beam lithography: A new approach," J. Vac. Sci. Technol. **B9**(6) 2996 (1991).

88. J. A. Liddle, S. D. Berger, C. J. Biddick, M. I. Blankey, K. J. Bolan, S. W. Bowler, K. Brady, R. M. Camarda, W. F. Connely, A. Crorken, J. Custy, R. C. Farrow, J. A. Felker, L. A. Fetter, B. Freeman, L.

R. Harriott, L. Hopkins, H. A. Huggins, C. S. Knurek, J. S. Kraus, D. A. Mixon, M. M. Mkrtchyan, A. E. Novembre, M. L. Peabody, W. M. Simpson, R. G. Tarascon, H. H. Wade, W. K. Waskiewicz, G. P. Watson, J. K. Williams, D. L. Windt, "The Scattering with Angular Limitation in Projection Electron-Beam Lithography (SCALPEL) System," Jpn. J. Appl. Phys. **34**, 6663 (1995).

89. J. A. Liddle, H. A. Huggins, S. D. Berger, J. M. Gibson, G. Weber, R. Kola, C. W. Jurgensen, "Mask fabrication for projection electron-beam lithography incorporating the SCALPEL technique," J. Vac. Sci. Technol. **B9**(6) 3000 (1991).

90. G. P. Watson, S. D. Berger, J. A. Liddle, W. K. Waskiewicz, "A background dose proximity effect correction technique for scattering with angular limitation projection electron lithography implemented in hardware", J. Vac. Sci. Technol. **B13**, 2504 (1995).

91. H. W. P. Koops, *Microcircuit Engineering 88* (North-Holland, New York, 1989) p.217.

92. G. E. Shedd and P. E. Russel, "The scanning tunneling microscope as a tool for nanofabrication," Nanotechnology **1**, 67 (1990).

93. N. C. MacDonald, W. Hofmann, L.-Y. Chen, J. H. Das, "Micro-machined electron gun arrays (MEGA)", Proc. SPIE **2522**, 220 (1995).

94. W. Hofmann, L.-Y. Chen, N. C. MacDonald, "Fabrication of integrated micromachined electron guns", J. Vac. Sci. Technol. **B13**, 2701 (1995).

95. N. Shimazu, K. Saito, M. Fujinami, "An approach to a high-throughput e-beam writing with a single-gun multiple-path system," Jpn. J. Appl. Phys. **34**, 6689 (1995).

96 . T. H. P. Chang, D. P. Kern, L. P. Murray, "Arrayed miniature electron beam columns for high throughput sub-100 nm lithography", J. Vac. Sci. Technol. **B10**, 2743 (1992).

97. D. A. Crewe, D. C. Perng, S. E. Shoaf, A. D. Feinerman, "Micromachined electrostatic electron source", J. Vac. Sci. Technol. **B10**, 2754 (1992).

98. G. W. Jones, S. K. Jones, M. D. Walters, B. W. Dudley, "Microstructures for control of multiple ion or electron beams", IEEE Trans. Electr. Dev. **36**, 2686 (1989).

99. E. Kratschmer, H. S. Kim, M. G. R. Thomson, K. Y. Lee, S. A. Rishton, M. L. Yu, T. H. P. Chang, "Sub-49nm resolution 1 keV scanning tunneling microscope field-emission microcolumn," J. Vac. Sci. Technol. **B12**, 3503 (1994).

100. E. Kratschmer, H. S. Kim, M. G. R. Thomson, K. Y. Lee, S. A. Rishton, M. L. Yu, T. H. P. Chang, "An electron-beam microcolumn with improved resolution, beam current, and stability", J. Vac. Sci. Technol. **B13**, 2498 (1995).

101. Cadence Design Systems, 555 River Oaks Parkway, San Jose, CA (USA) 408-943-1234. See also http://www.cadence.com.

102. Mentor Graphics Corp. Gateway Marketing Center, P.O. Box 5050, Wilsonville, OR 97070. 800-547-3000, fax: 503-685-8001. E-mail: gen-del@gateway.mentorg.com

103. Silvar Lisco, 703 E. Evelyn Av., Sunnyvale, CA 94086. 800-624-9978, 408-991-6000, fax: 408-737-9979.

104. Integrated Silicon Systems, P.O. Box 13665, Research Triangle Park, NC 27709. 800-422-3585.

105. Refer to the *Semiconductor International Buyer's Guide* issue for a list of other CAD vendors.

106. Design Workshop, 4226 St. John's, Suite 400 D. D. O. Quebec H9G 1X5, 514-696-4753, fax: 514-696-5351.

107. Tanner Research, 180 North Vinedo Av., Pasadena, CA 91107. 818-792-3000, fax: 818-792-0300.

108. DXF to GDSII conversion software is available from Artwork Conversion Software, 1320 Mission St. #5, Santa Cruz CA 95060 (408-426-6163.)

109. For information on ordering these programs and on the Berkeley Industrial Liaison Program, see http://www.eecs.berkeley.edu/ILP/Catalog/index.html

110. R. W. Hon, C. H. Sequin, *A Guide to LSI Implementation*, Second Edition, p.79. (XEROX Palo Alto Research Center, 3333 Coyote Rd., Palo Alto, CA 94304, 1980).

111. C. Mead, L. Conway, *Introduction to VLSI Systems* (Addison-Wesley, Reading MA 1980).

112. See http://info.broker.isi.edu/1/mosis

113. These rules provided by S. Reynolds, ISI (MOSIS) 4676 Admiralty Way, Marina del Rey, CA 90292.

114. Transcription Enterprises Limited, 101 Albright Way, Los Gatos, CA 95030. 408-866-1851, fax: 408-866-4839.

115. SIGMA-C GmbH, Rosenheimer Landstr. 74, D-85521, Munich, Germany, phone 49-89-609-6051, fax 49-89-609-8112, caprox@sigma-c.de. U.S. distributor: Raith Co., 6 Beech Rd, Islip, NY 11751, 516-224-1764, 516-224-2620 fax, 73164.1330@compuserve.com.

116. JEBCAD is sold by JEOL-USA, 111 Dearborn Rd, Peabody, MA 01960 (508-535-5900.) In Japan, JEOL Ltd., 1-2 Musashino 3-chome, Akishima Tokyo 196 (0425-42-2187.)

117. Design Workshop, 4226 St. John's, Suite 400 D. D. O. Quebec H9G 1X5, 514-696-4753, fax: 514-696-5351.

118. E. Reichmanis, L. F. Thompson, "Polymer materials for microlithography," in *Annual Review of Materials Science* vol. 17, R. A. Huggins, J. A. Giordmaine, J. B. Wachtman, Jr., eds. (Annual Reviews, Inc. Palo Alto, CA, 1987) p. 235.

119. E. Reichmanis, A. E. Novembre, "Lithographic resist materials chemistry," in *Annual Review of Materials Science* vol. 23, R. A. Laudise, E. Snitzer, R. A. Huggins, J. A.Giordmaine, J. B. Wachtman, Jr., eds. (Annual Reviews, Inc. Palo Alto, CA) 1993, p. 11.

120. C. Grant Willson, "Organic resist materials - theory and chemistry," in *Introduction to Microlithography*, L. F. Thompson, C. G. Willson, M. J. Bowden, eds., ACS Symposium Series 219 (American Chemical Society, Washington DC, 1983) p.87.

121. *Materials for Microlithography - Radiation-Sensitive Polymers,* L. F. Thompson, D. G. Willson, J. M. J. Fr*chet, eds., ACS Symposium Series 266 (American Chemical Society, Washington DC, 1984).

122. C. G. Willson, "Organic Resist Materials", and L. F. Thompson, "Resist Processing", in *Introduction to Microlithography,Second Edition,* L. F. Thompson, C. G. Willson, M. J. Bowden, eds. (American Chemical Society, Washington DC, 1994).

123. A. Weill, "The spin coating process mechanism," in *The Physics and Fabricaton of Microstructures and Microdevices*, M. J. Kelly, C. Weisbuch, eds., (Springer-Verlag, Berlin, 1986) p. 51.

124. T. Tanaka, M. Morigami, and N. Atoda, "Mechanism of resist pattern collapse during development process," Jpn. J. Appl.Phys **32**, 6059 (1993).

125. The program SELID is available from Sigma-C GmbH, Rosenheimer Landstr. 74 D-85521 Ottobrunn Germany, 49 89 609 60 51.

126. T. E. Everhart, in *Materials in Microlithography*, L. F. Thompson et al., eds. (American Chemical Society, Washington DC 1984).

127. Gold etch solution type TFA from Transene Co., Rowley MA.

128. Chrome etch type CR-14 from Cyantek Corp., 3055 Osgood Ct., Fremont CA 94538.

129. M. Kurihara, M. Arai, H. Fujita, H. Moro-oka, Y. Takahashi, H. Sano, "Primary processes in e-beam and laser lithographies for phase-shift mask manufacturing II," SPIE vol. 1809, *12th Annual BACUS Symposium*, 50 (1992).

130. C. A.Kondek, L. C. Poli, "A submicron e-beam lithography process using an overcoating conducting polymer for the reduction of beam charging effects on lithium niobate and quartz," Proc. SPIE vol. 2194 p.366 (1994).

131. M. Angelopoulos, J. M. Shaw, K. Lee, W. Huang, M. Lecorre, M. Tissier, "Lithographic applications of conducting polymers," J. Vac. Sci. Technol. **B9**(6) 3428 (1991).

132. M. Angelopoulos, N. Patel, J. M. Shaw, N. C. Labianca, S. A. Rishton, "Water soluble conducting polyanilines: Applications in lithography," J. Vac. Sci. Technol. **B11**(6) 2794 (1993).

133. I. Haller, M. Hatzakis, R. Srinivasan, "High-resolution positive resists for electron-beam exposure," IBM J. Res. Develop. **12** 251 (1968).

134. M. Hatzakis, "Electron resists for microcircuit and mask production," J. Electrochem. Soc. **116** 1033 (1969).

135. PMMA vendors include: OCG Microelectronic Materials Inc., 5 Garret Mountain Plaza, West Paterson, NJ 07424, 800-222-4868. Microlithography Chemical Corp., 1254 Chestnut St. Newton, MA 02164 617-965-5511 617-965-5818 fax. Mead Chemical Co., 10750 County Rd. 2000, PO Box 748, Rolla, MO 65401. 314-364-8844.

136. G. H. Bernstein, D. A. Hill, "On the attainment of optimum developer parameters for PMMA resist," Superlattices and Microstructures **11** (2) 237 (1992).

137. B. P. Van der Gaag, A. Sherer, "Microfabrication below 10nm," Appl. Phys. Lett. **56** 481 (1990).

138. D. W. Keith, R. J. Soave, M. J. Rooks, "Free-standing gratings and lenses for atom optics," J. Vac. Sci. Technol. **B9** (6) 2846 (1991).

139. W. C. B. Peatman, P. A. D. Wood, D. Porterfield, T. W. Crowe, M. J. Rooks, "Quarter-micrometer GaAs Schottky barrier diode with high video responsivity at 118 m," Appl. Phys. Lett. **61** 294 (1992).

140. R. C. Tiberio, G. A. Porkolab, M. J. Rooks, E. D. Wolf, R. J. Lang, A. D. G. Hall, "Facetless Bragg reflector surface-emitting AlGaAs/GaAs lasers fabricated by electron-beam lithography and chemically assisted ion-beam etching", J. Vac. Sci. Technol. **B9** 2842 (1991).

141. Note that this liftoff process allows the use of ultrasonic agitation because chrome sticks very well to silicon. The ultrasonic process causes lines of aluminum to peal off the surface. A common belief is that once the substrate is dry, the metal cannot be made to separate from the surface. This is not necessarily true. If the metal pattern adheres well to the substrate (e.g., Cr or Ti), then further

ultrasonic agitation in the solvent may well continue the liftoff process and improve the yield of devices.

142. T. Tada, "Highly sensitive positive electron resists consisting of halogenated alkyl -chloroacrylate series polymer materials," J. Electrochem. Soc. **130** 912 (1983).

143. Toray Marketing and Sales, 1875 S. Grant St., Suite 720, San Mateo, CA 94402. 415-341-7152. Toray Industries, 1-8-1 Mihama Urayasu Inc., Chiba, Japan.

144. K. Nakamura, S. L. Shy, C. C. Tuo, C. C. Huang, "Critical dimension control of poly-butene-sulfone resist in electron beam lithography," Jpn. J. Appl. Phys. **33**, 6989 (1994).

145. M. Widat-alla, A. Wong, D. Dameron, C. Fu, "Submicron e-beam process control," Semiconductor International (May 1988), p. 252.

146. Pre-spun mask plates are sold by Hoya Electronics Co., Ft. Lee, NJ.; Balzers Optical Co., Marlborough, MA; see the Semiconductor International Buyer's Guide for other vendors.

147. Mead Chemical Co., 10750 County Rd. 2000, PO Box 748, Rolla, MO 65401. 314-364-8844.

148. Nippon Zeon is represented in the US by Nagase California Corp., 710 Lakeway, Suite 135, Sunnyvale, CA 94086. 408-773-0700.

149. K. Kurihara, K. Iwadate, H. Namatsu, M. Nagase, H. Takenaka, K. Murase, "An electron beam nanolithography system and its application to Si nanofabrication," Jpn. J. Appl. Phys. **34** 6940 (1995).

150. T. Nishida, M. Notomi, R. Iga, T. Tamamura, "Quantum wire fabrication by e-beam lithographyusing high-resolution and high-sensitivity e-beam resist ZEP-520," Jpn. J. Appl. Phys. **31**, Pt. 1, no.12B, 4508 (1992).

151. J. Pacansky, R. J. Waltman, "Solid-state electron beam chemistry of mixtures of diazoketones in phenolic resins: AZ resists," J. Phys. Chem. **92** 4558 (1988).

152. Hoechst Celanese Corp, AZ Photoresist Products, 70 Meister Ave., Somerville, NJ 08876. 908-429-3500.

153. M. Kurihara, M. Komada, H. Moro-oka, N. Hayashi, H. Sano, "EBR900 processes in e-beam and laser beam lithographies for photomask production", Proc. SPIE **2437**, 240 (1995).

154. A. E. Novembre, R. G. Tarascon, O. Nalamasu, L. Fetter, K. J. Bolan, C. S. Knurek, "Electron-beam and x-ray lithographic characteristics of the optical resist ARCH", Proc. SPIE **2437**, 104 (1995).

155. OCG Microelectronic Materials Inc., 5 Garret Mountain Plaza, West Paterson, NJ 07424, 800-222-4868.

156. Shipley Inc., 455 Forest St., Marlboro, MA 01752. 800-343-3013.

157. D. Macintyre, S. Thoms, "High resolution electron beam lithography studies on Shipley chemically amplified DUV resists," presented at the MNE Conference, September 1996; to appear in *Micro- and Nano-engineering 96, Procedings of the International Conference on Micro- and Nano-engineering,* S. P. Beaumont ed., vol. 29.

158. E. Reichmanis, L. F. Thompson, "Polymer materials for microlithography," in *Annual Review of Materials Science*, v.17, R. A. Huggins, J. A. Giordmaine, J. B. Wachtman Jr., eds. (Annual Reviews, Palo Alto, 1987) p.238.

159. T. Yoshimura, Y. Nakayama, S. Okazaki, "Acid-diffusion effect on nanofabrication in chemical amplification resist," J. Vac. Sci. Technol. **B10**(6) 2615 (1992).

160. E. A. Dobisz, C. R. K. Marrian, "Sub-30nm lithography in a negative electron beam resist with a vacuum scanning tunneling microscope," Appl. Phys. Lett. **58**(22) 2526 (1991).

161. A. Claßen, S. Kuhn, J. Straka, A. Forchel, "High voltage electron beam lithography of the resolution limits of SAL601 negative resist," Microelectronic Engineering **17** 21 (1992).

162. D. A. Mixon, A. E. Novembre, W. W. Tai, C. W. Jurgensen, J. Frackoviak, L. E. Trimble, R. R. Kola, G. K. Celler, "Patterning of x-ray masks using the negative-acting resist P(SI-CMS)," J. Vac. Sci. Technol. **B11**(6) 2834 (1993).

163. A. E. Novembre, D. A. Mixon, C. Pierrat, C. Knurek, M. Stohl, "Dry etch patterning of chrome on glass optical masks using P(SI-CMS) resist," Proc. SPIE **2087** 50 (1993).

164. C. W. Lo, W. K. Lo, M. J. Rooks, M. Isaacson, H. G. Craighead, A. E. Novembre, "Studies of 1 and 2 keV electron beam lithography using silicon containing P(SI-CMS) resist", J. Vac. Sci. Technol. **B13** 2980 (1995).

165 . K. J. Stewart, M. Hatzakis, J. M. Shaw, D. E. Seeger, E. Neumann, "Simple negative resist for deep ultraviolet, electron beam, and x-ray lithography", J. Vac. Sci. Technol. **B7** 1734 (1989).

166. K. G. Chiong, S. Wind. D. Seeger, "Exposure characteristics of high-resolution negative resists", J. Vac. Sci. Technol. **B8** 1447 (1990).

167. K. G. Chiong, F. J. Hohn, "Resist patterning for sub-quarter micron device fabrications", Proc. SPIE **1465** 221 (1991).

168. N. LaBianca, J. D. Gelorme, "High aspect ratio resist for thick film applications", Proc. SPIE **2438** 846 (1995).

169. W. Moreau, C. H. Ting, "High sensitivity positive electron resisit," US Patent 3934057, 1976.

170. S. Mackie, S. P. Beaumont, Solid State Technology **28** 117 (1985).

171. M. J. Rooks, C. C. Eugster, J. A. del Alamo, G. L. Snider, E. L. Hu, "Split-gate electron waveguide fabrication using multilayer poly(methyl methacrylate)," J. Vac. Sci. Technol. **B9**(6) 2856 (1991).

172. Microlithography Chemical Corp., 249 Pleasant St., Watertown, MA 02172. 617-926-3322, -2919 fax.

173. M. Hatzakis, "PMMA copolymers as high sensitivity electron resists," J. Vac. Sci. Technol. **16**(6) 1984 (1979). M. Hatzakis, "High sensitivity resist system for lift-off metallization," U.S. Patent No. 4024293 (1977).

174. P(MMA-MAA) and PMMA may be purchased from OCG Microelectronic Materials Inc., 5 Garret Mountain Plaza, West Paterson, NJ 07424, 800-222-4868; or from the Microlithography Chemical Corp., 249 Pleasant St., Watertown, MA 02172. 617-926-3322, -2919 fax.

175. R. E. Howard, E. L. Hu, L. D. Jackel, "Multilevel resist for lithography below 100nm," IEEE Trans. Electron. Dev. **ED-28**(11) 1378 (1981).

176. G. J. Dolan, "Offset masks for lift-off photoprocessing," Appl. Phys. Lett. **31**, 337 (1977).

177. R. E. Howard, D. E. Prober, "Nanometer-scale fabrication techniques," in *VLSI Electronics: Microstructure Science* vol. 5, (Academic Press, New York, 1982).

178. H. Takenaka, Y. Todokoro, "A PMMA/PMGI two layer resist system for stable lift-off processing," Proc. SPIE **1089** 132 (1989).

179. M. P. de Grandpre, D. A. Vidusek, M. W. Legenza, "A totally aqueous developable bilayer resist system," Proc. SPIE **539**, 103 (1985). M. W. Legenza, D. A. Vidusek, M. P. Grandpre, "A new class of bilevel and mono-level positive resist systems based on a chemically stable imide polymer," Proc. SPIE **539**, 250 (1985).

180. R. C. Tiberio, J. M. Limber, G. J. Galvin, E. D. Wolf, "Electron beam lithography and resist processing for the fabrication of T-gate structures," Proc. SPIE **1089**, 124 (1989).

181. A. N. Broers, "Micromachining by sputtering through a mask of contamination laid down by an electron beam," in *Proceedings of the First International Conference on Electron and Ion Beam Science and Technology*, R. Bakish, ed. (Wiley, New York, 1964) p.191.

182. R. Voss, R. B. Laibowitz, A. N. Broers, "Niobium nanobridge DC SQUID," Appl. Phys. Lett. **37** 656 (1980).

183. C. P. Umbach, S. Washburn, R. A. Webb, R. Koch, M. Bucci, A. N. Broers, R. B. Laibowitz, "Observation of the h/e Aharonov-Bohm interference effects in sub-micron diameter, normal metal rings," J. Vac. Sci. Technol. **B4** 383 (1986).

184. P. Mankiewich, H. G. Craighead, T. R. Harrison, A. Dayen, "High resolution electron beam lithography on CaF_2", Appl. Phys. Lett. **44** 468 (1984).

185. E. Kratschmer, M. Isaacson, "Nanostructure fabrication in metals, insulators, and semiconductors using self-developing metal inorganic resist," J. Vac. Sci. Technol. **B4**(1) 361 (1986).

186. M. Isaacson, A. Muray, "In situ vaporization of very low molecular weight resists using 1/2 nm diameter electron beams," J. Vac. Sci. Technol. **19**, 1117 (1981).

187. W. Langhenrich, A. Vescan, B. Spangenberg, H. Beneking, Microelectronics Engineering **17**, 287 (1992). W. Langhenrich, H. Beneking, Jpn. J. Appl. Phys. **32**, 6248 (1993).

188. J. Fujita, H. Watanabe, Y. Ochiai, S. Manako, J. S. Tsai, S. Matsui, "Sub-10 nm lithography and development properties of inorganic resist by scanning electron beams", J. Vac. Sci. Technol. **B13**, 2757 (1995).

189. D. R. Allee, X. D. Pan, A. N. Broers, C. P. Umbach, "ultra-high resolution electron beam patterning of SiO_2: A review," in *Science and Technology of Mesoscopic Structures*, S. Namba, C. Hanmaguchi, T. Ando, eds. (Springer-Verlag, Tokyo, 1991) p. 362.

190. M. J. Lercel, G. F. Redinbo, F. D. Pardo, M. Rooks, R. C. Tiberio, P. Simpson, H. G. Craighead, C. W. Sheen, A. N. Parikh, D. L. Allara, "Electron beam lithography with monolayers of alkylthiols and alkylsiloxanes," J. Vac. Sci. Technol. **B12**(6) 3663 (1994).

191. R. C. Tiberio, H. G. Craighead, M. Lercel, T. Lau, C. W. Sheen, D. L. Allara, "Self assembled monolayer electron beam resist on GaAs," Appl. Phys. Lett. **62**, 476 (1993).

192. S. W. J. Kuan, C. W. Frank, Y. H. Y. Lee, T. Eimori, D. R. Allee, R. F. W. Pease, R. Browning, "Ultrathin Poly(MMA) resist films for microlithography," J. Vac. Sci. Technol. **B7**, 1745 (1989).

193. M. Böttcher, L. Bauch, "Surface imaging by silylation for low voltage electron-beam lithography," J. Vac. Sci. Technol. B12, 3473 (1994).

194. C. Pierrat, S. Tedesco, F. Vinet, T. Mourier, M. Lerme, B. Dal'Zotto, J. C. Guibert, "PRIME process for deep UV and E-beam lithography", Microelectronic Engineering, **11**, 507 (1990).

195. C. Pierrat, "New model of polymer silylation: application to lithography", J. Vac. Sci. Technol. **B10**, 2581 (1992).

196. M. Irmscher, B. Höfflinger, R. Springer, "Comparative evaluation of chemically amplified resists for electron-beam top surface imaging use," J. Vac. Sci. Technol. **B12**, 3925 (1994).

197. Portions of the *GDSII Stream Format Manual*, Documentation No. B97E060, Feb. 1987, reprinted with permission of Cadence Design Systems, Inc., 555 River Oaks Parkway, San Jose, CA 95134. 408-943-1234. See also the web site http://www.cadence.com.

198. A useful set of GDSII utilities is available for the VMS operating system. This set includes programs for syntax checking, dumping to ASCII, building from ASCII, rotating and scaling cells, printing cell hierarchies, printing data extents, and displaying layer occupation. For purchase information contact the Cornell NanoScale Facility at 607-255-2329, or information@cnf.cornell.edu.